Advances in Solid State Photo-Detectors

with single photon sensitivity

G.Collazuol
Dipartimento di Fisica ed Astronomia
Universita` di Padova

Overview

- SSPD for **single photon**... mainly **SiPM**
- **Physics** and **technology** key features
- Main SiPM **parameters**
- **Comparison** among photo-detectors
- Few examples of **Cherenkov** light readout with SiPM

...for a more extensive review → GC at IDPASC 2013 (Siena)

SSD with internal gain

Reverse biased junction: internal gain via impact ionization in high E field

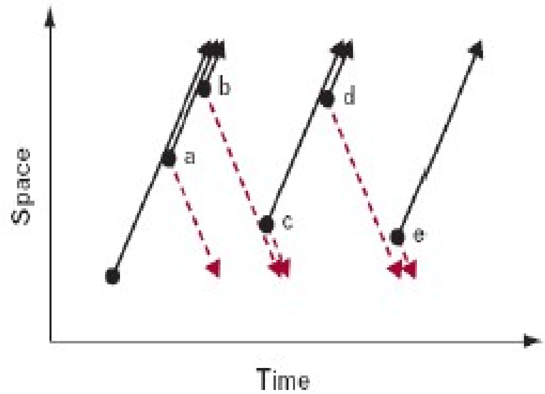

APD: avalanche photo-diode

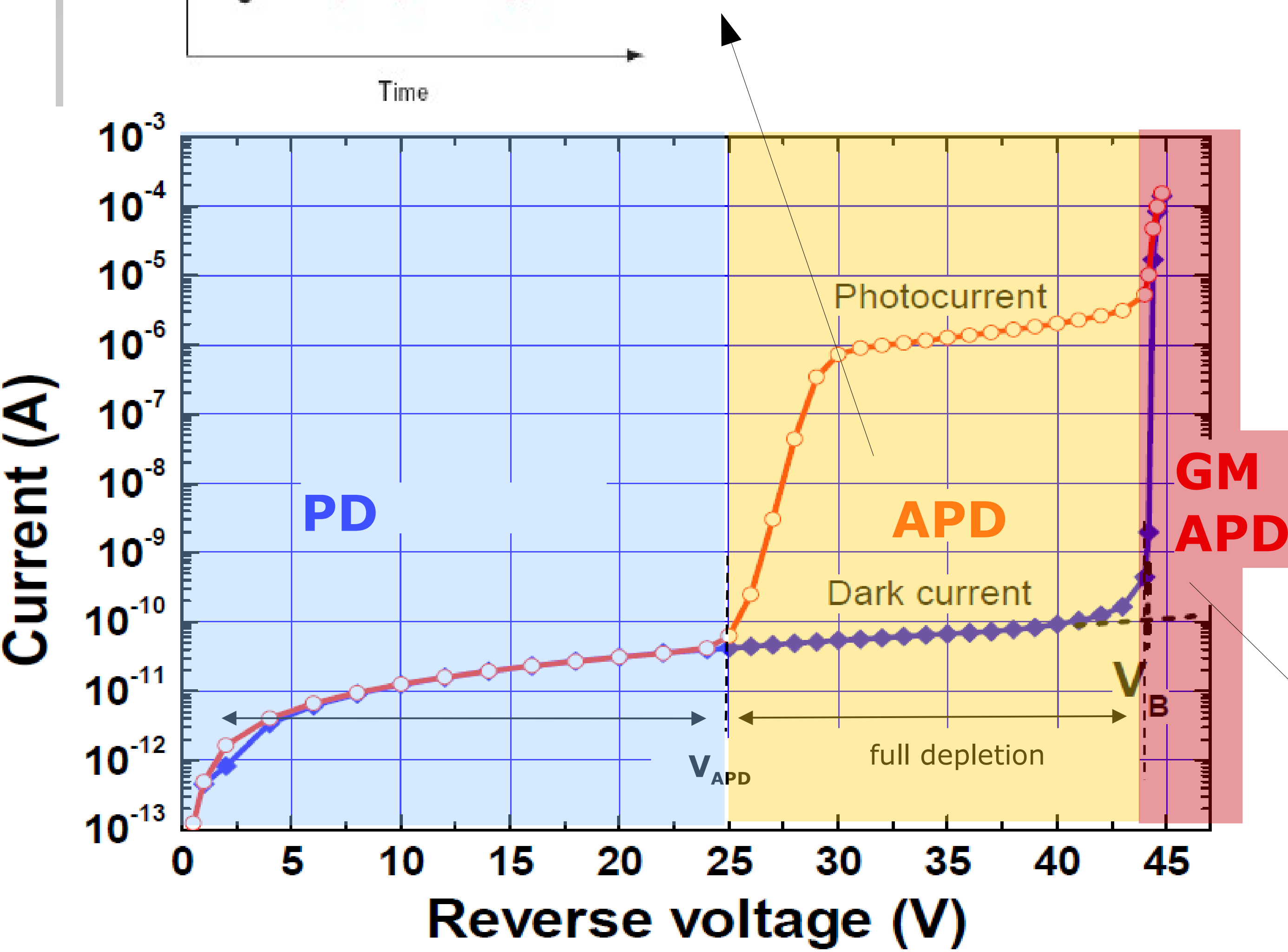

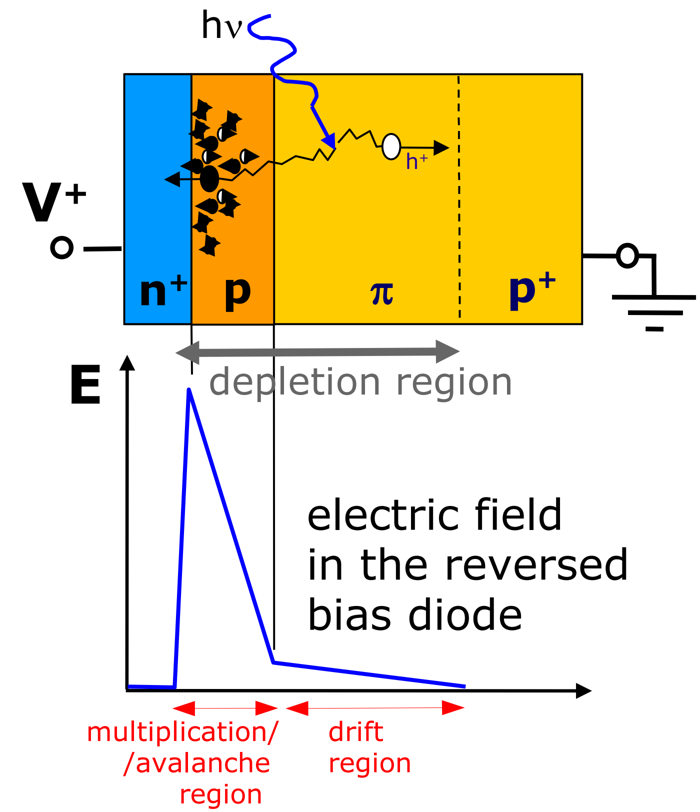

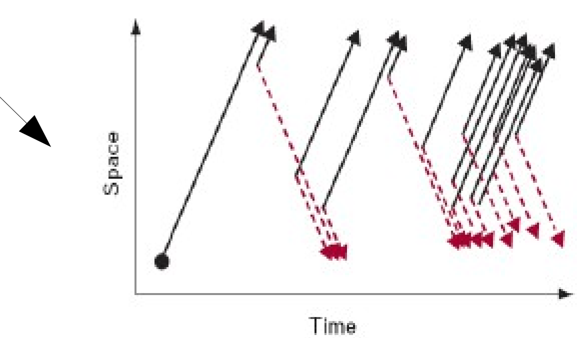

Geiger Mode APD

SSD with internal gain

APD: avalanche photo-diode

- Bias **below** V_{bd} ($V_{APD} < V < V_{bd}$)
- Linear Mode/ **amplifier** device
- Multiplication < 10^3 (lim. by fluctuations)
- **Sensitivity ~ 5 ph.e** (room temperature)

  (1ph.e. at low T with slow electronics...)

Reverse biased junction: internal gain via impact ionization in high E field

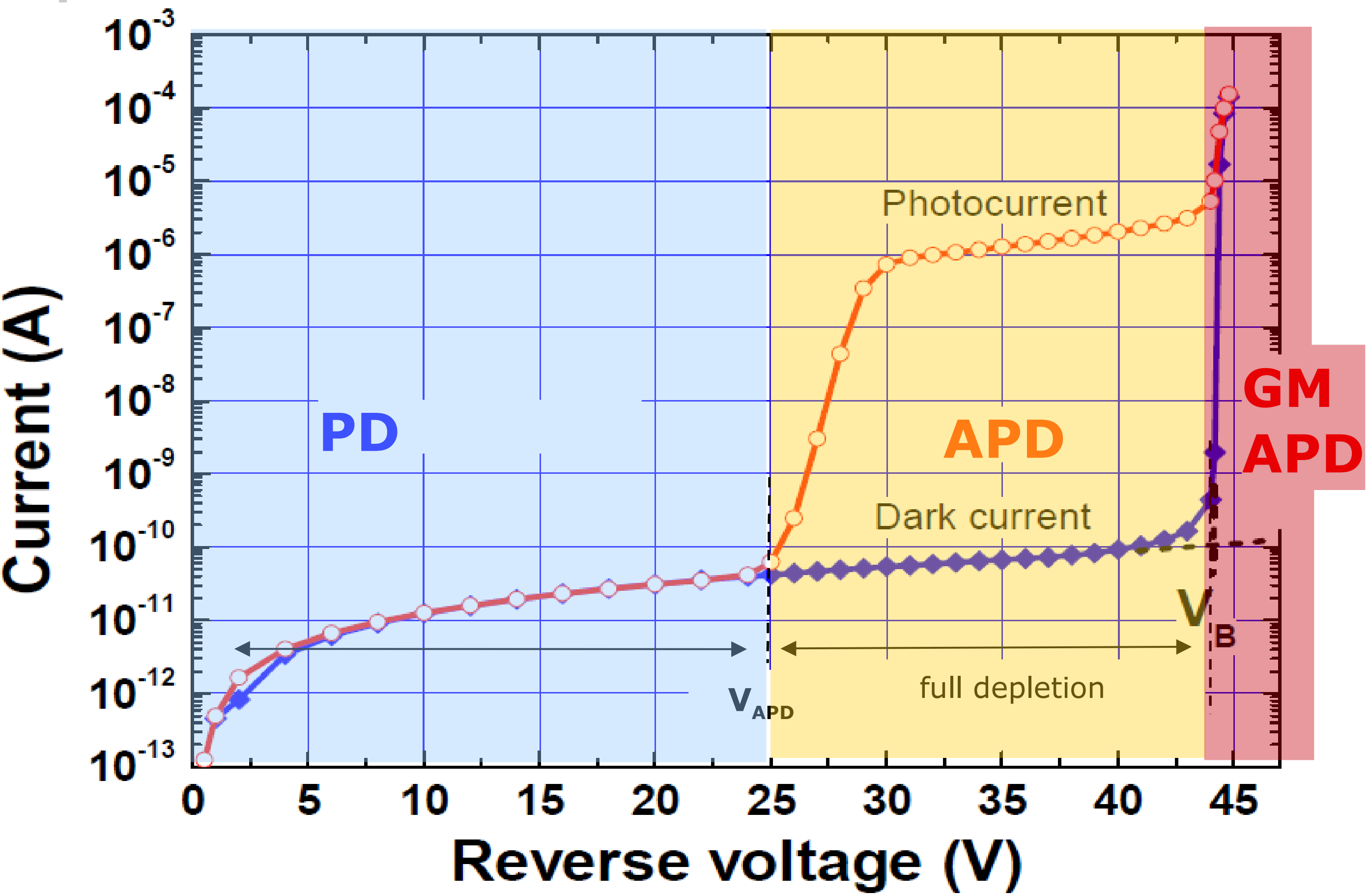

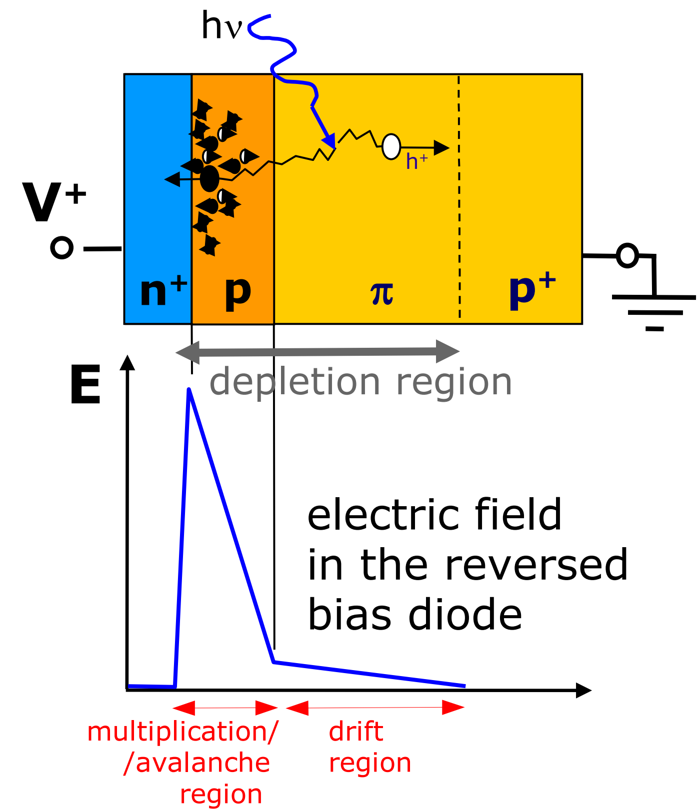

GM-APD: Geiger Mode

- Bias **above** V_{bd} (a few V)
- **binary** device
- Gain: ~10^6 (lim. by noises)
- **Single ph.e. resolution**
- Limited by dark count rate
- **Need Quenching/Reset**

GM-APD Operation model – passive quenching

Diode (capacitor) fast discharge
and slow recharge

charge stored defines Gain
→ Gain ~ C ΔV
$\Delta V = V_{bias} - V_{bd}$ "Over-Voltage"

currents internal / external

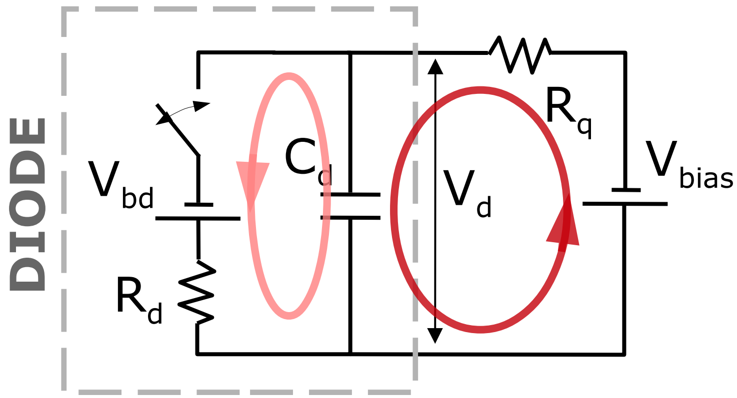

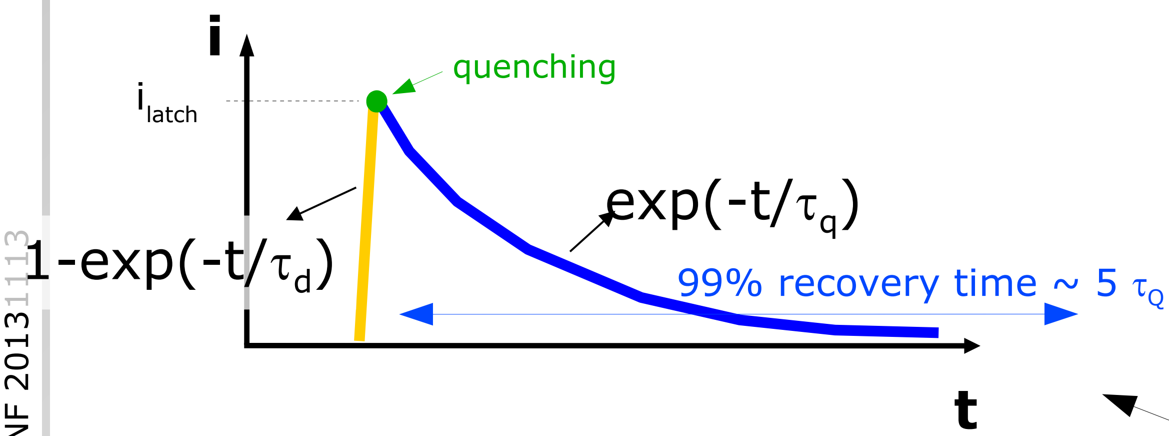

Rise time $\tau_d = R_d C_d$ ≪ Fall time (recovery) $\tau_q = R_q C_d$

pulse shape (ideal)

Gain → linear with ΔV (≠ APD)
→ no intrinsic fluctuations !!! (≠ APD)
→ independent of T at fixed ΔV (≠ APD)

Rise time T dependence (weak) due to R_d

Recovery time T dependence (strong) due to R_q
C_d is independent of T

The Silicon PM: array of GM-APD

Single GM-APD gives **no information** on light intensity → use array of GM-APDs' first proposed in the late '80-ies by Golovin and Sadygov

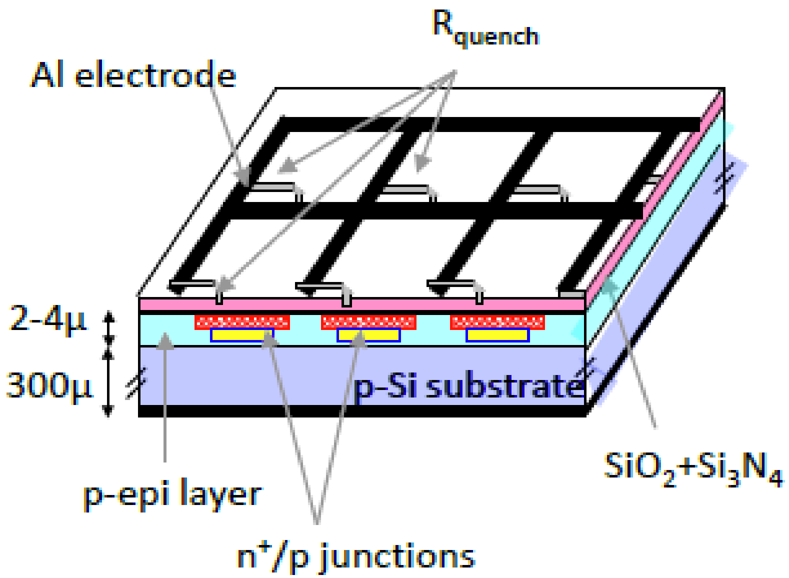

A SiPM is segmented in tiny GM-APD cells and connected in parallel trough a decoupling resistor, which is also used for quenching avalanches in the cells

Each element is independent and gives the same signal when fired by a photon

Σ of binary signals → analog signal

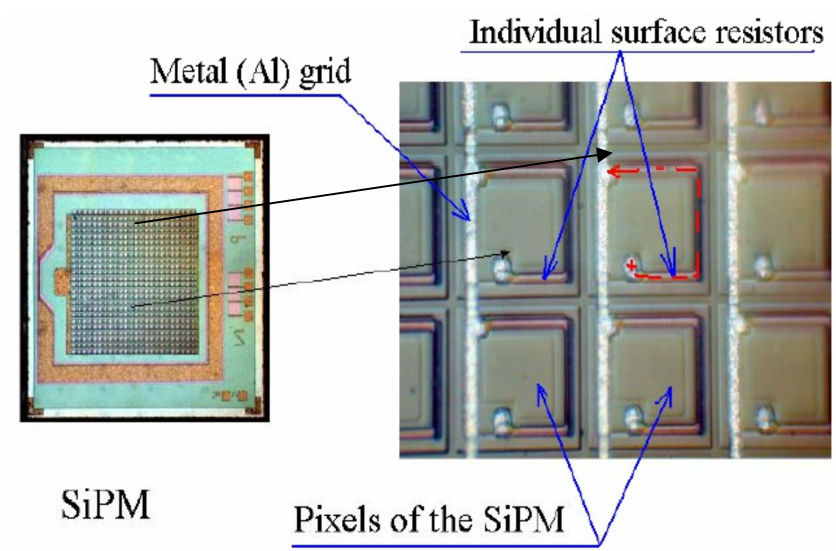

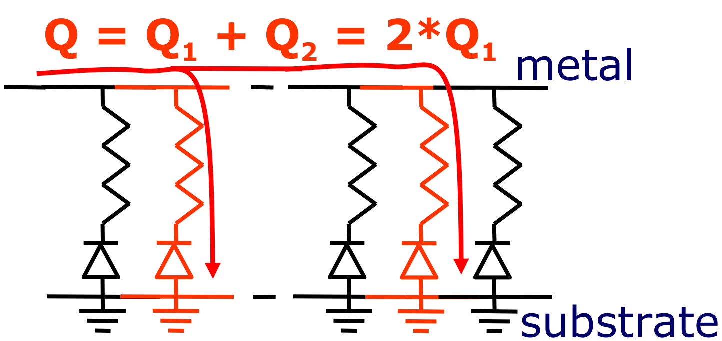

Output ∝ number incident photons

The Silicon PM: array of GM-APD

Single GM-APD gives **no information** on light intensity → use array of GM-APDs' first proposed in the late '80-ies by Golovin and Sadygov

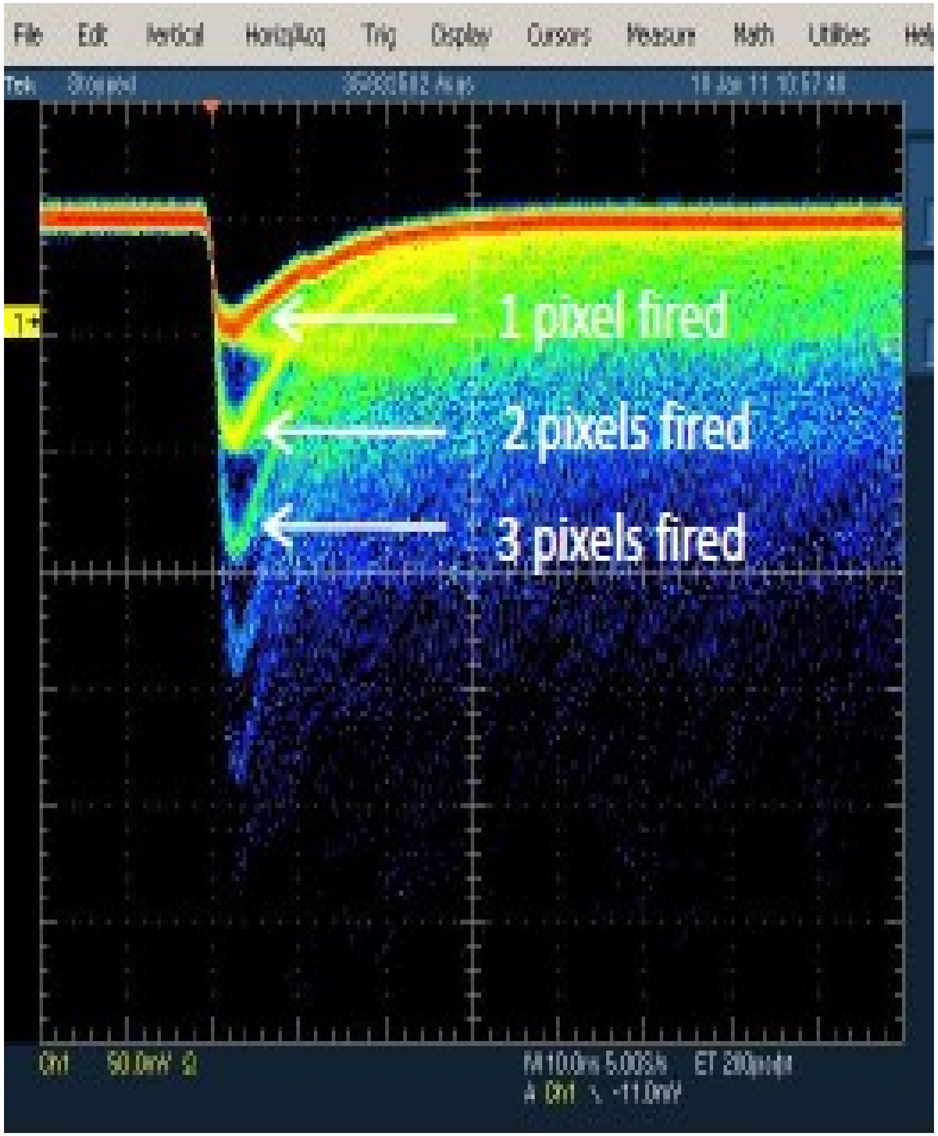

A SiPM is segmented in tiny GM-APD cells and connected in parallel trough a decoupling resistor, which is also used for quenching avalanches in the cells

Each element is independent and gives the same signal when fired by a photon

Σ of binary signals → analog signal

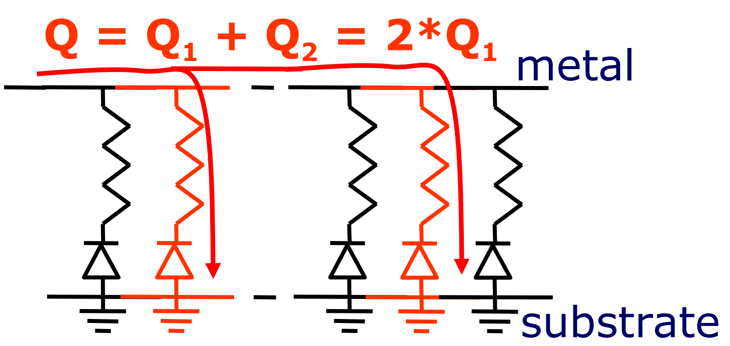

Output $\propto$ number incident photons

Today: few examples

ZECOTEK MAPD-3N

FBK-AdvanSiD

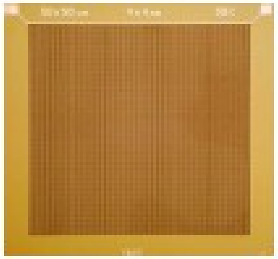

HAMAMATSU S10985

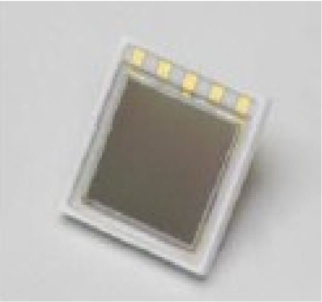

KETEK PM3350

STMicroelectronics

Producer	Reference	Area (mm^2)	PDE max @ 25 °C *	Dark Count Rate (Hz) @ 25°C *	Gain *
ZECOTEK	MAPD-3N	3 x 3	30% @ 480 nm	$9.10^5 - 9.10^6$	10^5
FBK - AdvanSiD	ASD-SiPM4S	4 x 4	30% @ 480 nm	$5.5\ 10^7$ - $9.5\ 10^7$	$4.8\ 10^6$
HAMAMATSU	S10985-50C	6 x 6	50% @ 440 nm (includes afterpulses & crosstalk)	$6.10^6 - 10.10^6$	$7.5\ 10^5$
KETEK	PM3350	3 x 3	40% @ 420 nm	4.10^6	$2\ 10^6$
STMicrolectronics	SPM35AN	3,5 x 3,5	16% @ 420 nm	$7.5\ 10^6$	$3.2\ 10^6$

** datasheet data*

Ongoing R&D to increase the active area at KETEK, AdvanSiD, Excelitas (6 x 6 mm^2)

Other solution to get larger area : connection of several channels of a matrix

Physics & Technology
Key features

- Custom vs CMOS technologies → close up of a cell
- Quenching and Reset modes
- Analog vs Digital SiPM

Arranging SPAD into packed matrices

Transition single SPAD to packed GM-APD matrices (SiPMs) is not just design

Need addressing new issues:

• a third factor enters in the photo-detection efficiency (PDE): the **fill factor** that for small cell size can be quite low

• how to control the **dark rate** because
- limited space for gettering techniques
- high probability to include noisy cells in a device

• optical **cross-talk** among cells

• **yield** and **uniformity** in performances

• **electronics** (integrated, hybrid, external)

Silicon technology – few examples

Custom technology

SiPM “RGB” FBK – external electronics

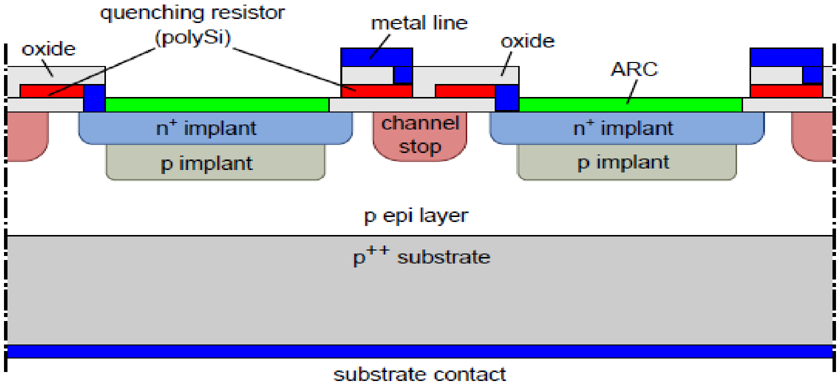

N.Serra et al JINST 8 (2013) P03019

CMOS HV technology

intergated electronics

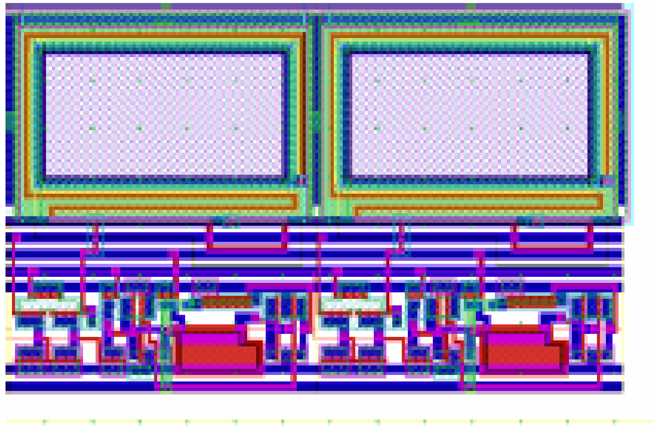

Stapels et al Procs. SPIE 7720 2009

Custom CMOS technology

SPAD array - hybrid electronics

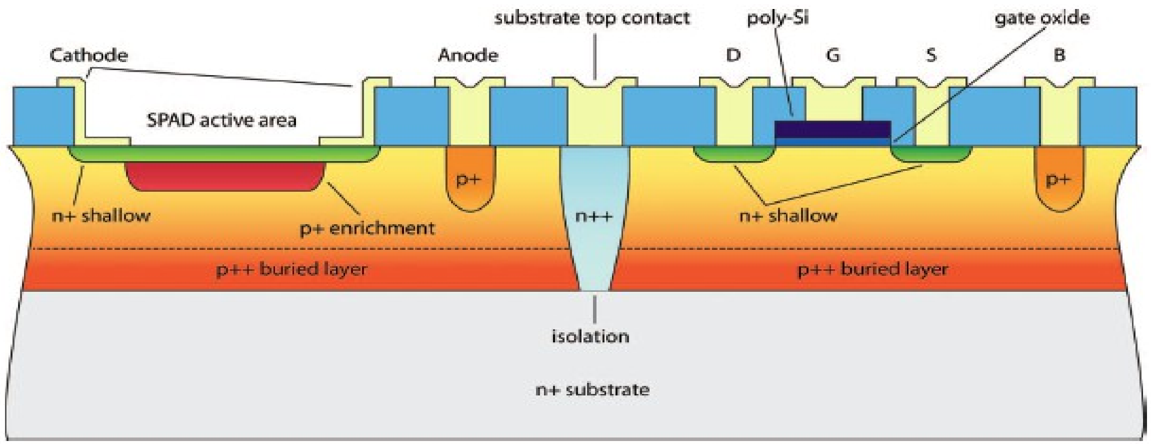

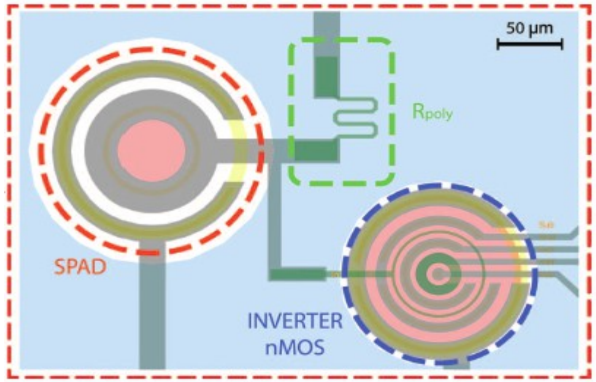

Cammi et al Rev Sci Instr 83 (2012) 033104

Close up of a cell – custom process

Shallow-Junction APD

Example of implementation

C.Piemonte NIM A 568 (2006) 224

Optical window → Anti-Reflective Coating (ARC)
note: light absorption in Si, SiO_2

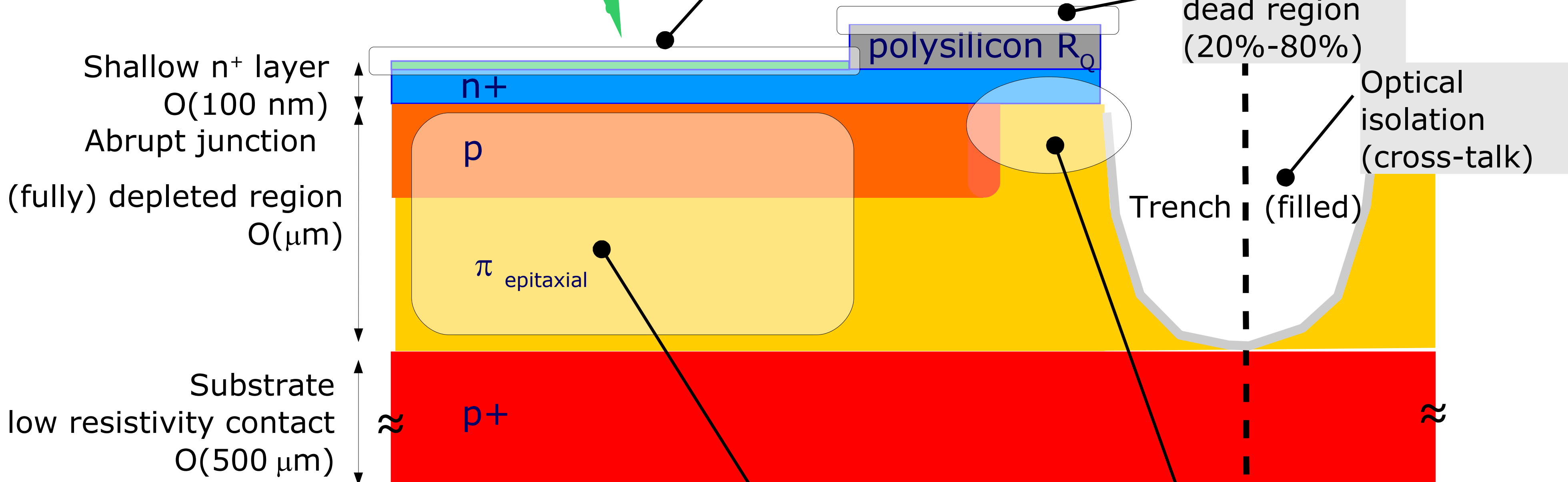

Active volume

- no micro-plasma's high quality epitaxial
- doping / E field profile engineering

Critical region:

- Leakage current
- Surface charges
- Guard Ring for
  - preventing early edge-breakdown
  - isolating cells
  - tuning E field shape

→impact on Fill Factor

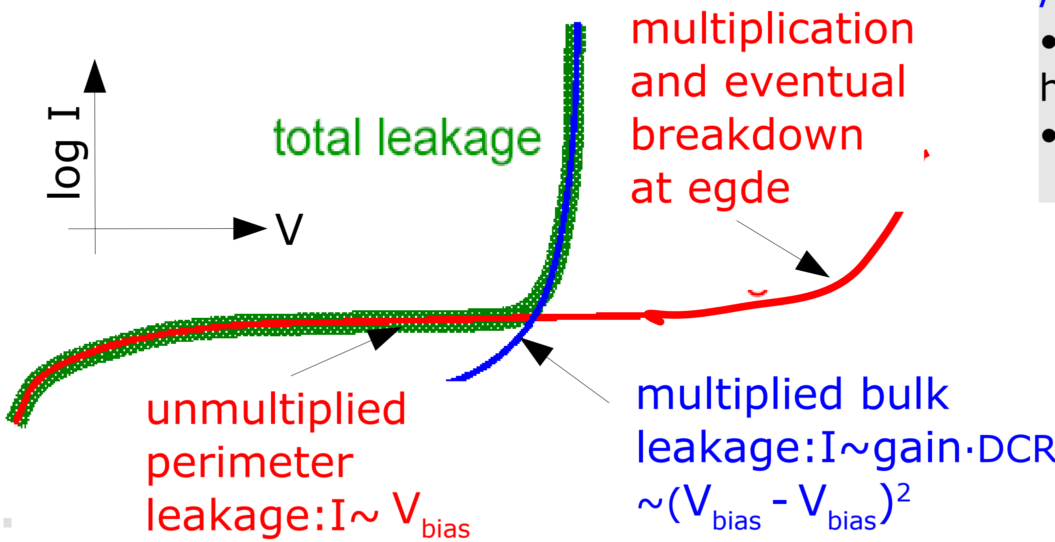

Close up of a cell - CMOS

Key elements for CMOS SiPMs
- **APD cell isolation** from CMOS circuitry
- **guard ring**

APD integration into CMOS

Example of implementation *T.Frach in US patent 2010/0127314*

Note
- extended CMOS processes exploited
- careful design of cell isolation and guard ring

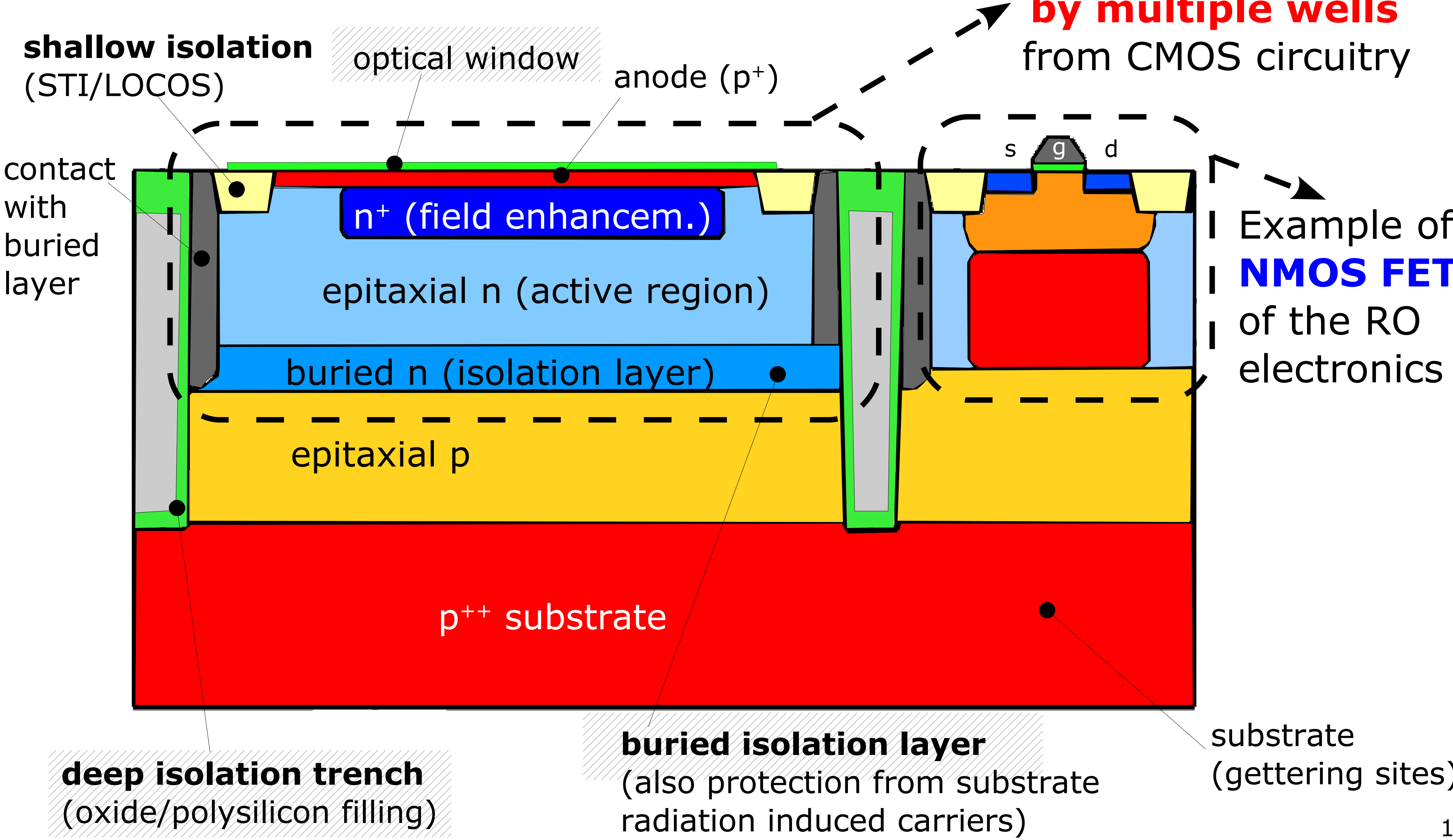

Passive / Active quenching and recharge

Passive Quenching and Reset

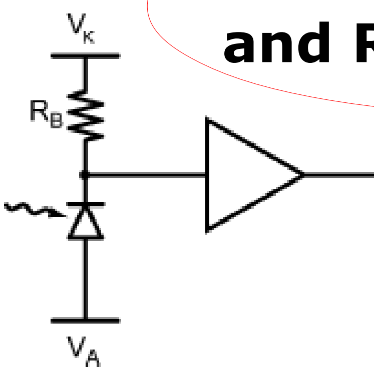

SiPM

Passive Quenching Active Reset

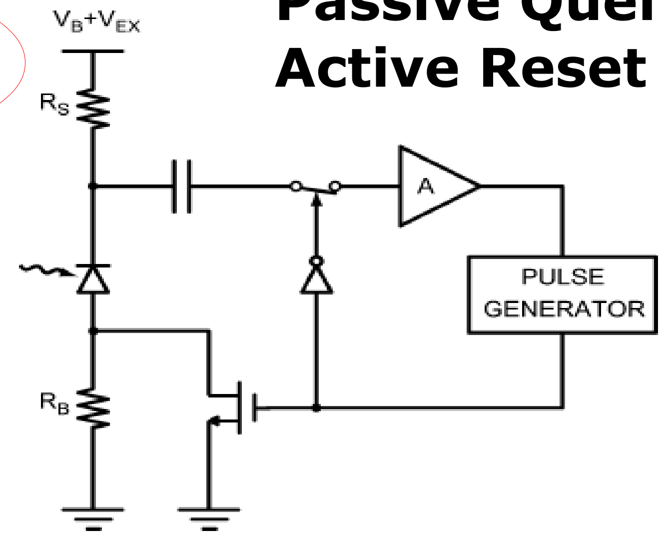

Active Quenching and Reset

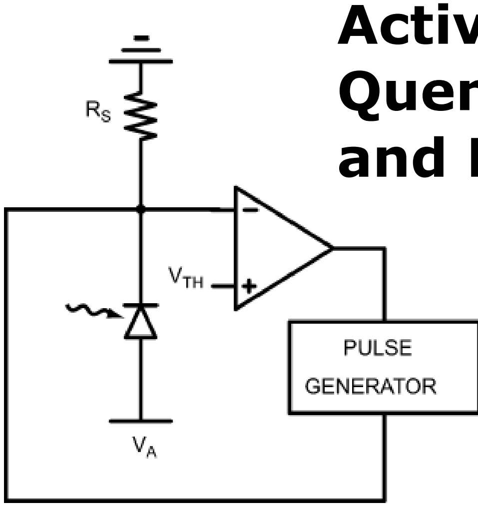

Mixed Active/Passive Quenching Active Reset

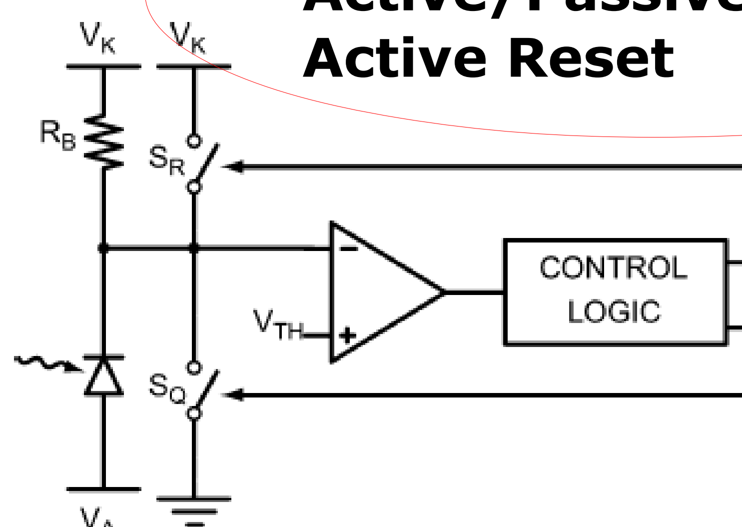

modern SPAD arrays

Gallivanoni et al IEEE TNS 57 (2010) 3815

Passive / Active quenching and recharge

Rq~ few 100kΩ

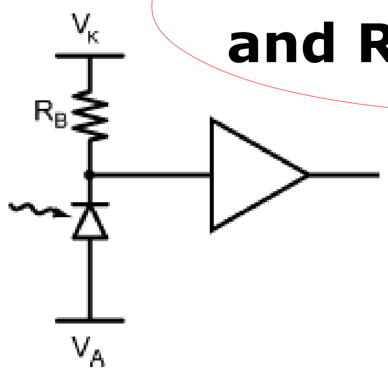

Passive Quenching and Reset

SiPM

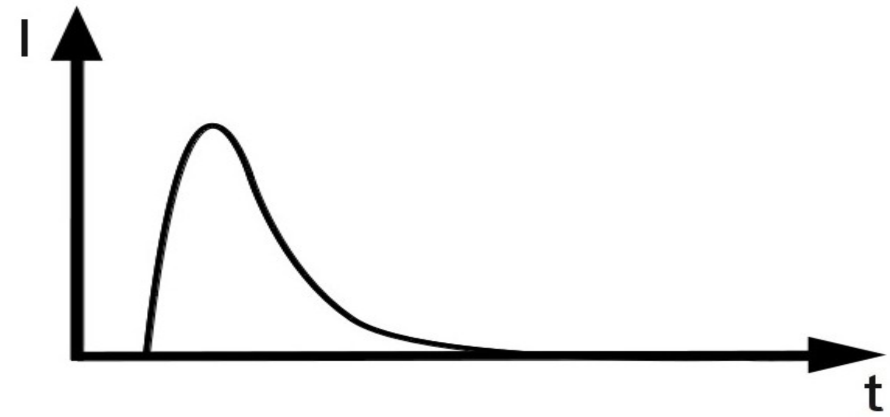

- "Quenching resistor" regulates both **quenching** and **recharge**
- Simple concept but tricky to implement (high-ohmic resistors needed)
- Used in most SiPMs as the summation can be easily implemented
- Limit the recharge current to < 20μA (Rq ~ ΔV/20μA)
- Recovery time: ~ Rq x Cd
- Output is charge pulse: Gain G = Cd x ΔV
- Output signal compatible with that of PMTs → re-use of readout infrastructure

Passive / Active quenching and recharge

- Sense the voltage at the diode terminal
- Use transistors to actively **discharge/recharge** the diode
  → controlled amount of charge → reduced after-pulsing and cross-talk
- Flexibility: programmable timing possible, disabling of faulty cells
- But: requires SPAD/CMOS or 3D integration (cost)
- In case of SPAD/CMOS integration, electronics area affects fill factor
- Fast digital signals (gate delays of ~30ps, rise/fall times ~90ps), low parasitics

Separation of **photon number**, **time of arrival**
and **position** information
right **at the detection element**
might potentially enable
new detector concepts

Mixed
Active/Passive Quenching
Active Reset

already "digital" signal

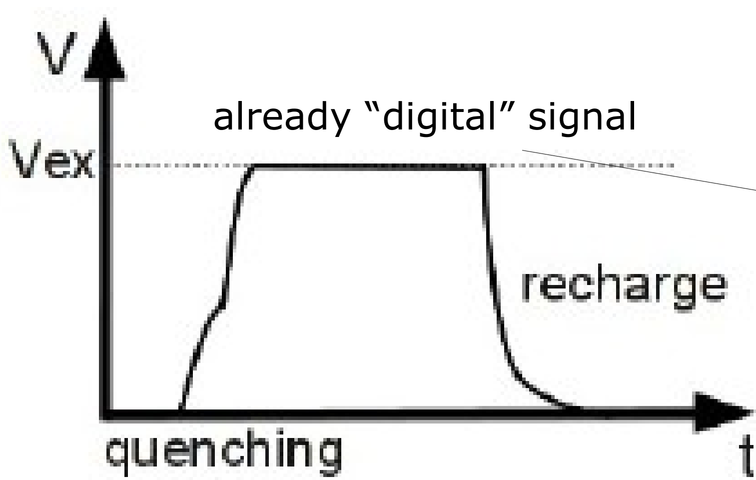

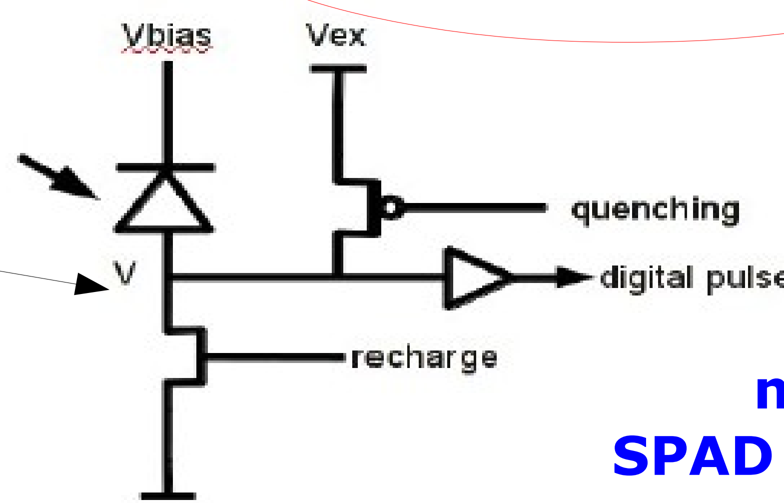

modern
SPAD arrays

Mixed mode Quenching and Recharge

Digital-SiPM cell & its electronics

- Cell area ~ 30x50μm^2
- Fill Factor ~ 50%

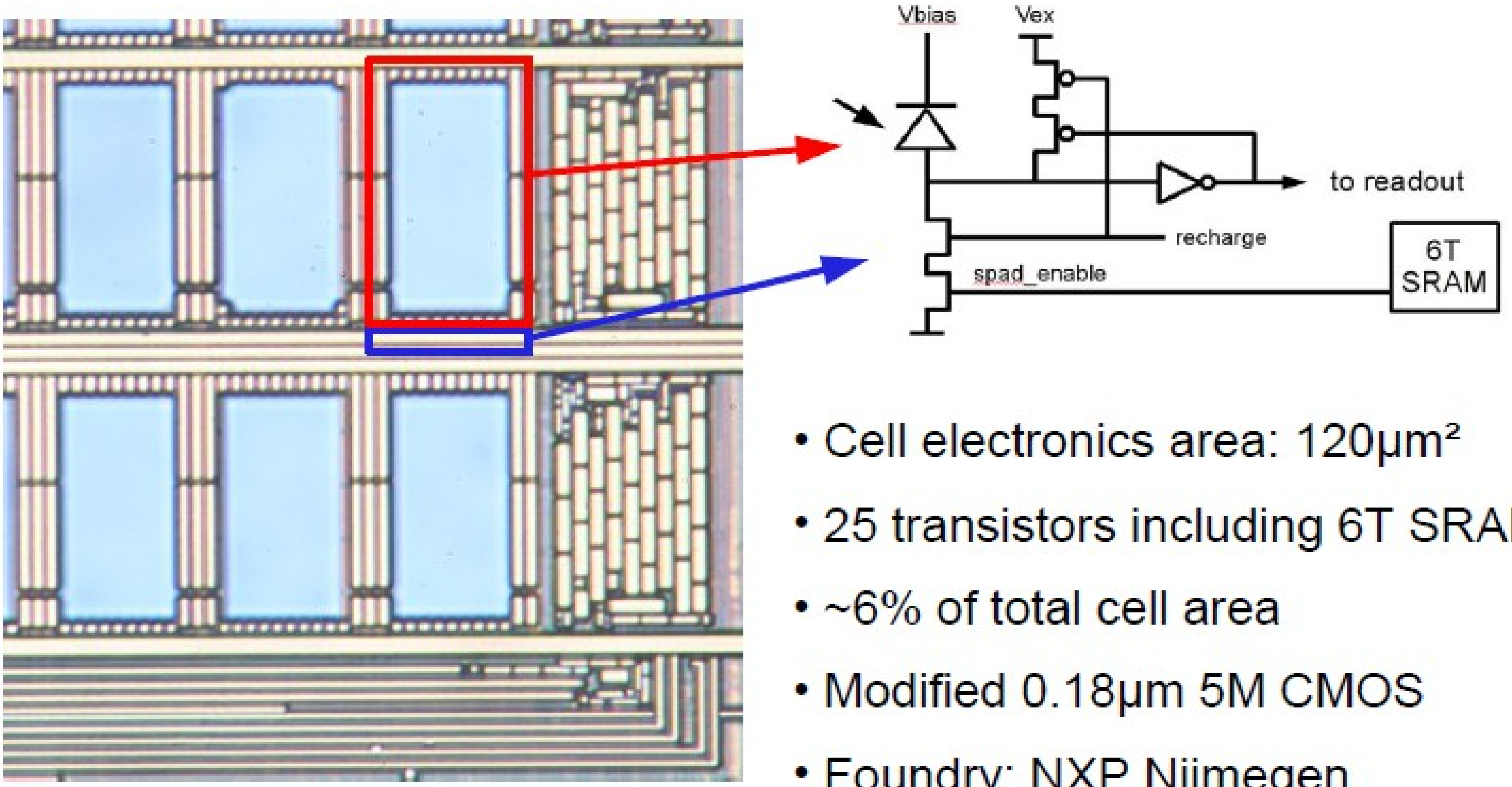

- Cell electronics area: 120µm²
- 25 transistors including 6T SRAM
- ~6% of total cell area
- Modified 0.18µm 5M CMOS
- Foundry: NXP Nijmegen

T.Frach at LIGHT 2011

Analog vs Digital SiPM

Analog SiPM

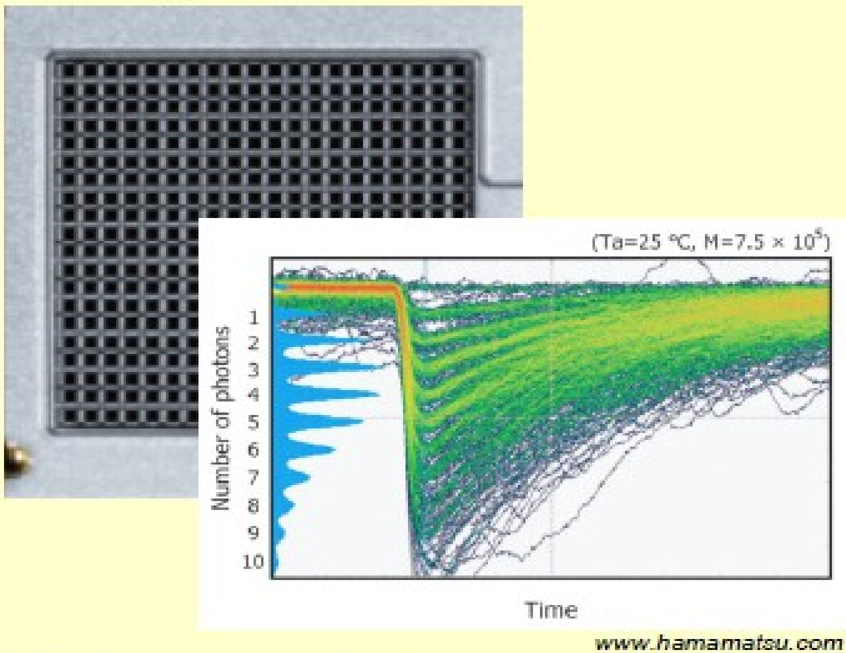

- Cells connected to common readout
- Analog sum of charge pulses
- Analog output signal

Digital SiPM Philips

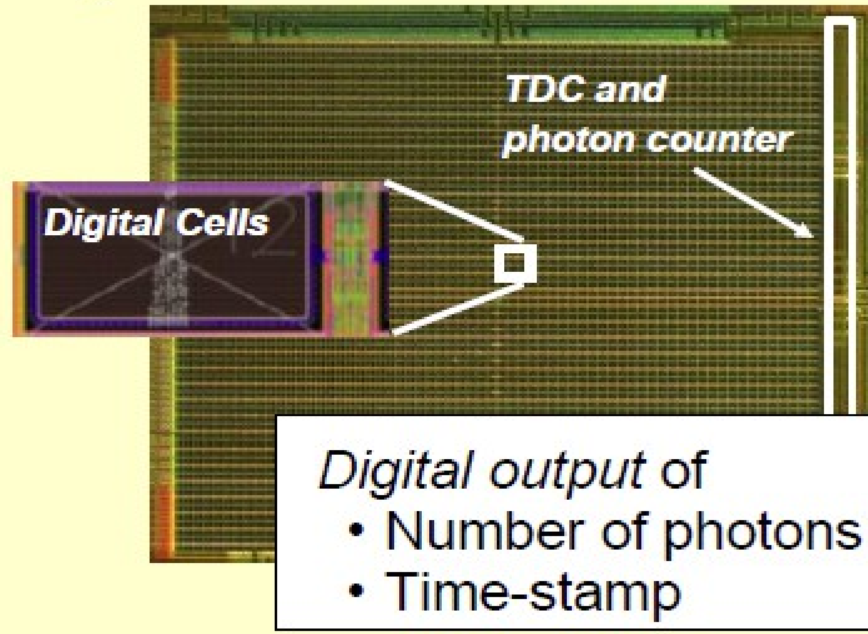

- Each diode is a digital switch
- Digital sum of detected photons
- Digital data output

T.Frach at Heraeus Seminar 2013

Analog vs Digital SiPM

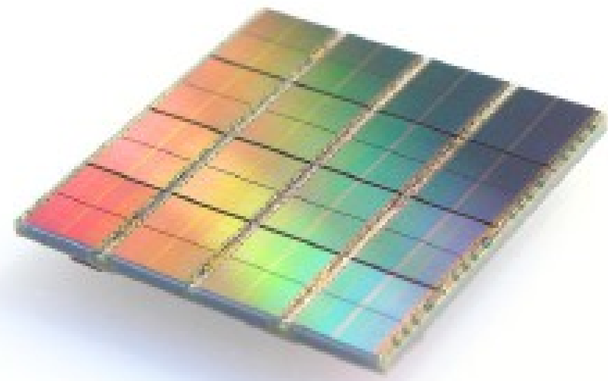

Analog Silicon Photomultiplier

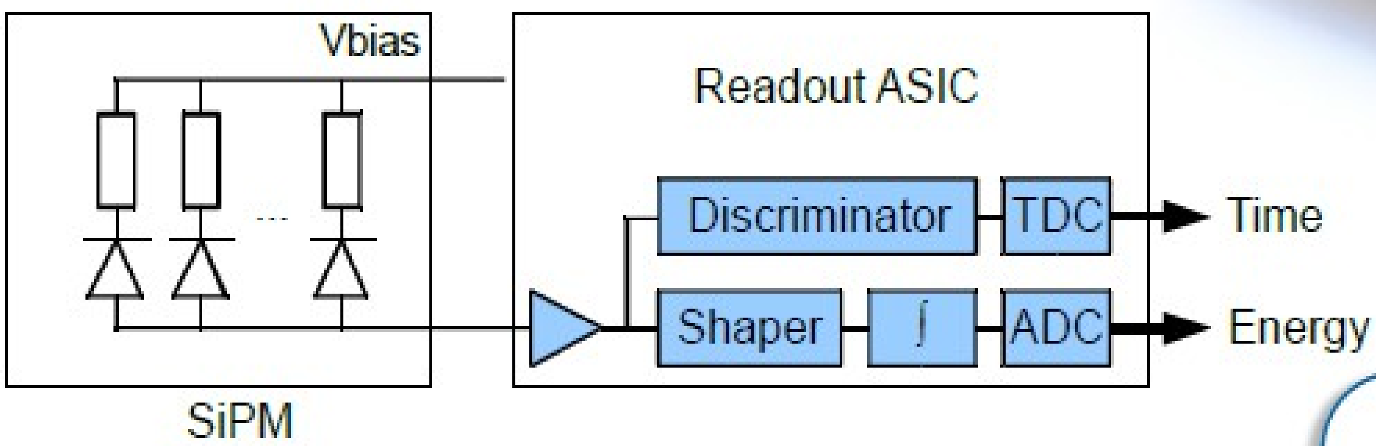

Digital Silicon Photomultiplier

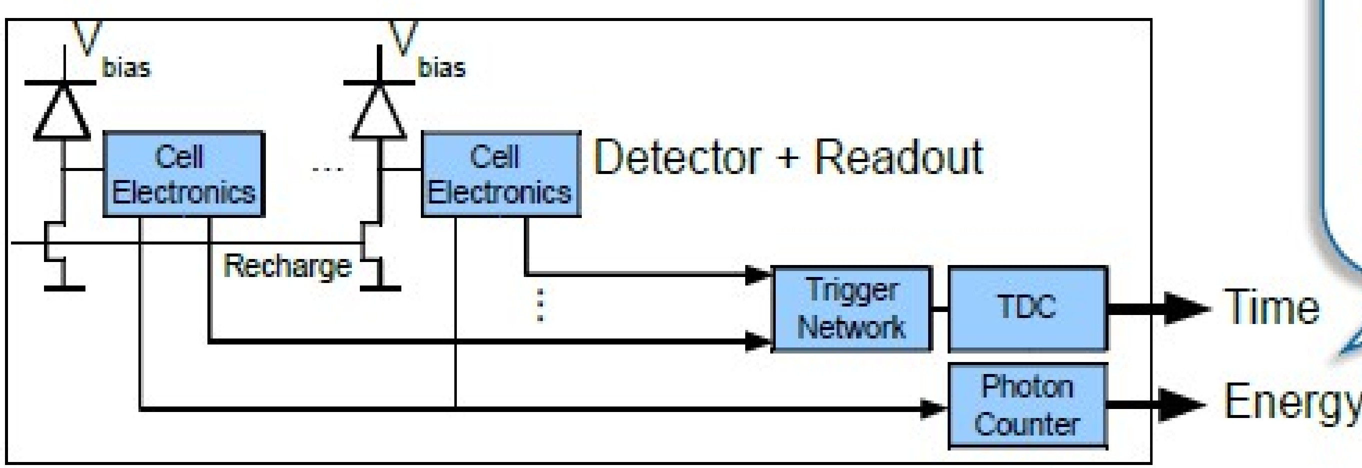

dSiPM provides a digital timestamp and the photon count for each light pulse, without the need of any analog front-end electronics

!!! control over individual SPADs

Main parameters

Gain, Pulse shape,
Dynamic Range, Linearity

related to the recharge of the diode capacitance from V_{bd} to V_{bias} during the avalanche quenching time after I_{latch} is reached

Primary noise:
→ thermally generated

pulses triggered by non-photo-generated carriers (thermal / tunneling generation in the bulk or in the surface depleted region around the junction)

Correlated noise:
→ afterpulses, cross-talk

carriers can be trapped during an avalanche and then released triggering another avalanche

photo-generation during the avalanche discharge. Some of the photons can be absorbed in the adjacent cell possibly triggering new discharges

Photo-detection efficiency

$PDE = QE * P_{01} * \varepsilon$

QE = quantum efficiency
P_{01} = avalanche triggering prob.
ε = geometrical fill factor

Time resolution

Related to the photo-generation and to the avalanche propagation

Pulse shape, Gain and Response

(mainly for passive mode)

- Detailed electrical model
- Gain and its fluctuations
- Response non-linearity

Actual pulse shape and Gain

Waveform (Dark noise)

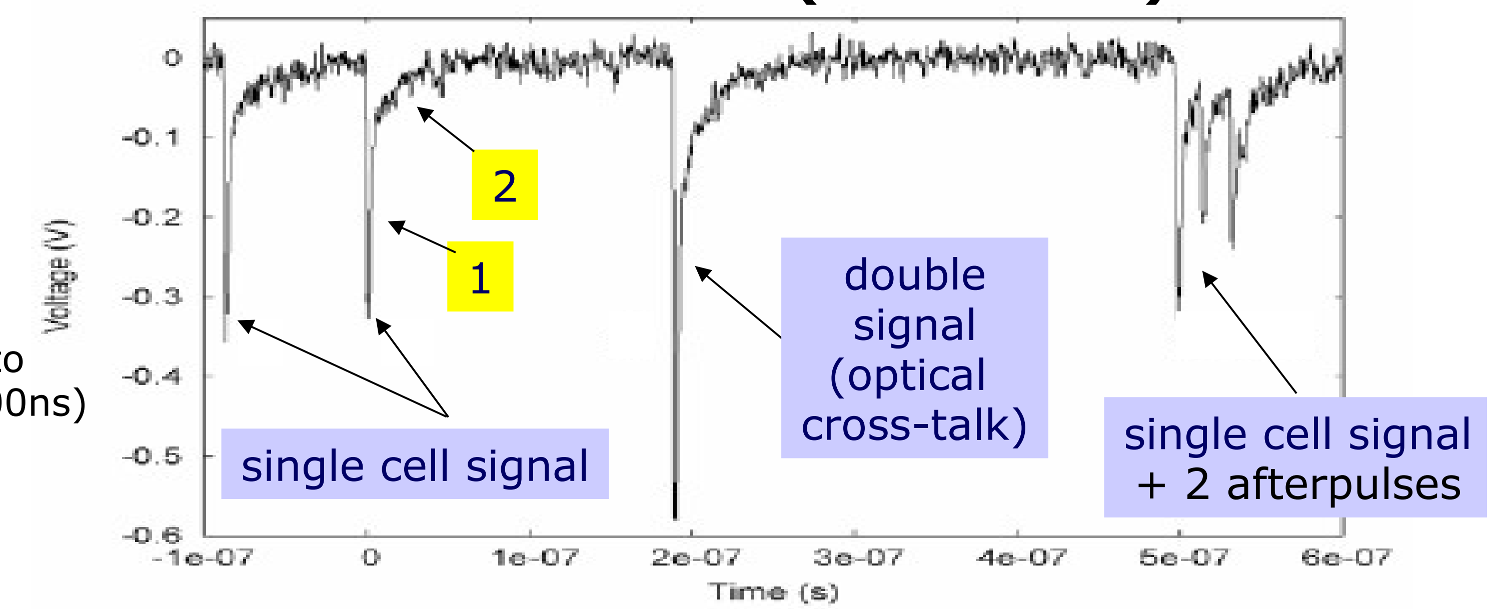

Pulse shape

1. fast component (parasitic transient)

2. slow component due to (99% recovery time ~100ns)

Charge spectrum

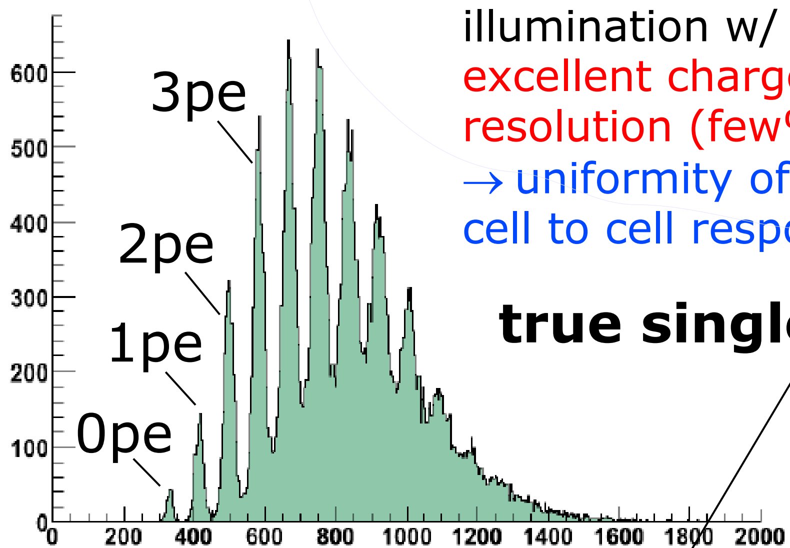

illumination w/ LED
excellent charge resolution (few%)
→ uniformity of cell to cell response

true single ph.e

NOTE: gain easily measured

Gain

linear up to ΔV~5V
→ proper quenching

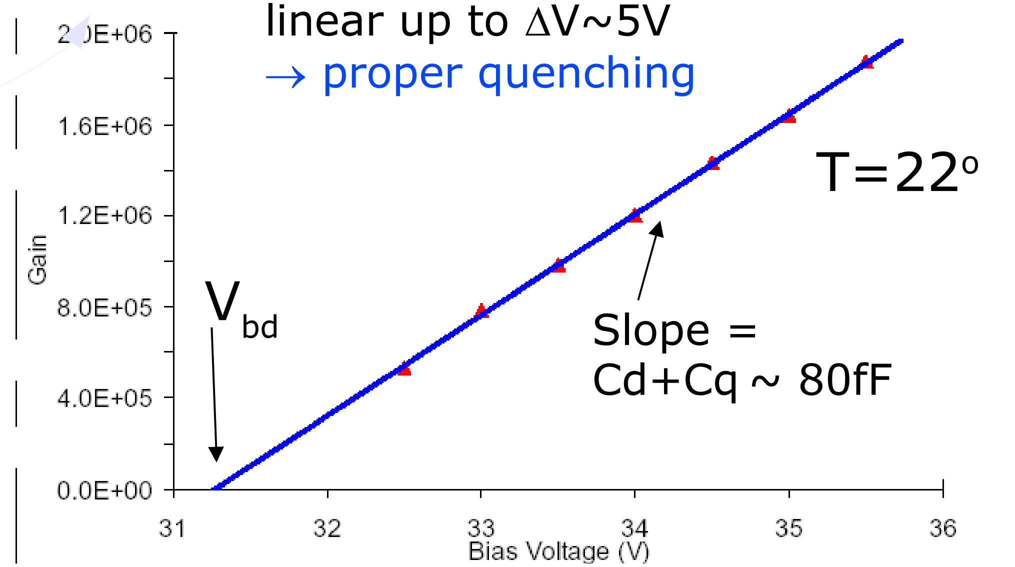

Gain and its fluctuations

$$G = \Delta V (C_q + C_d) / q_e$$

→ Gain is linear if ΔV in quenching regime

but

there are various sources of response non-linearity (ie non-proportionality to number of photons → next slides)

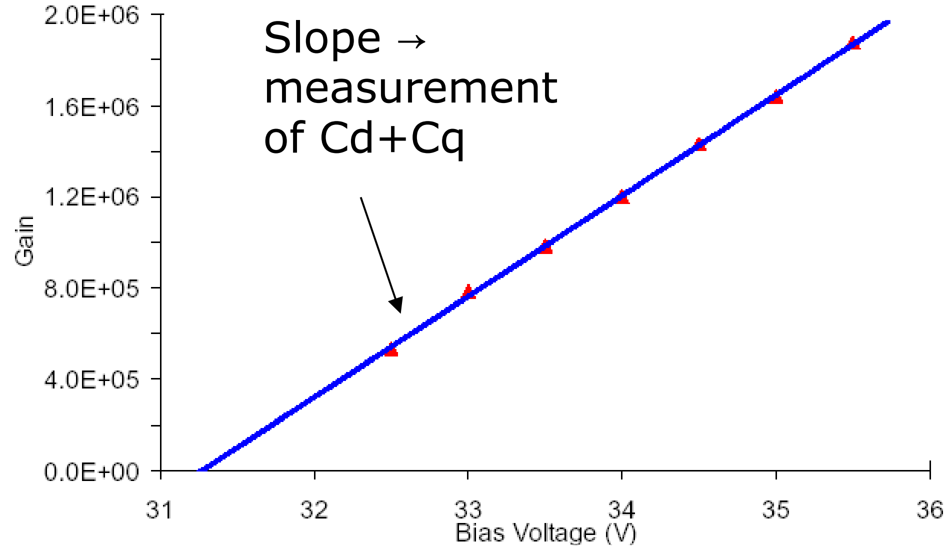

SiPM gain fluctuations (intrinsic) differ in nature compared to APD where the statistical process of internal amplification shows a characteristic fluctuations

$$\frac{\delta G}{G} = \frac{\delta V_{bd}}{V_{bd}} \oplus \frac{\delta C_{dq}}{C_{dq}}$$

cell to cell uniformity (active area and volume) control at % level

- doping densities (Poisson): $\delta V_{bd} \geq 0.3V$ *Shockley, Sol. State Ele. 2 (1961) 35*
- doping, epitaxial, oxide (processing): $\delta V_{bd} \sim O(0.1V)$

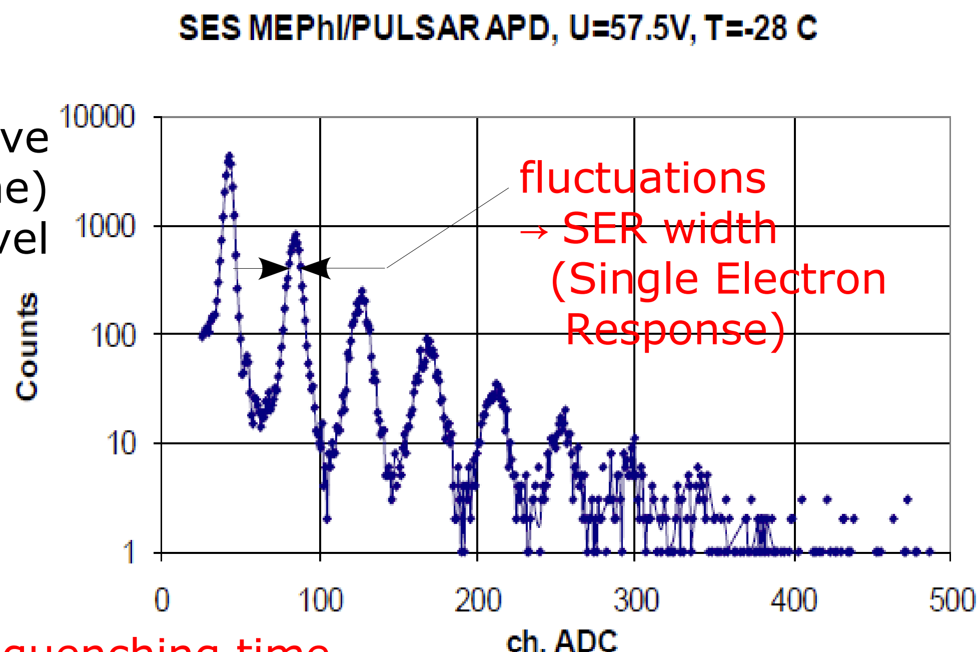

In addition δG might be due to fluctuations in quenching time
… and of course after-pulses contribute too (not intrinsic → might be corrected)

Improved V_{bd} uniformity

Engineering high electric field & depletion/drift layer profiles

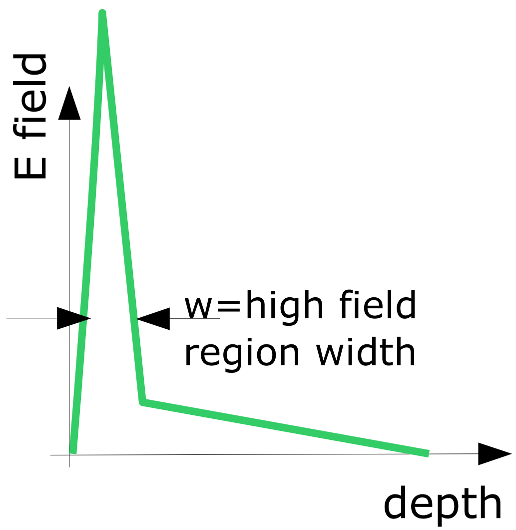

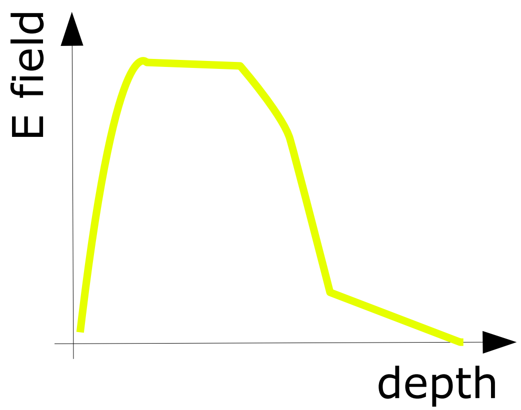

→ Improved break-down voltage uniformity

- wafer level
- among wafers

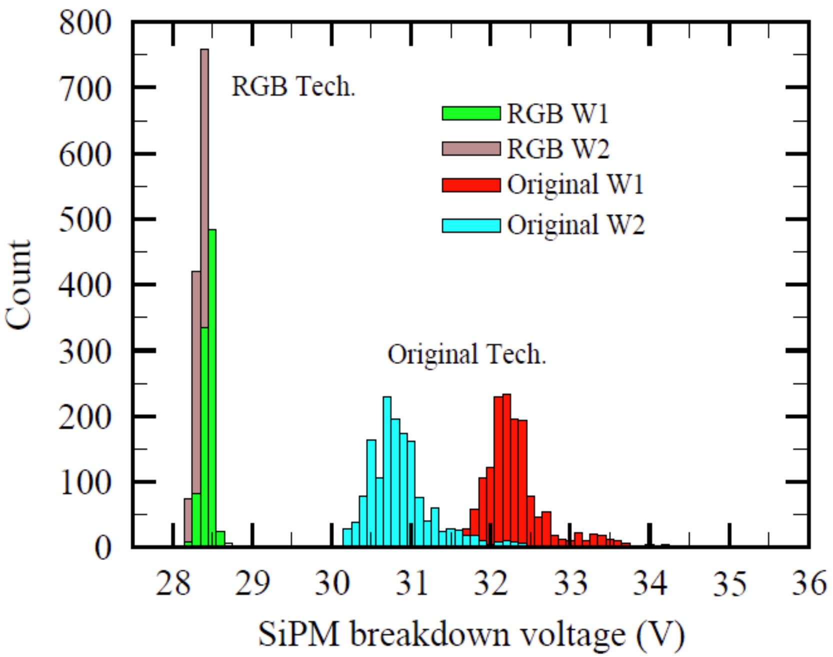

Recent progresses in FBK-Advansid devices

N.Serra: "Characterization of new FBK SiPM technology for visible light detection", JINST 2013 JINST 8 P03019

Response Non-Linearity

Non-proportionality of charge output w.r.t. number of photons (i.e. response) at level of several % might show up even in quenching regime (negligible quenching time), depending on ΔV and on the intensity and duration of the light pulse.

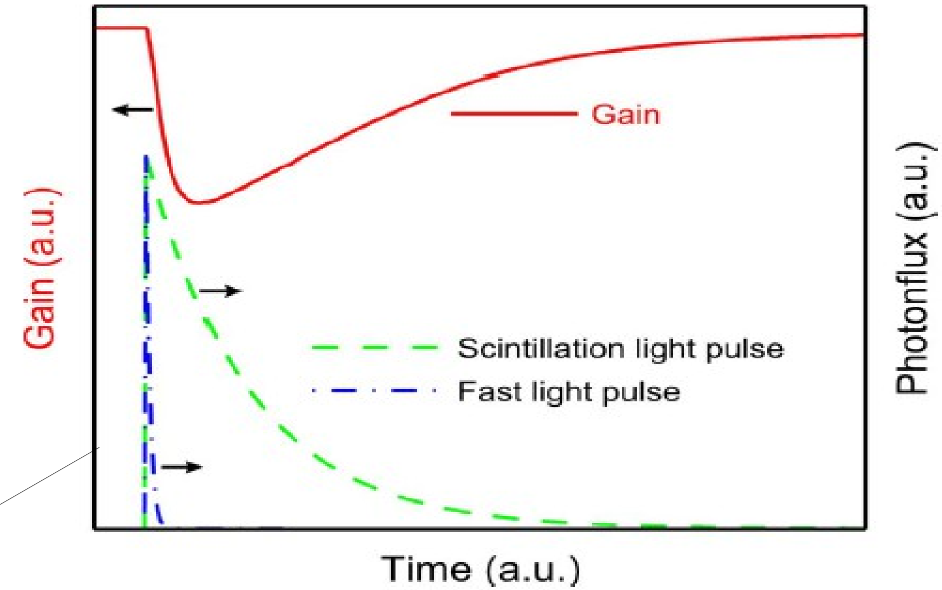

Main sources are:

- finite number of pixels
- finite recovery time
- after-pulses, cross-talk
- drop of ΔV during the light pulse

due to relevant signal current on (large) series resistances (eg ballast)

T.van Dam IEEE TNS 57 (2010) 2254
Detailed model to estimate non-lin. corrections

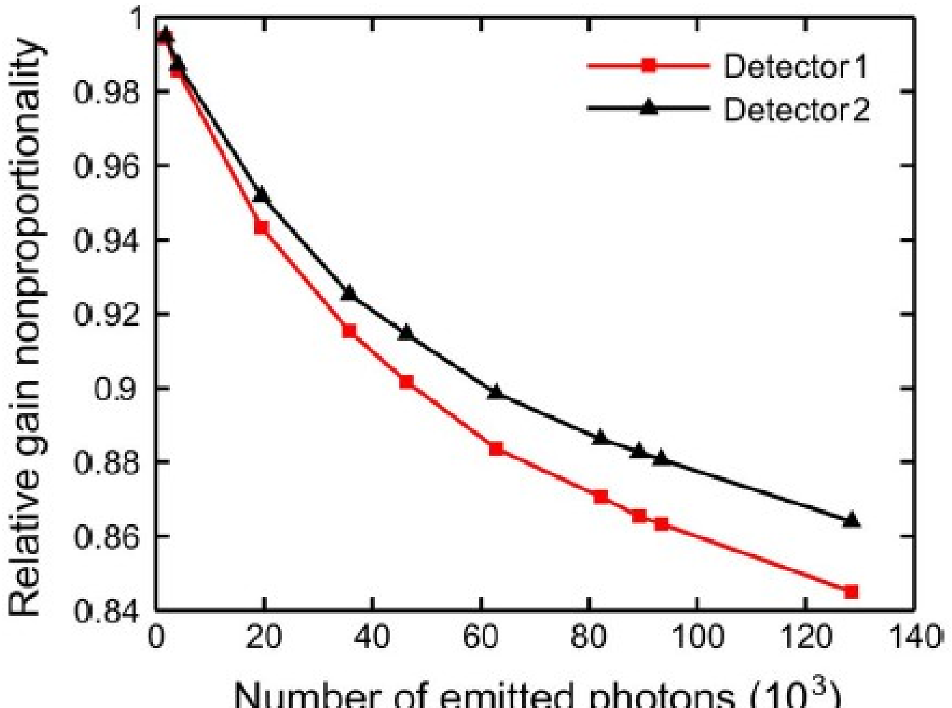

Finite number of cells is main contribution in case number of photons ~ O(number of cells) (dynamic range not adequate to application)

→ saturation $n_{fired} = n_{all}\left(1 - e^{-\frac{n_{phot.}PDE}{n_{all}}}\right)$

→ loss of energy resolution

see Stoykov et al JINST 2 P06500 and Vinogradov et al IEEE NSS 2009 N28-3

Dynamic range and non-linearity

analog SiPM output =
sum of binary cell's output

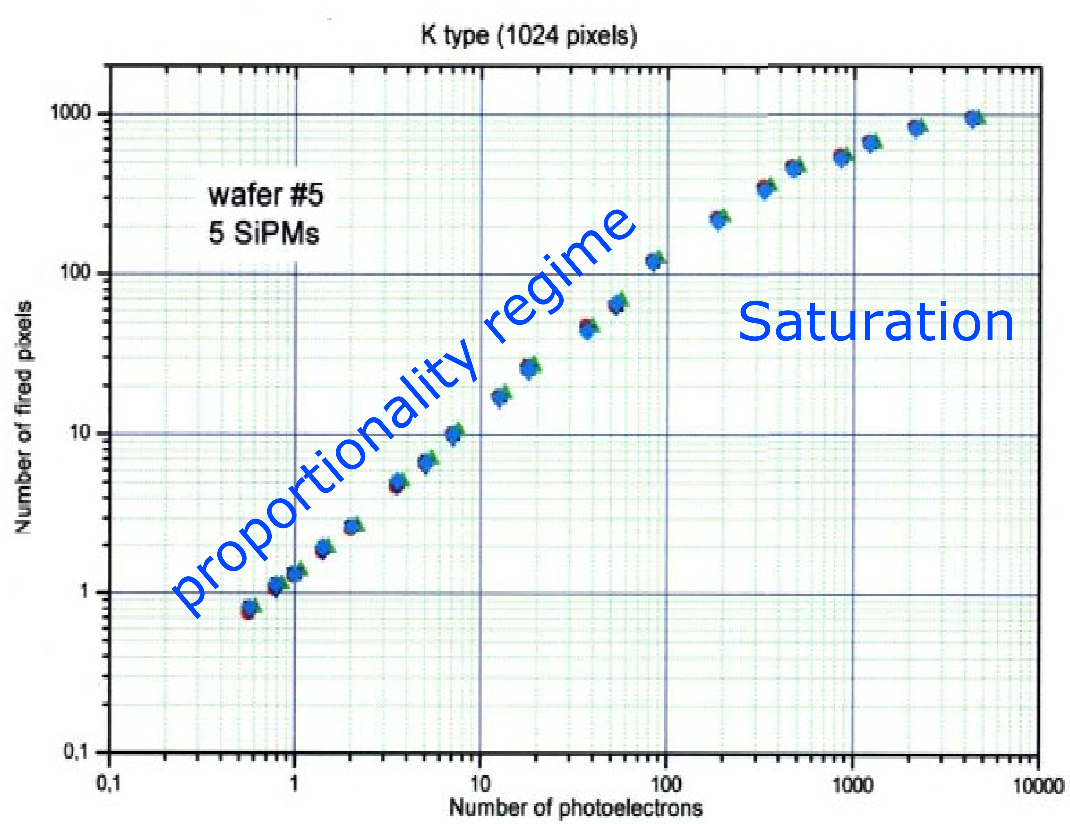

- Due to **finite number of cells** → signal **saturation**

- Correction possible BUT
→ **degraded resolution**

$$A \approx N_{firedcells} = N_{total} \cdot (1 - e^{-\frac{N_{photon} \cdot PDE}{N_{total}}})$$

eg: 20% deviation from linearity
if 50% of cells respond

➡ Best working conditions: $N_{photo\text{-}electrons} < N_{SiPM\ cells}$

Additional complications:
1) need correction to $N_{fired\text{-}cells}$ due to cross-talk and after-pulse
2) effective dynamic range depends on recovery time and time scale of signal burst

Tinier cell → better whole performance

Latest MPPC tiny cell by Hamamatsu

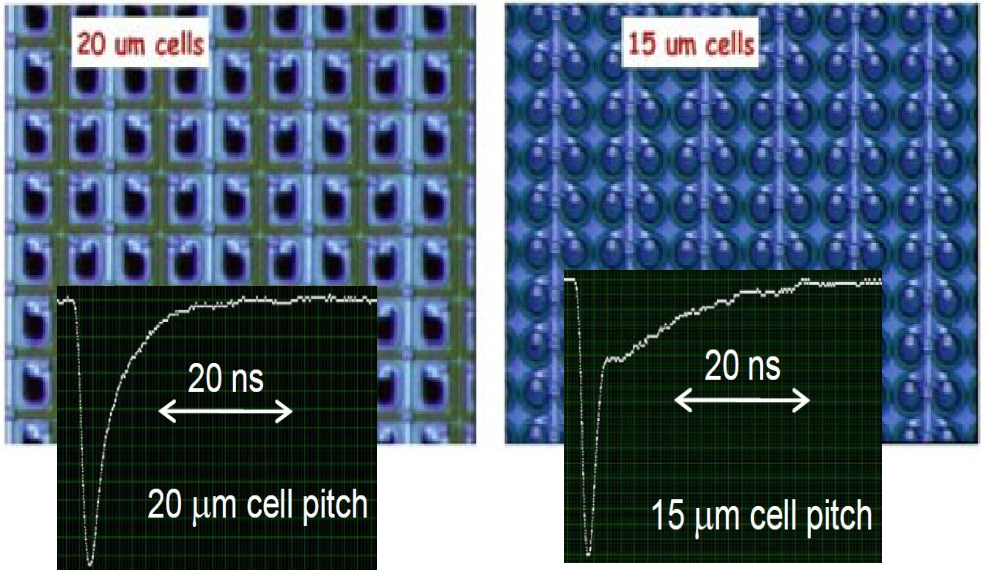

Different types available or in preparation:

- tiny cells (→ 15µm)
  → HPK, FBK-Advansid(*), NDL, MPI-LL

  (*) fill factor → 50% !!!
- micro cells (→ µm)
  → Zecotek, AmplititionTechn.

SiPMs NDL (Bejiing)

Zhang et al NIM A621 (2010) 116
Han at NDIP 2011

- type: n-on-p, Bulk Rq
- high cell density (10000/mm²)
- fast recovery (5ns)
- low gain
- **better timing**

→ dynamic range

→ less after-pulsing
→ less cross-talk
→ radiation hardness

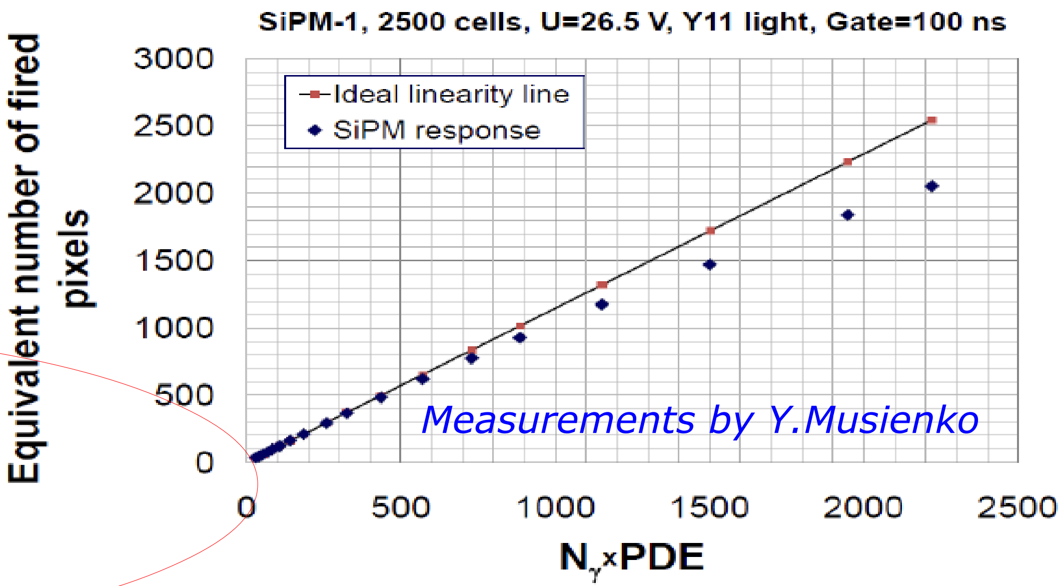

Measurements by Y.Musienko

Noise sources

Primary noise

→ dark counts

pulses triggered by non-photo-generated carriers (thermal / tunneling generation in the bulk or in the surface depleted region around the junction)

Correlated noise:

→ After-pulsing

→ Cross-Talk

"optical"

carriers can be trapped during an avalanche and then released triggering another avalanche

photo-generation during the avalanche discharge. Some of the photons can be absorbed in the adjacent cell possibly triggering new discharges

Dark current vs T   sources of DCR

contribution to DCR
from diffusion of minority
carriers negligible below 350K

Noise mainly comes from the high E Field region (no whole depletion region)

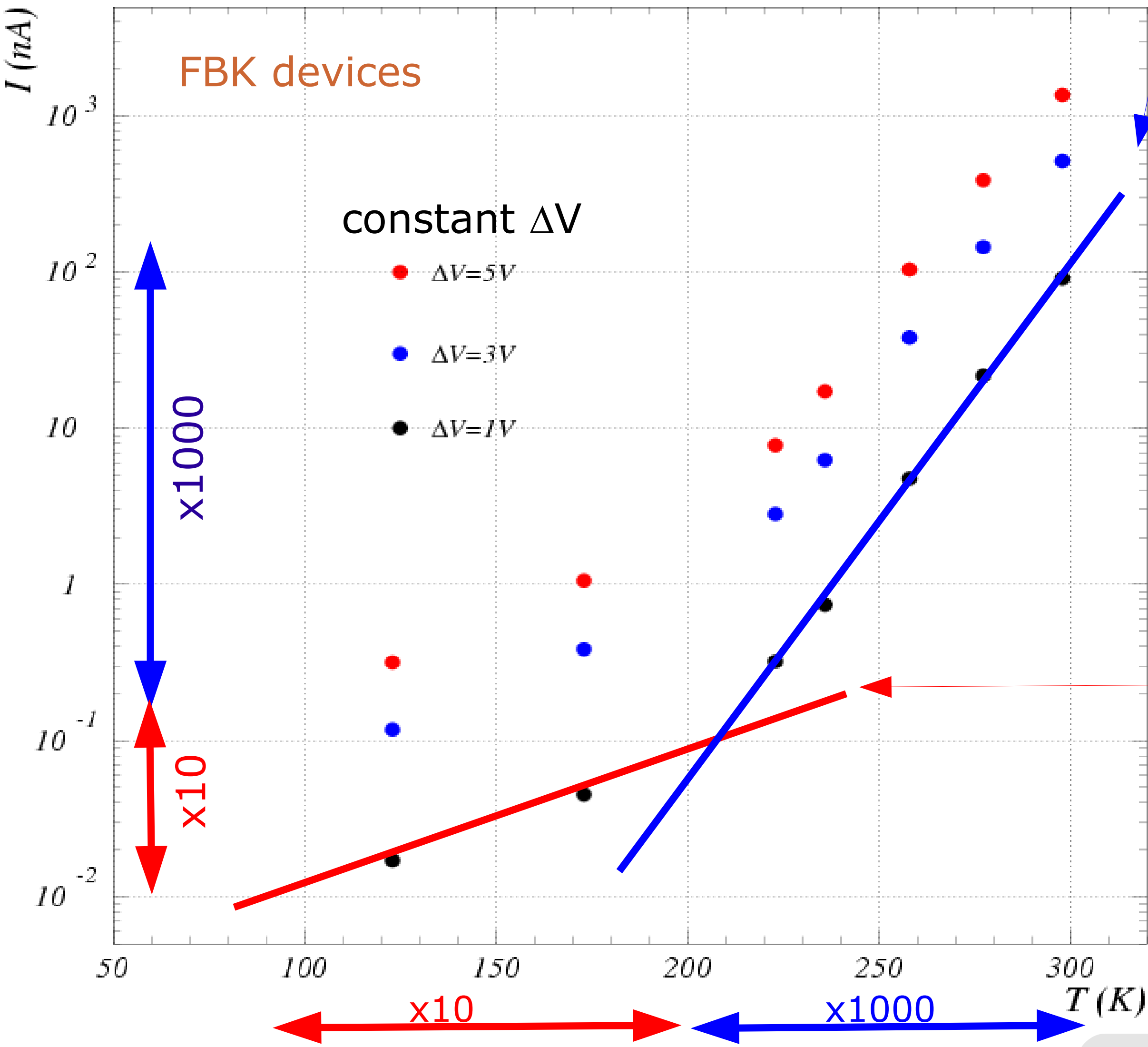

1) Generation/Recombination SRH noise (enhanced by trap assisted tunneling)

$$I_{reverse} \sim T^{1.5} \exp\frac{-E_{act}}{K_B T}$$

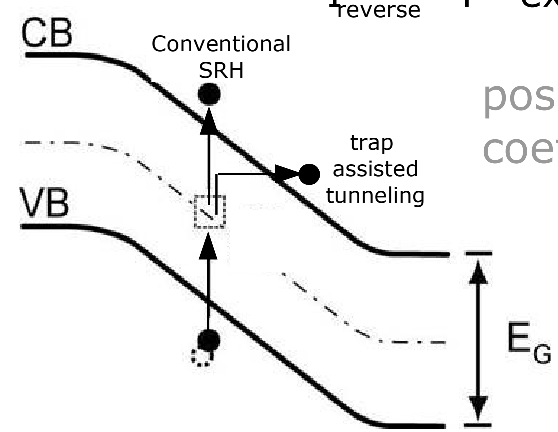

positive T coefficient

2) Band-to-band Tunneling noise (strong dependence on the Electric field profile)

negative T coefficient

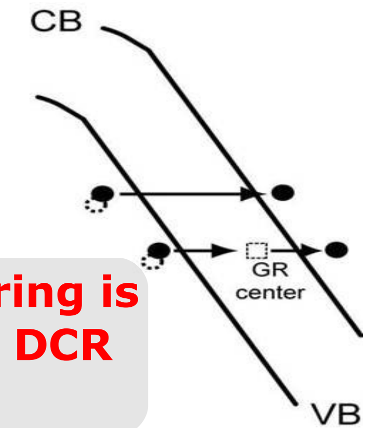

Tunneling noise dominating for T<200K
(sharp high E field region → higher noise)

E field engineering is crucial for min. DCR (esp. at low T)

Dark Count Rate

- DCR → linear dependence due to $P_{01} \propto \Delta V$ (→ same as PDE vs ΔV)
  → non-linear at high ΔV due to cross-talk and after-pulsing → $\propto \Delta V^2$
- DCR scales with active surface (not with volume: high field region)

Engineering high electric field & depletion/drift layer profiles

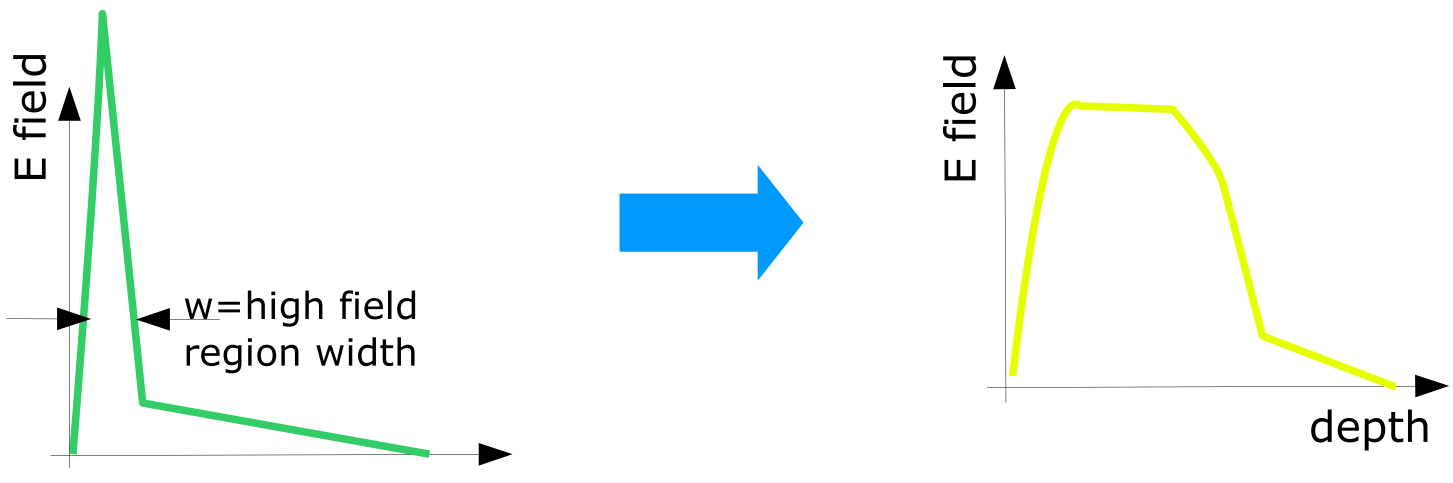

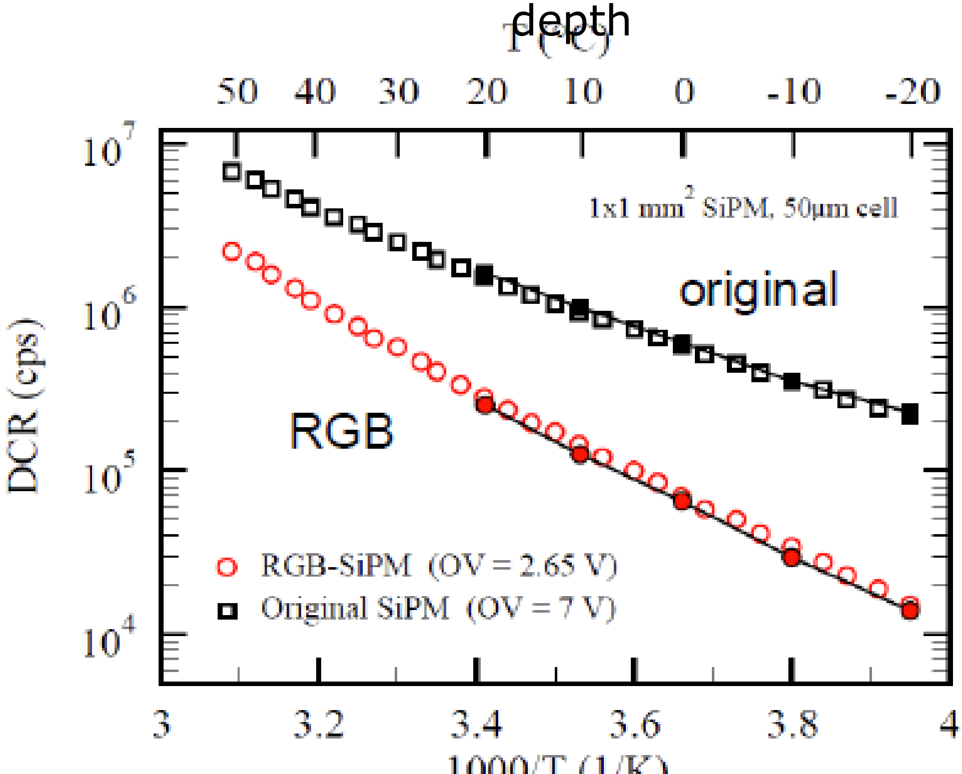

RGB has a much lower noise and a steeper temperature dependence:

→ **less tunneling**

Recent progresses in FBK-Advansid devices

Dark Count Rate

- DCR → linear dependence due to $P_{01} \propto \Delta V$ (→ same as PDE vs ΔV)
  → non-linear at high ΔV due to cross-talk and after-pulsing → $\propto \Delta V^2$
- DCR scales with active surface (not with volume: high field region)

KETEK PM 3350 (p^+-on-n, shallow junction)
3x3mm² active area pixel size 50x50 μm²

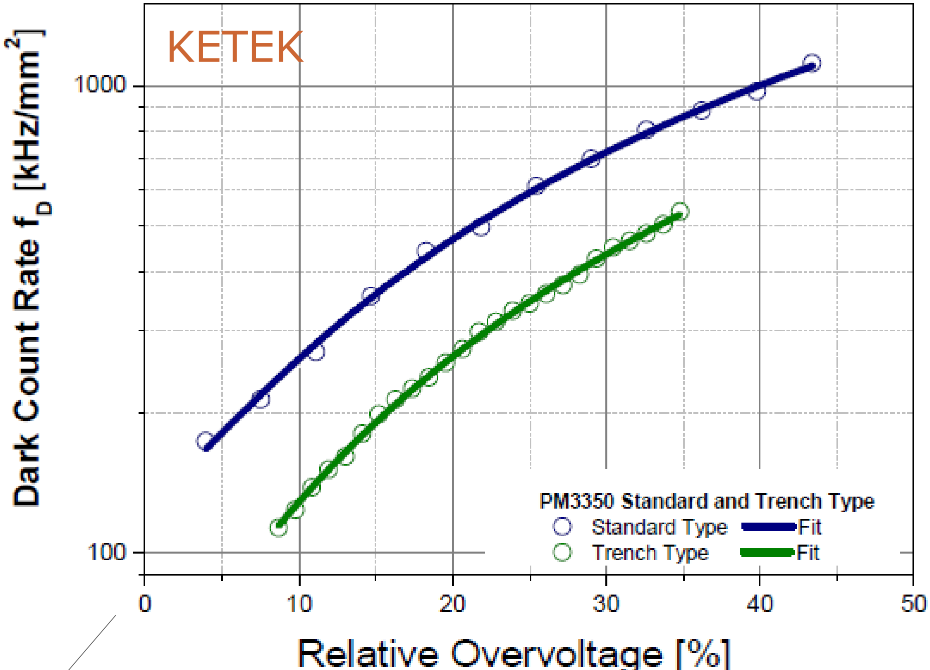

V_{bd} ~ 25V

F.Wiest – AIDA 2012 at DESY

Critical issues:

- quality of epitaxial layer
- gettering techniques
- Electric field → tunneling

Exelitas 1st generation SiPM 2011
(p^+-on-n) 1x1mm²

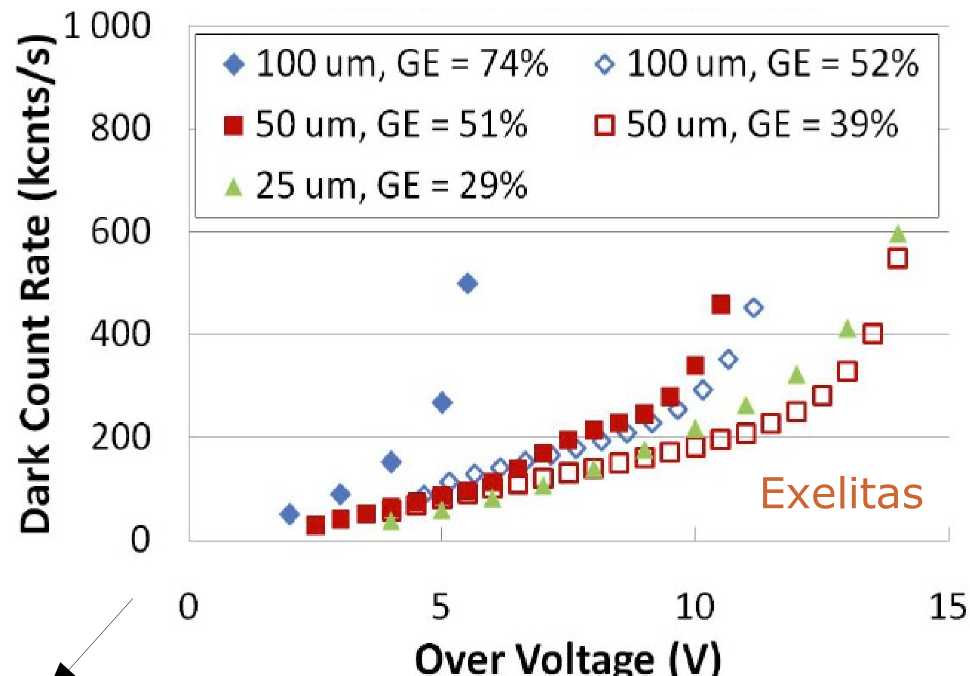

V_{bd} ~ 140V

P.Berard – NDIP 2011

Latest Hamamatsu and FBK devices below ~100kHz/mm²

Dark Count Rate: digital-SiPM (Philips)

Control over individual SPADs enables detailed device characterization

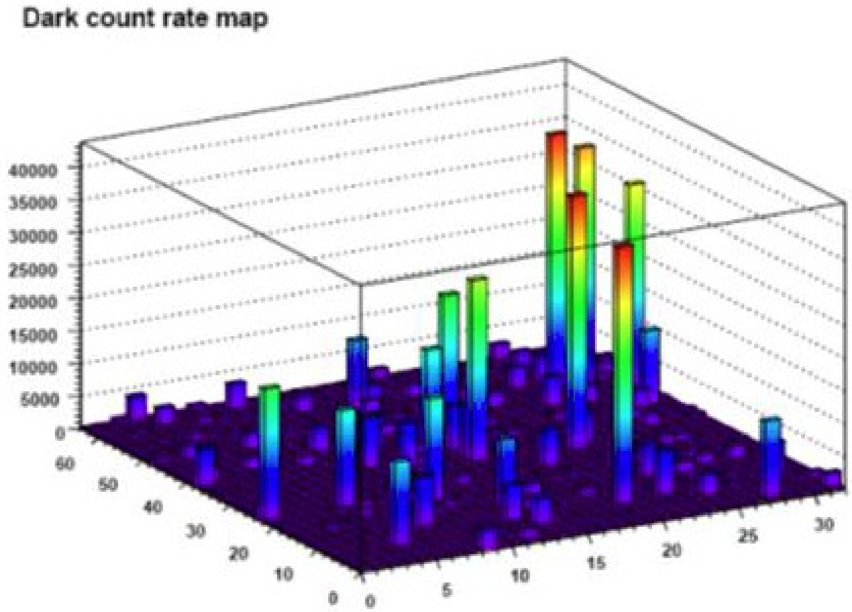

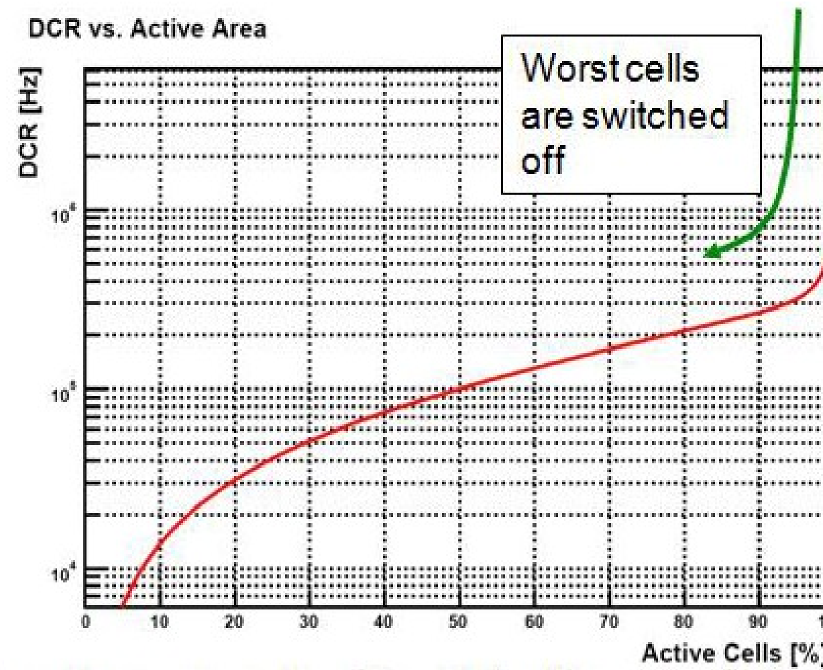

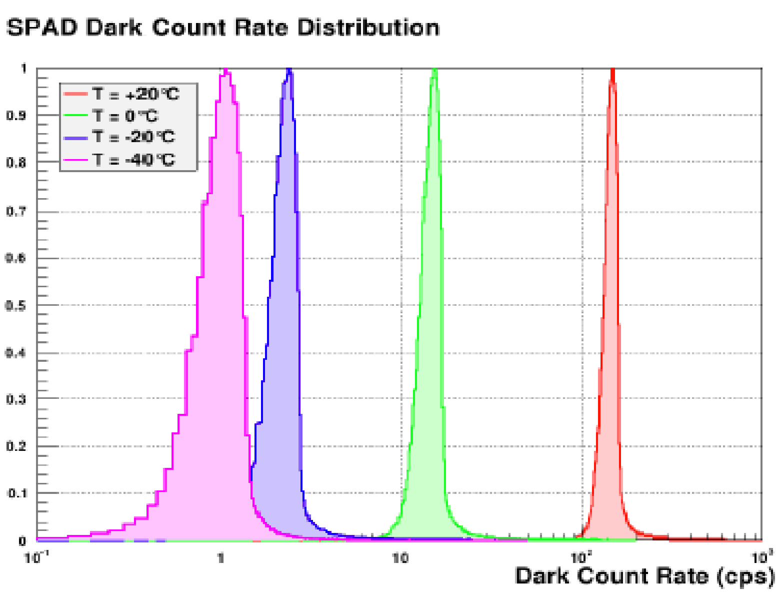

- Over 90% good diodes
  (dark count rate close to average)
- Typical dark count rate (DCR) at 20°C and ΔV=3.3V ~150Hz / diode
- Low DCR ~1-2Hz/diode at -40°C

T.Frach at Heraeus Seminar 2013

After-Pulsing Carrier trapping and delayed release

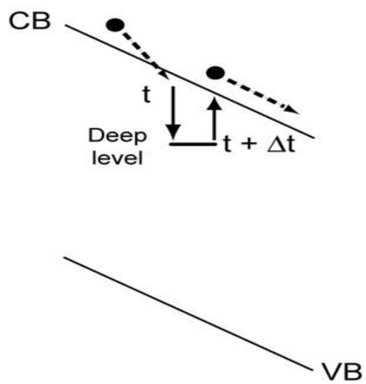

$$P_{afterpulsing}(t) = P_c \cdot \frac{\exp(-t/\tau)}{\tau} \cdot P_{01} \quad \propto \Delta V^2$$

~Few % level
at 300K

avalanche triggering probability
$\propto \Delta V(t)$

τ : trap lifetime
depends on trap level position

quadratic
dependence
on ΔV

P_c : trap capture probability
$\propto$ carrier flux (current) during avalanche $\propto \Delta V$
$\propto$ N traps

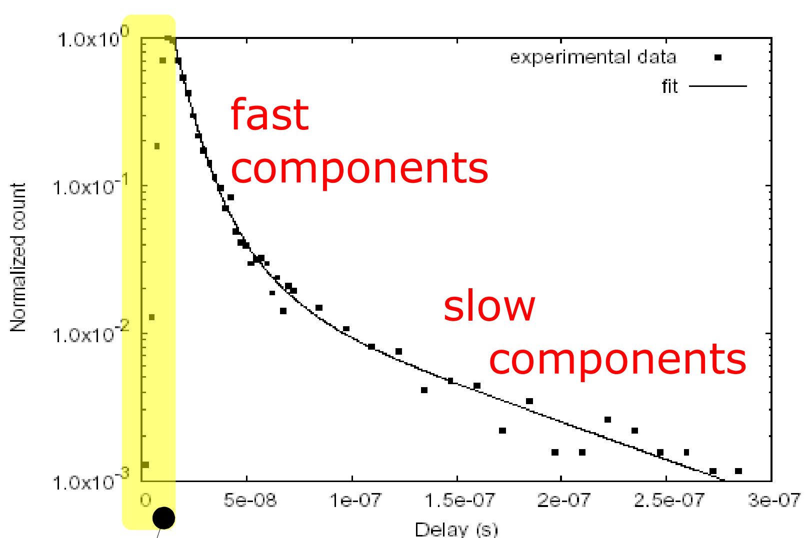

Fig. 10. Spectrum of the delay time from the primary pulse to the after-pulse.

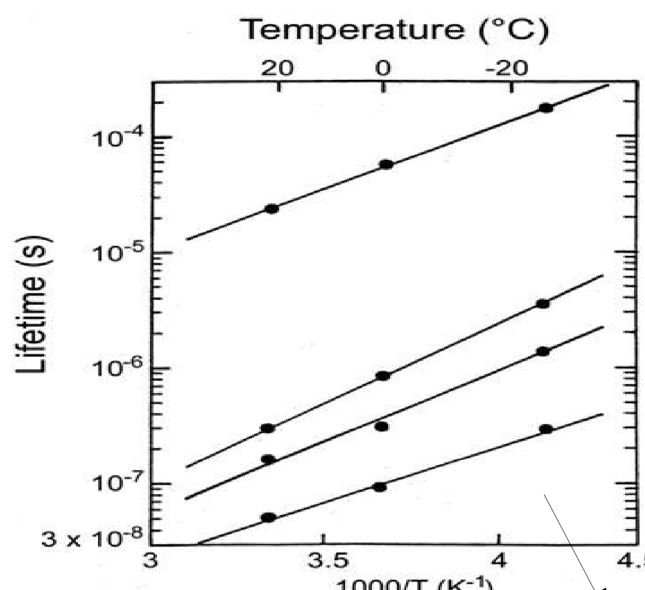

S.Cova, A.Lacaita,
G.Ripamonti, IEEE EDL (1991)

not trivial
dependence on T

Only partially sensitive to after-pulsing during recovery
ie recovery hides After-pulses (does not cancel them)

Optical cross-talk

Avalanche luminescence (NIR)

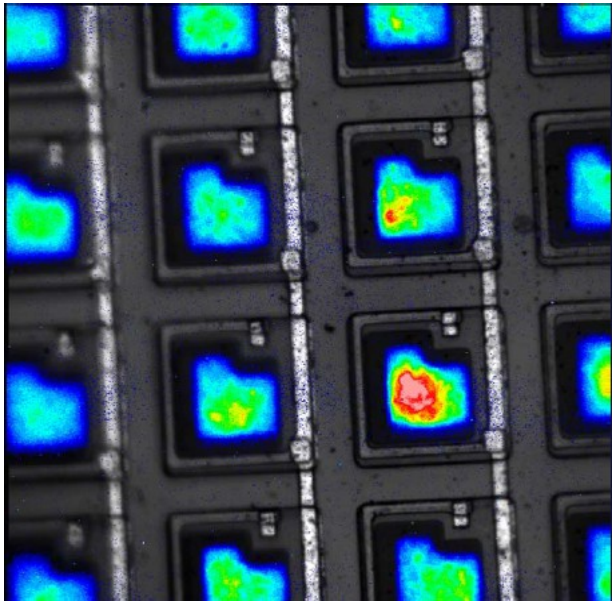

N.Otte, SNIC 2006

Carriers' luminescence (spontaneous direct relaxation in the conduction band) during the avalanche: probability 3.10^{-5} per carrier to emit photons with E> 1.14 eV

A.Lacaita et al. IEEE TED (1993)

Photons can induce avalanches in neighboring cells. Depends on distance between high-field regions

ΔV^2 dependence on over-voltage:
- carrier flux (current) during avalanche $\propto \Delta V$
- gain $\propto \Delta V$

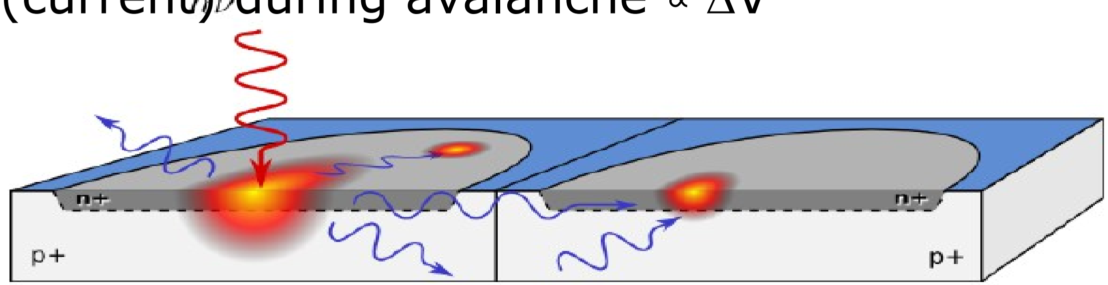

Counteract:
- optical isolation between cells

by trenches filled with opaque material
- low over-voltage operation helps

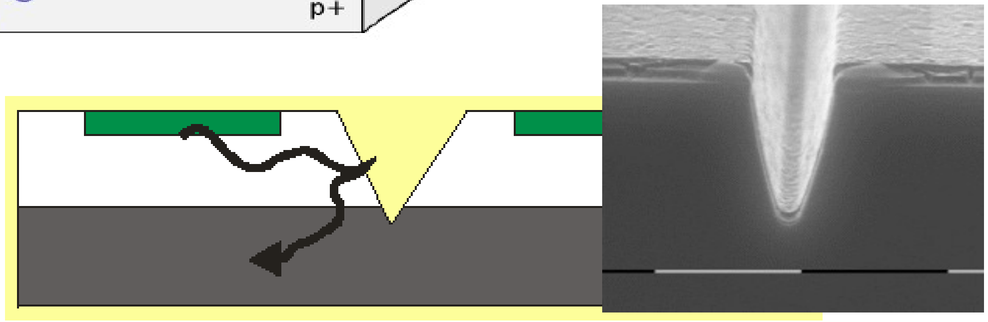

It can be reduced to a level below % in a wide ΔV range

Correlated noise sources

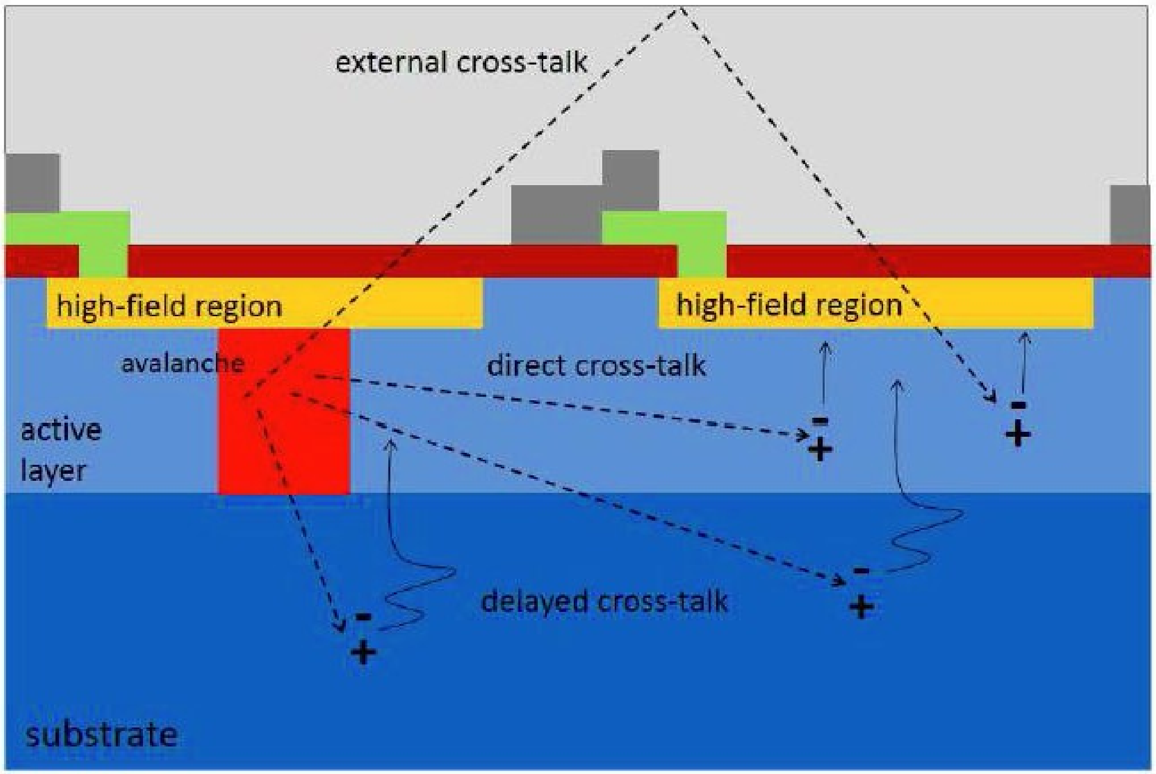

Some paths for optical cross-talk

A.Ferri IPRD 2013

- Trenches to avoid direct and delayed cross-talk…
- buried junction to avoid out-diffusion…
- **lower gain → use tiny cells (passive quenching)**
  → or active quenching devices

Recent devices from Hamamatsu (2013)

Reduced After-pulsing and Cross-Talk rates...
(... not simultaneously in the same device)

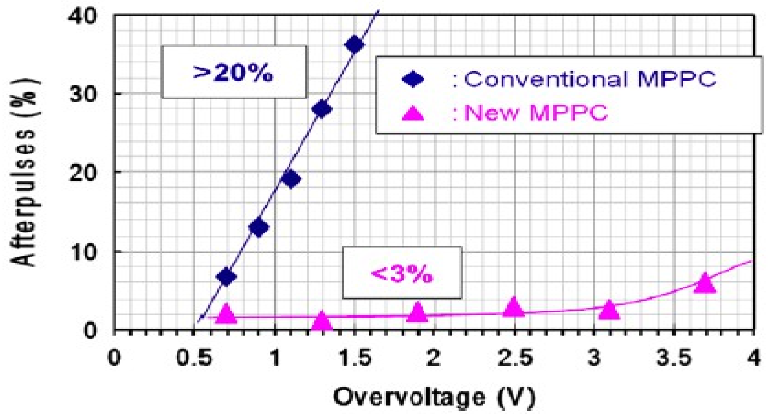

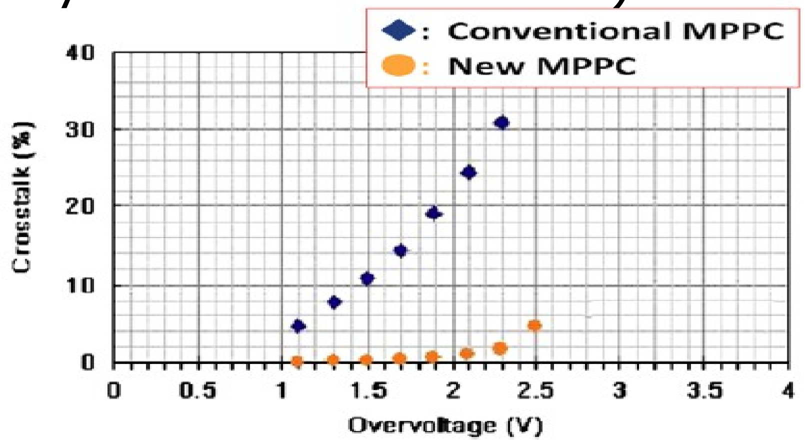

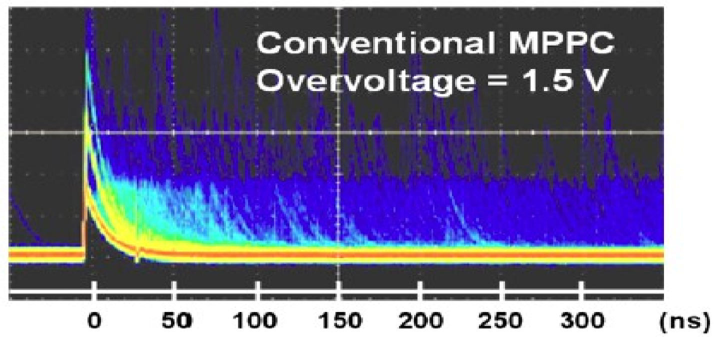

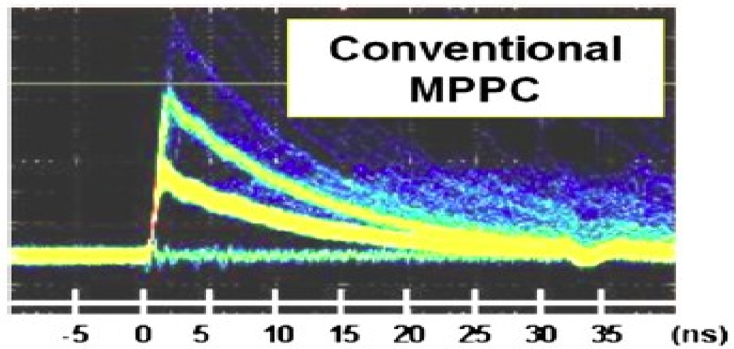

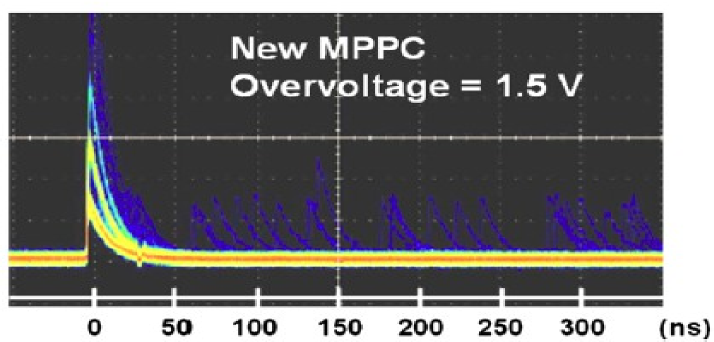

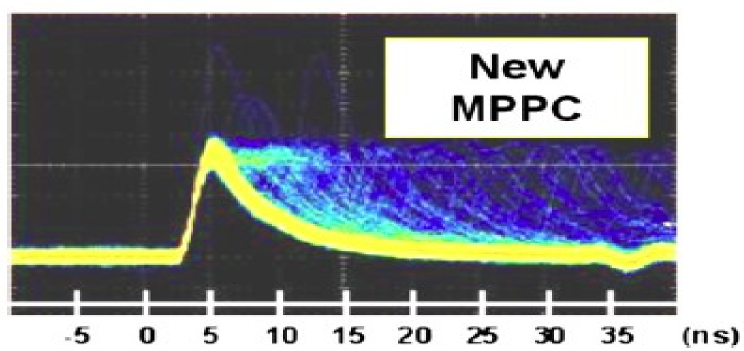

K.Sato et al Vienna Conference on Instrumentation 2013

Photo-Detection Efficiency - PDE

- Three factors
- Recent improvements
- UV and VUV enhanced devices

Photo-Detection Efficiency (PDE) – 3 factors

QE: carrier Photo-generation

probability for a photon to generate a carrier that reaches the high field region

→ λ and T dependent

→ ΔV independent if full depletion at V_{bd}

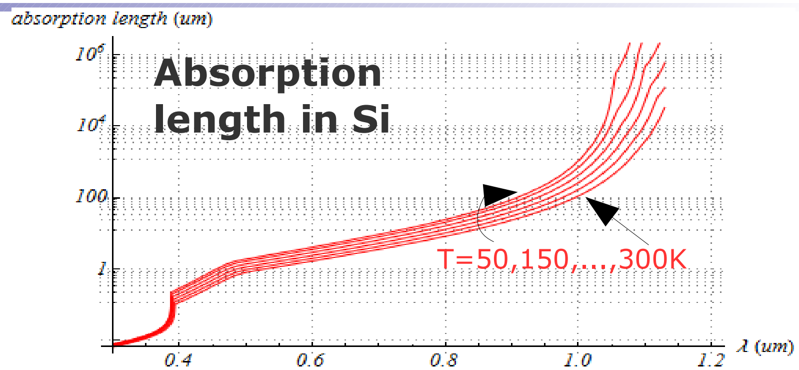

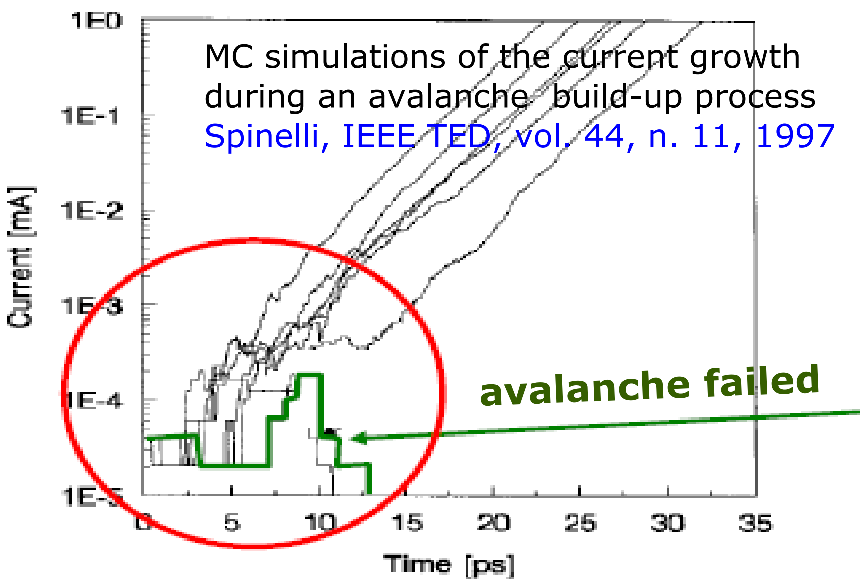

P_{01} : avalanche triggering probability

probability for a carrier traversing the high-field to generate the avalanche

→ λ, T and ΔV dependent

FF: geometrical Fill Factor

fraction of dead area due to structures between the cells, eg. guard rings, trenches

→ moderate ΔV dependence (cell edges)

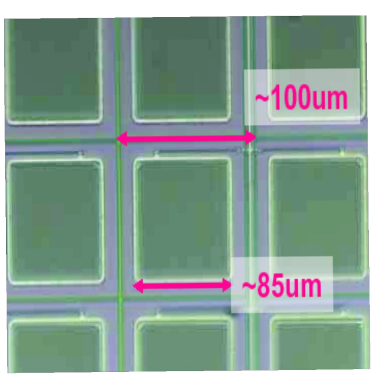

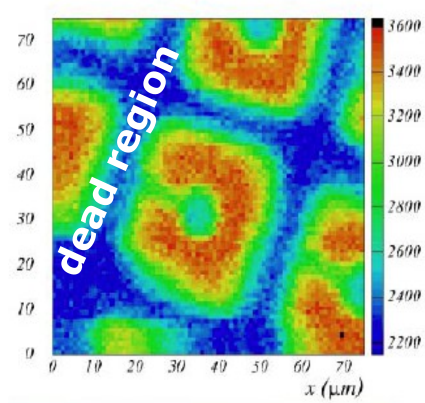

QE → PDE dependence on wavelength λ

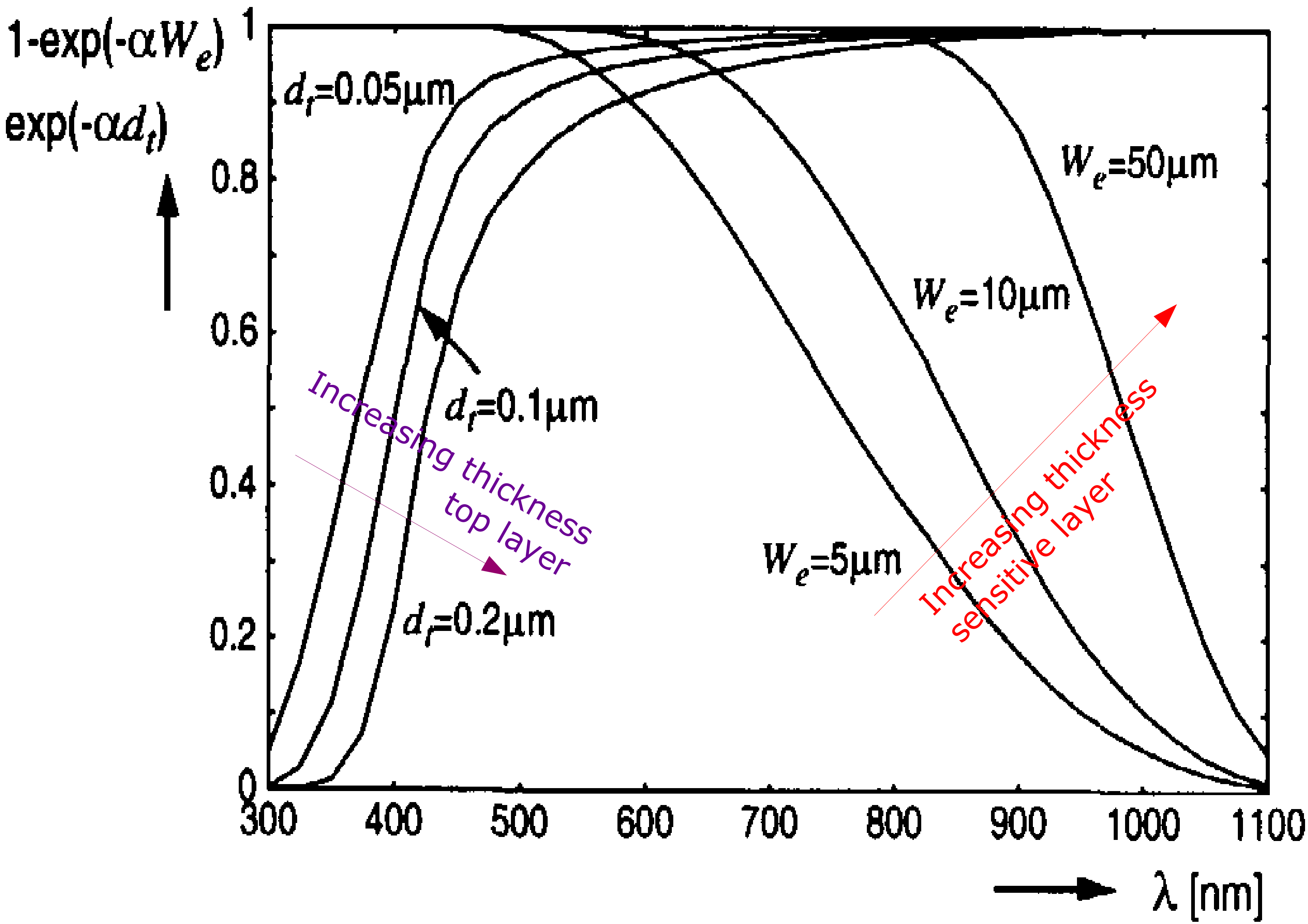

W.Knidt PhD Thesis 1999

QE → PDE dependence on wavelength λ

FBK single diode (2006) photo-voltaic regime ($V_{bias} \sim 0$ V)

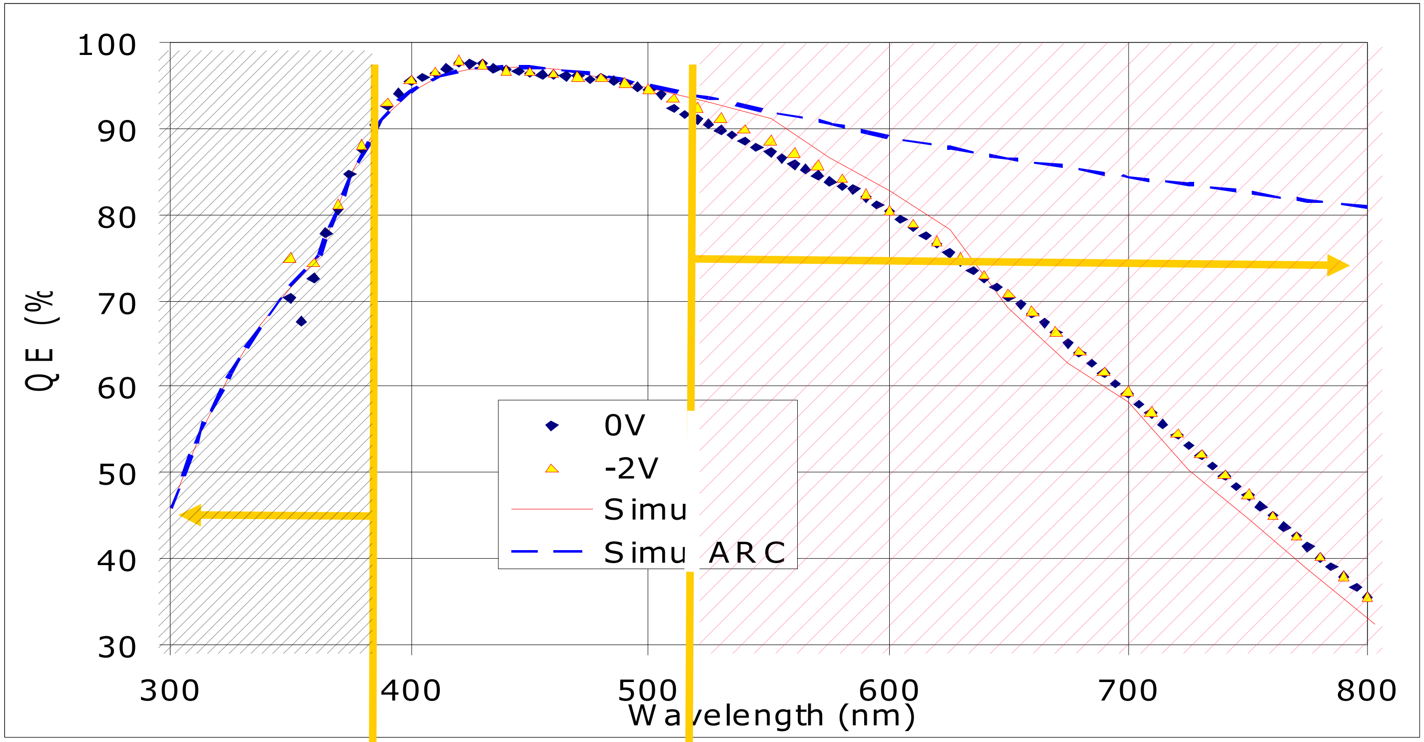

limited by
ARC Transmittance
&
Superficial
Recombination

limited by the
small π layer thickness

Most critical issue for **Deep UV SiPM**
note: reduced superficial recombination
in n-on-p wrt p-on-n

Avalanche Trigg. Probability → PDE vs λ

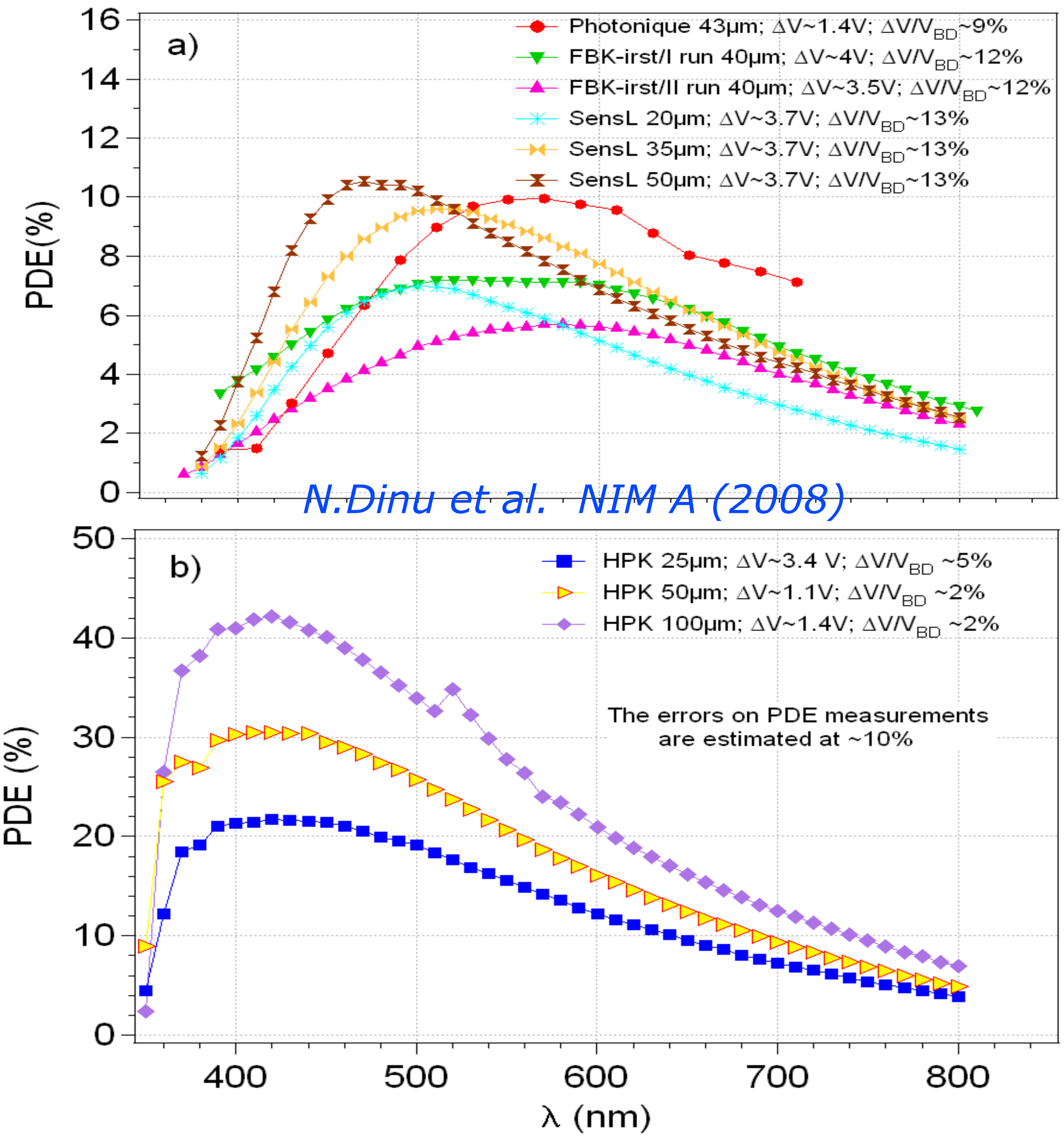

Fig. 5a) The PDE vs. λ of the Photonique, FBK-irst and SensL devices and b) HPK

n-on-p structures

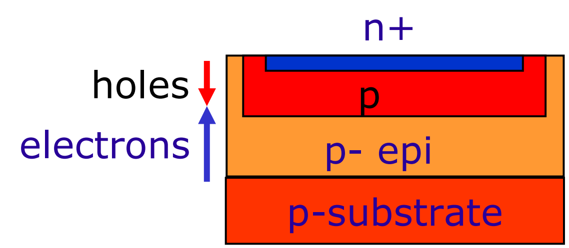

Ionization rate in Silicon

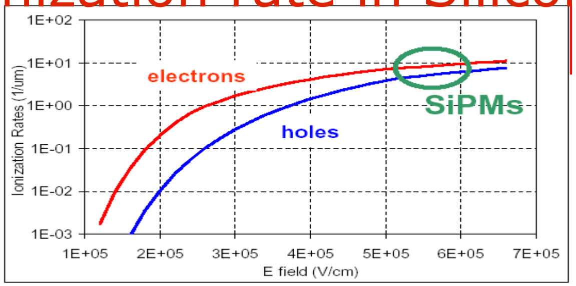

p-on-n structure

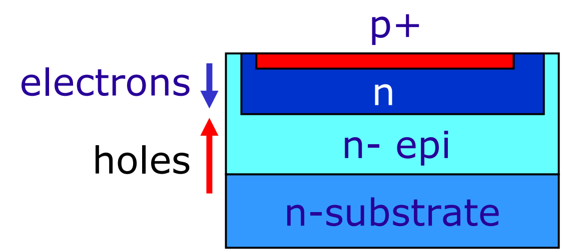

(shallow junctions)

Improving PDE

→ PDE peak constantly improving for many devices
→ every manufacturer shape PDE for matching target applications
→ UV SiPM eg from MePhi/Excelitas (see *E.Popova at NDIP 2011*)
→ VUV SiPMs in development too

Barlow – LIGHT 2011

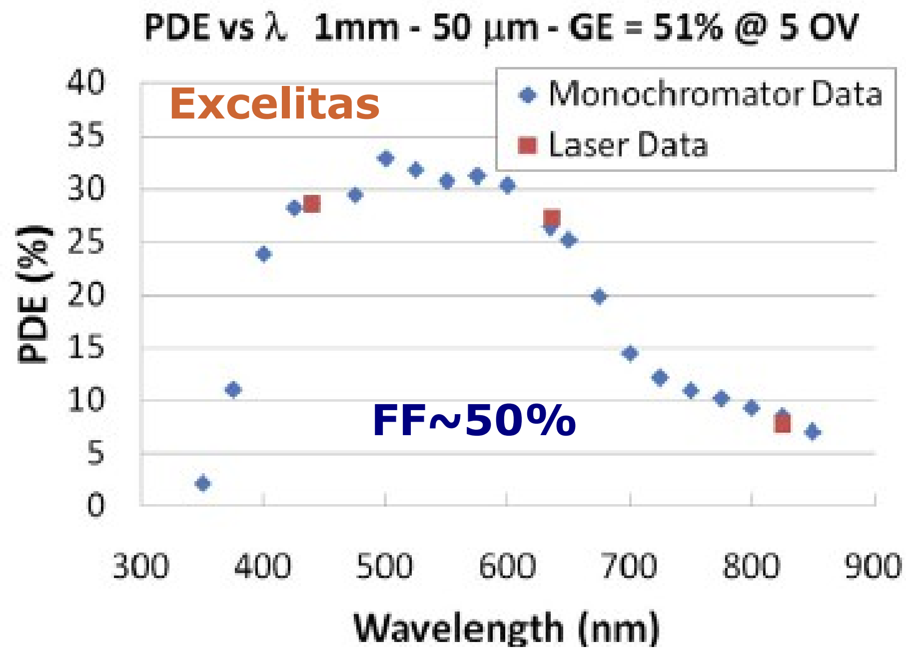

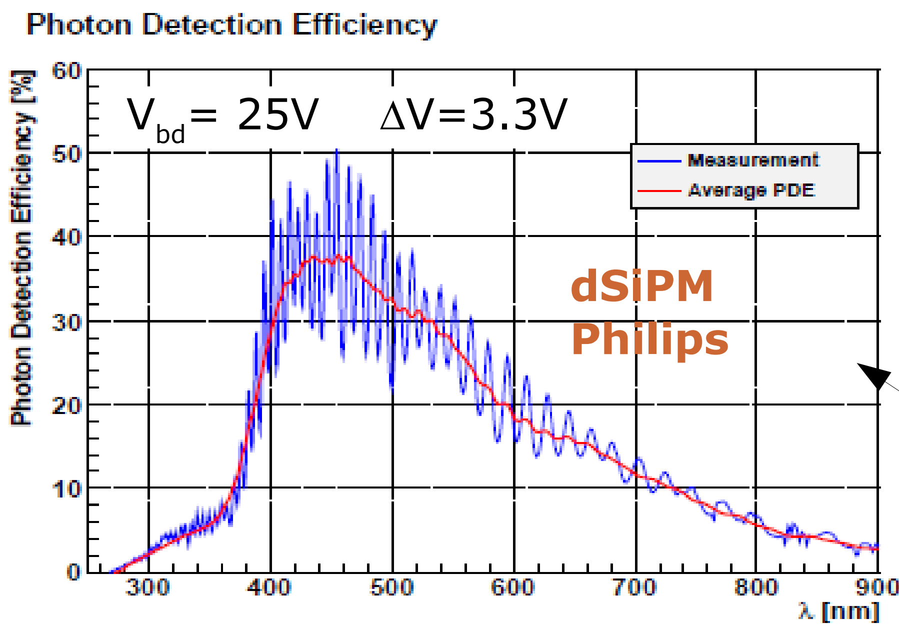

T.Frach 2012 JINST 7 C01112

F.Wiest – AIDA 2012 at DESY

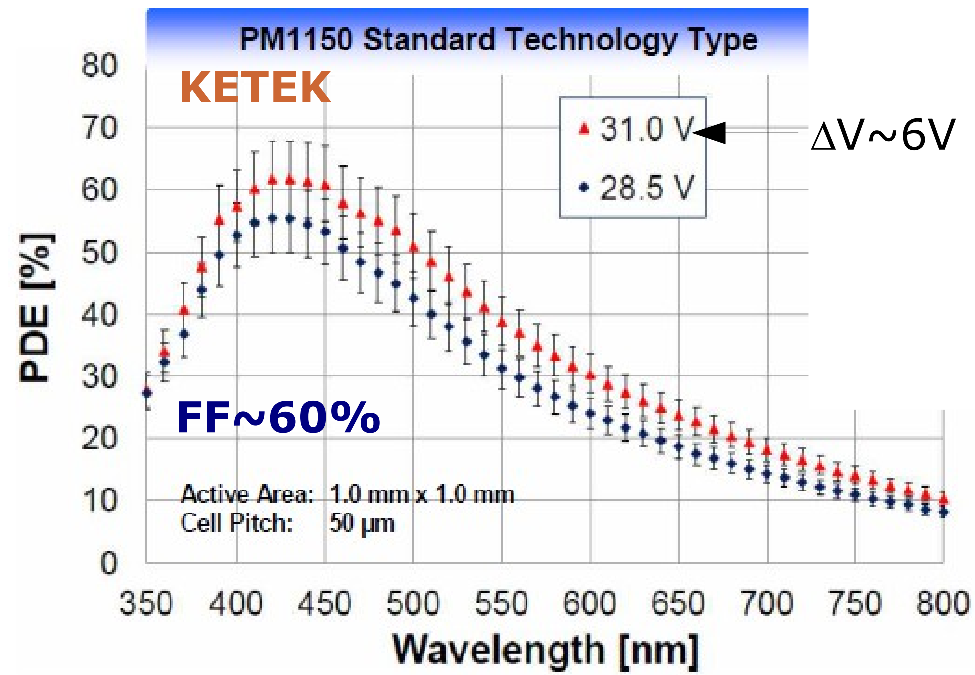

dSiPM (latest sensor 2011)
→ up to now no optical stack optimization
→ no anti-reflecting coating
→ potential improvement up to 60% peak PDE (*Y.Haemish at AIDA 2012*)

UV and VUV SiPM development

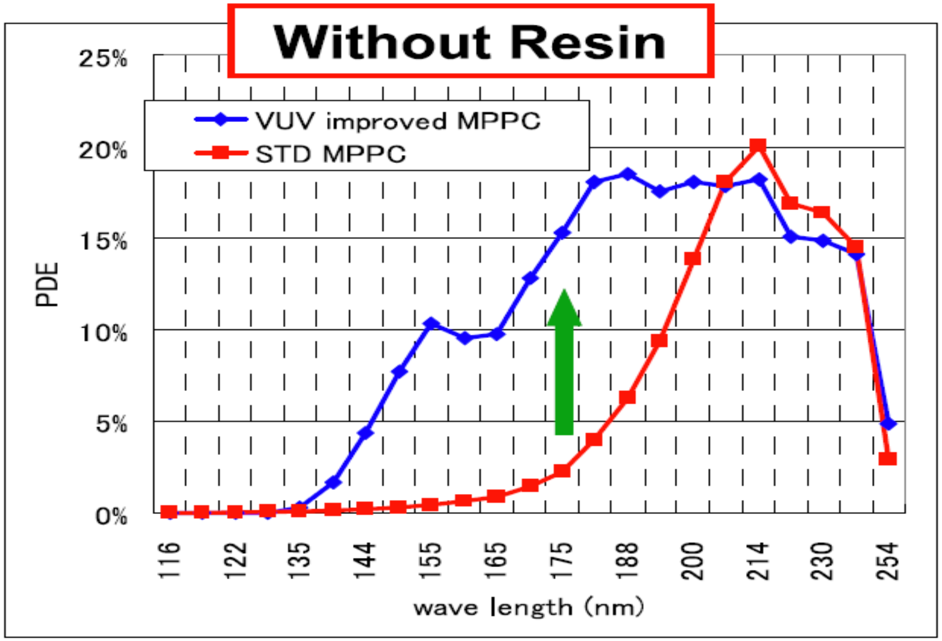

Sato et al (**Hamamatsu**) - Vienna Conf. on Instr. 2013

Hamamatsu
VUV-enhanced MPPC

→ removal of protection coating
→ optimization of the parameters
- thinner junction
- optimized superficial layers

...

New windows for applications in fundamental Physics experiments

- **Dark matter detection**
  ZEPLIN, LUX, DARWIN, XENON100
- **Double beta decay measurement**
  EXO
- **Search for rare decay mode**
  MEG

FBK - Advansid
NUV-SiPM (Near-UV)

- PDE (350nm) ~ 27 % (FF = 45 %)
- DCR = 200 kHz @ 20°C (ΔV = 5V)

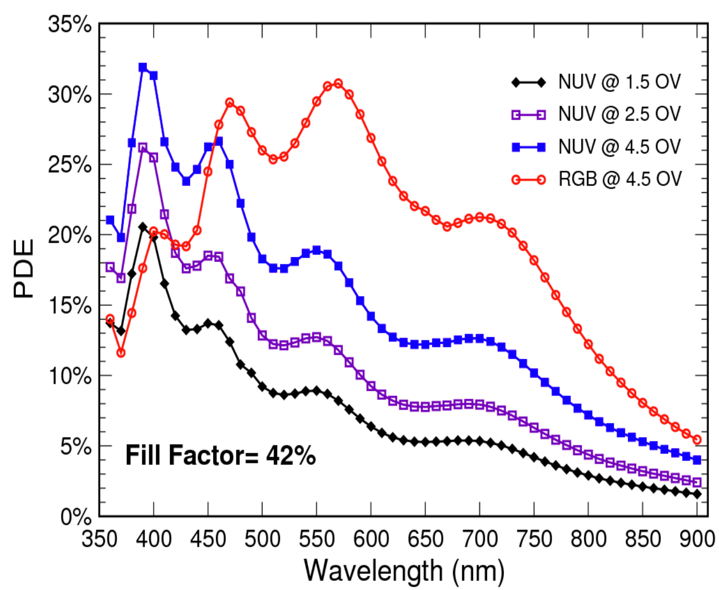

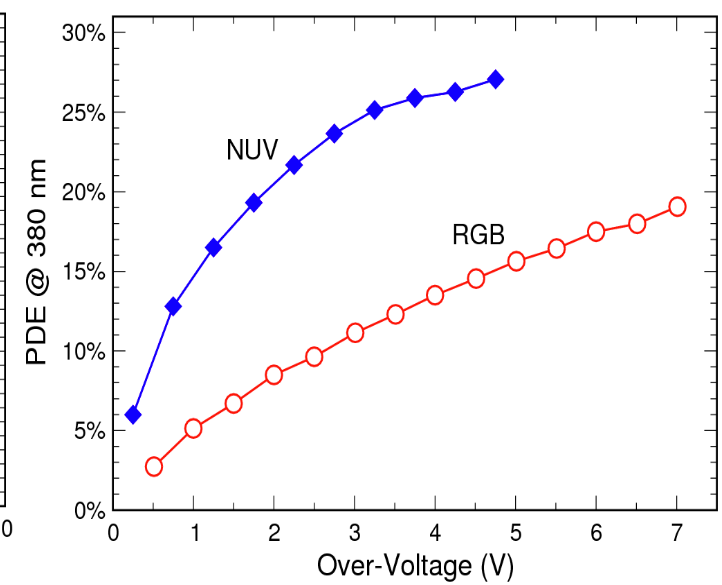

A.Ferri at IDPASC 2013

Timing fluctuations

• **SiPM are intrinsically very fast**

Two timing components (related to avalanche developement)

1) prompt → gaussian time jitter well below **100ps** (depending on ΔV, and λ)

2) delayed → non-gaussian tails up to **few ns** (depending on λ)

• **Optimization of devices for timing**

→ use of fast signal shape component

→ use pulse shape analysis, better than CFD … don't use ToT (for single photon)

Timing jitter: prompt and delayed components

1) Prompt component: gaussian with time scale O(100ps)

Statistical fluctuations in the avalanche:

- **Longitudinal** build-up (minor contribution)
- **Transversal** propagation (main contribution)

  - via multiplication assisted diffusion (dominating in few μm thin devices)
  A.Lacaita et al. APL and El.Lett. 1990

  - via photon assisted propagation (dominating in thick devices – O(100μm))
  PP.Webb, R.J. McIntyre RCA Eng. 1982
  A.Lacaita et al. APL 1992

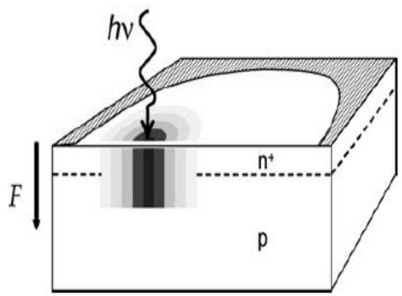

Multiplication assisted diffusion

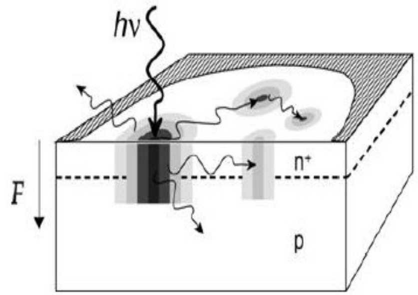

Photon assisted propagation

Fluctuations due to
a) impact ionization statistics

b) variance of longitudinal position of photo-generation: finite drift time even at saturated velocity
note: saturated ve ~ 3 vh
(n-on-p are faster in general)

→ Jitter at minimum → **O(10ps)**
(very low threshold → not easy)

Fluctuations in shock-wave due to
c) variance of the transverse diffusion speed v_{diff}

d) variance of transverse position of photo-generation: slope of current rising front depends on transverse position

→ Jitter → **O(100ps)**
(usually threshold set high)

Timing jitter: prompt and delayed components

2) delayed component: non-gaussian tails with time scale O(ns)

Carriers photo-generated in the neutral regions above/beneath the junction and reaching the electric field region by diffusion

G.Ripamonti, S.Cova Sol.State Electronics (1985)

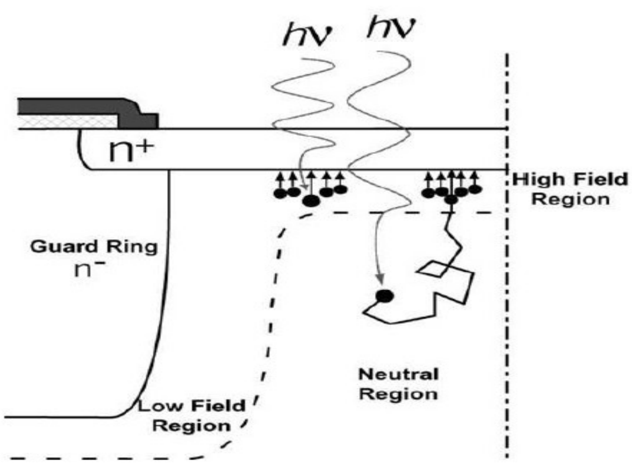

S.Cova et al. NIST Workshop on SPD (2003)

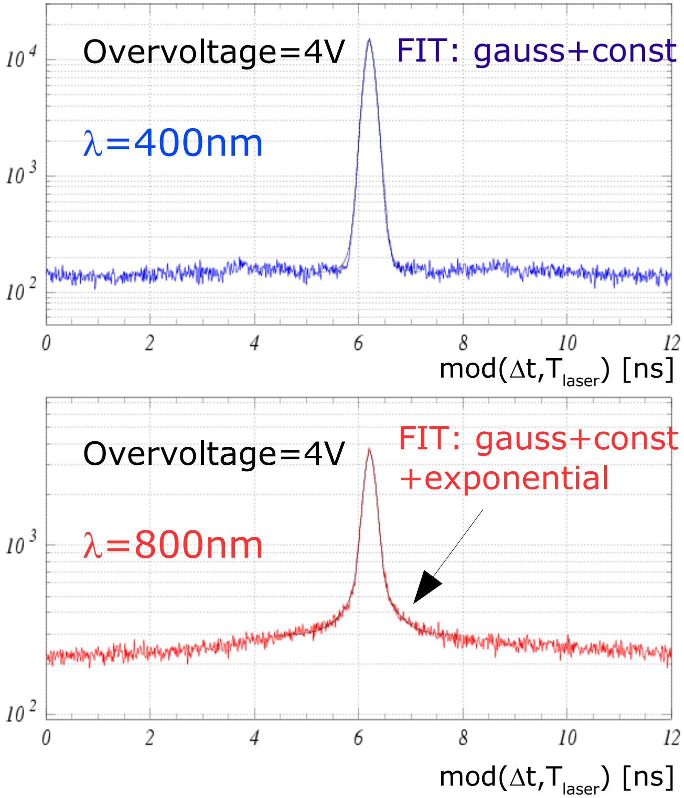

G.C. et al NIMA 581 (2007) 461

tail lifetime: $\tau \sim L^2 / \pi^2 D$ ~ up to some ns
L = effective neutral layer thickness
D = diffusion coefficient

→ **Neutral regions** underneath the junction : timing tails for long wavelengths
→ **Neutral regions** in APD entrance: timing tails for short wavelengths

Single photon pulse shape (Rising and falling edges)

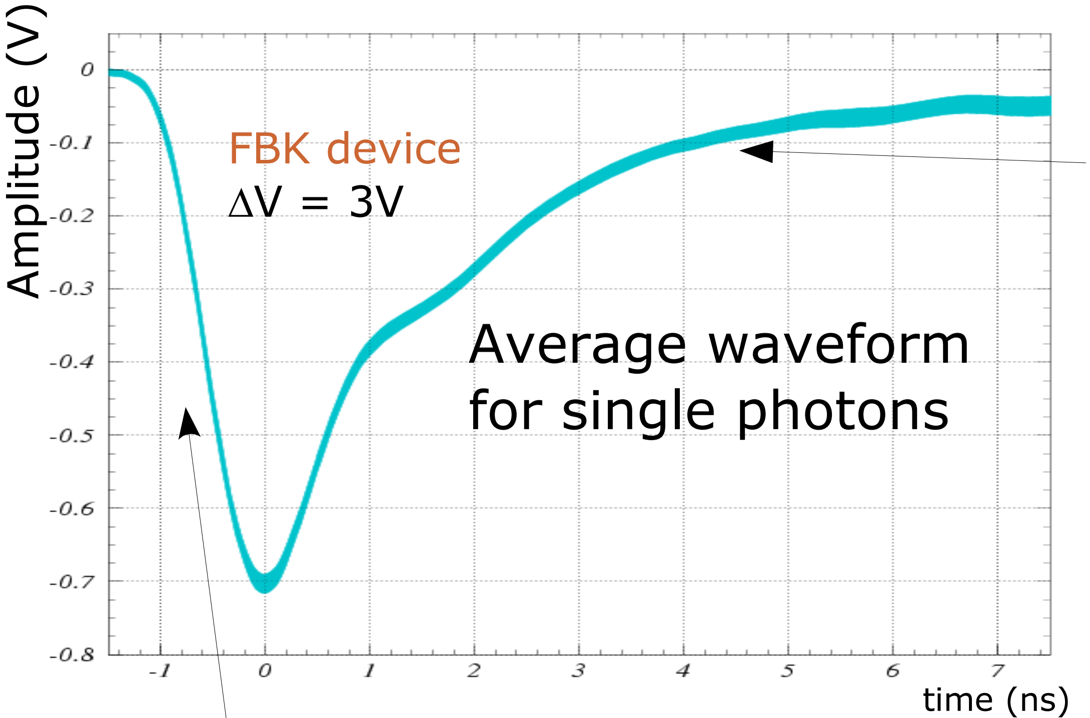

Falling signal shape fluctuates considerably (due eg to after-pulses) → signal tail is non useful for timing, if not detrimental

note: using Time-over-Threshold method for slew correction might lead to worse resolution in case of single photon pulses

Reminder:

$$\frac{dI}{dt} \sim \frac{\sqrt{D}}{R_{sp}\sqrt{\tau}}$$

$$\tau \sim \frac{1}{1-(E_{max}/E_{breakdown})^n}$$

Rise-time depends on **ΔV, T** and **impact position** ie **signal shape is not constant**, then:
1) CFD method only partially effective in canceling time walk effects
2) any **digital timing filter** should account for shape variations (ΔV, T)

For comparison about waveform method and various digital algorithms see *Ronzhin et al NIM A 668 (2012) 94*

Single Photon Timing Resolution: impact position → cell size dependence

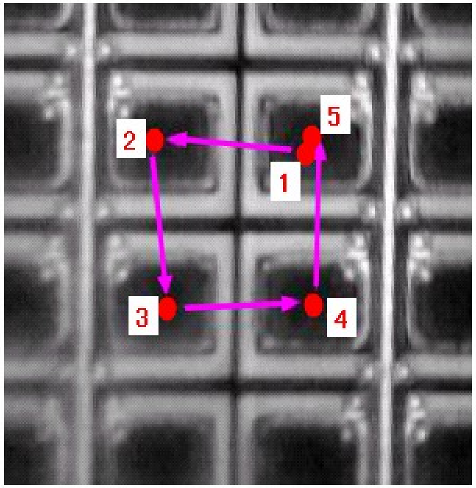

	FWHM (ps)	FWTM (ps)
1	199	393
2	197	389
3	209	409
4	201	393
5	195	383

K.Yamamoto PD07

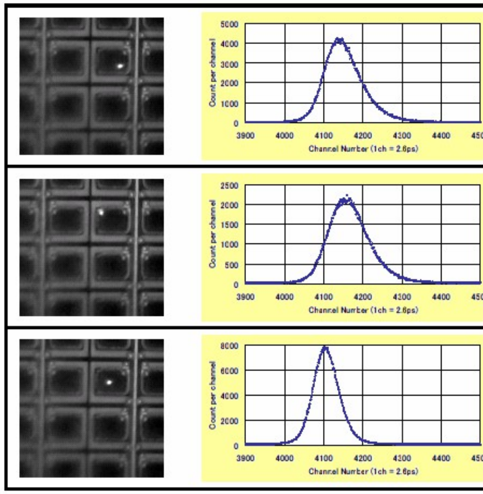

FWHM = 263 ps

FWHM = 294 ps

FWHM = 192 ps

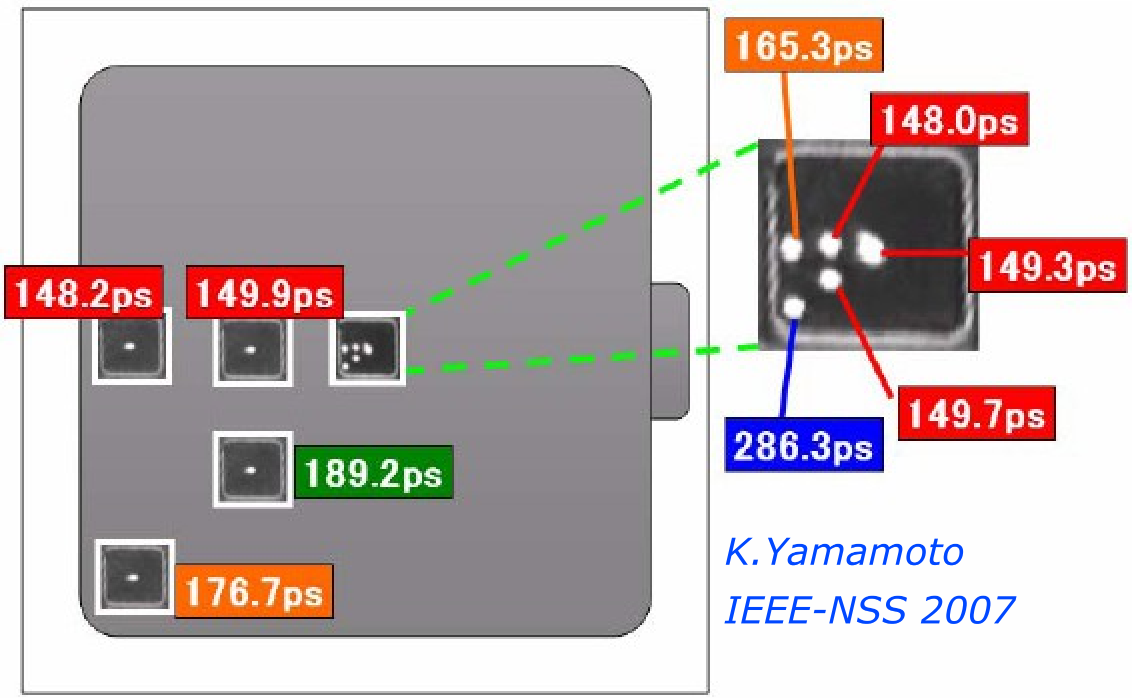

K.Yamamoto
IEEE-NSS 2007

Larger jitter if photo-conversion at the border of the cell

Due to:

1) slower avalanche front propagation

2) lower E field at edges

→ cfr PDE vs position

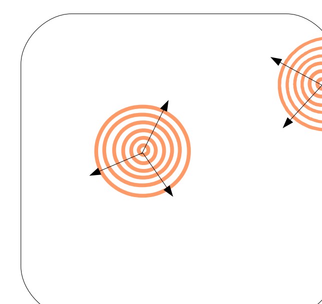

Data include the system jitter (common offset, not subtracted)

SPTR: FBK devices – shallow junction

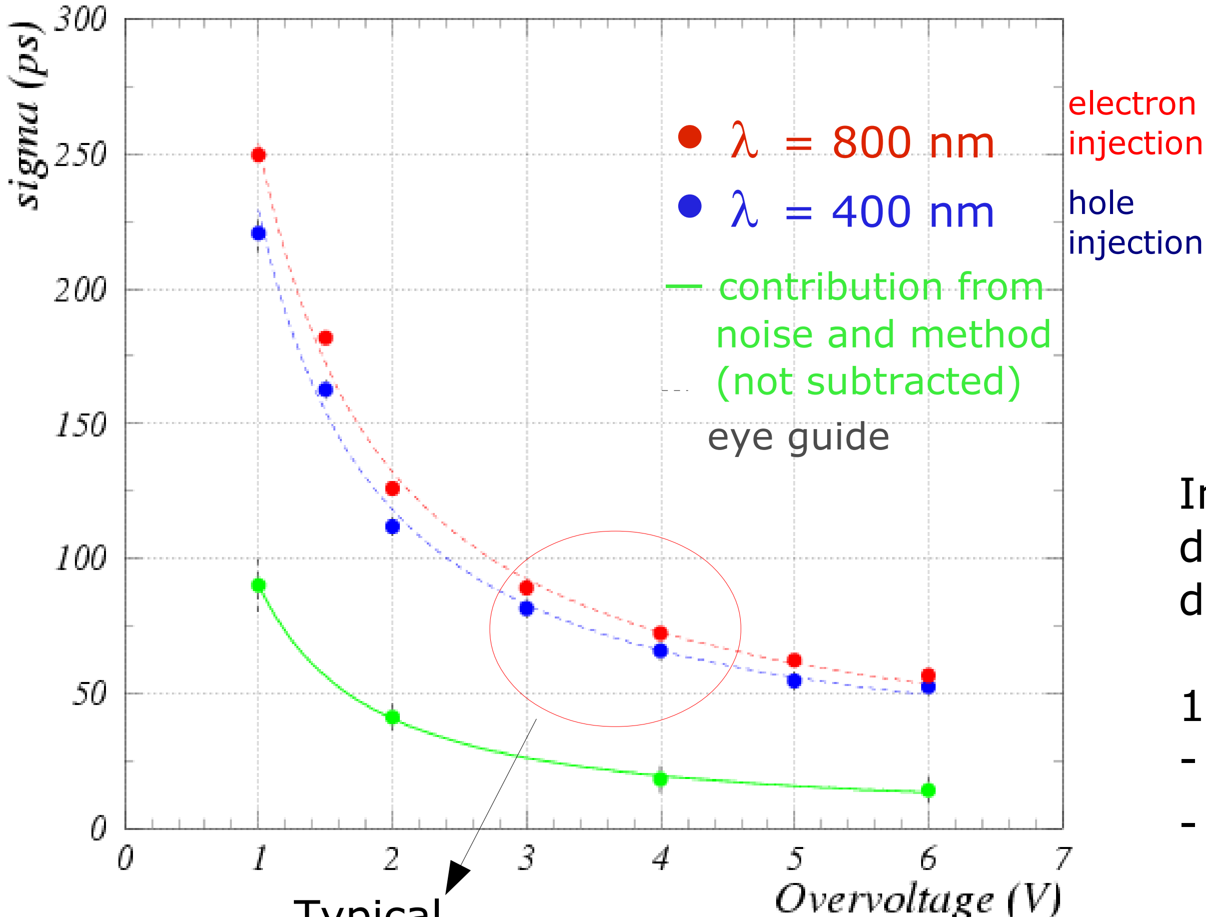

Typical working region

G.C. et al NIMA 581 (2007) 461

NOTE: good timing performances kept up to 10MHz/mm² photon rates

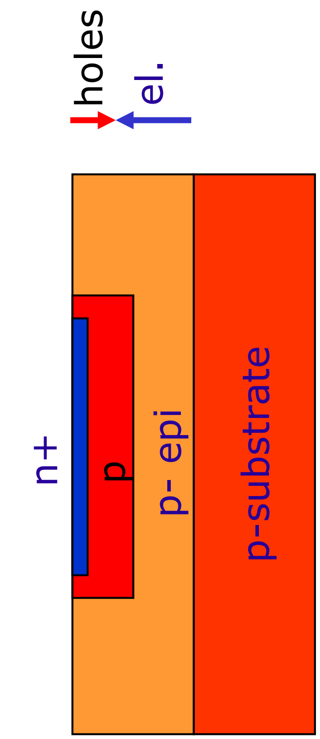

In general due to drift, resolution differences

1) high field junction position
- shallow junction: $\sigma_t^{red} > \sigma_t^{blue}$
- buried junction: $\sigma_t^{red} < \sigma_t^{blue}$

2) n^+-on-p smaller jitter than p^+-on-n due to electrons drifting faster in depletion region (but λ dependence)

3) above differences more relevant in thick devices than thin

SiPM equivalent circuit and pulse shape

Single cell model → $(R_d||C_d)+(R_q||C_q)$

SiPM + load → $(||Z_{cell})||C_{grid} + Z_{load}$

Signal = slow pulse ($\tau_{d\ (rise)}$, $\tau_{slow\ (fall)}$) +

+ fast pulse ($\tau_{d\ (rise)}$, $\tau_{fast\ (fall)}$)

- $\tau_{d\ (rise)} \sim R_d(C_q+C_d)$
- $\tau_{fast\ (fall)} = R_{load}\ C_{tot}$ (fast; parasitic spike)
- $\tau_{slow\ (fall)} = R_q\ (C_q+C_d)$ (slow; cell recovery)

F.Corsi, et al. NIM A572 (2007) 416

S.Seifert et al. IEEE TNS 56 (2009) 3726

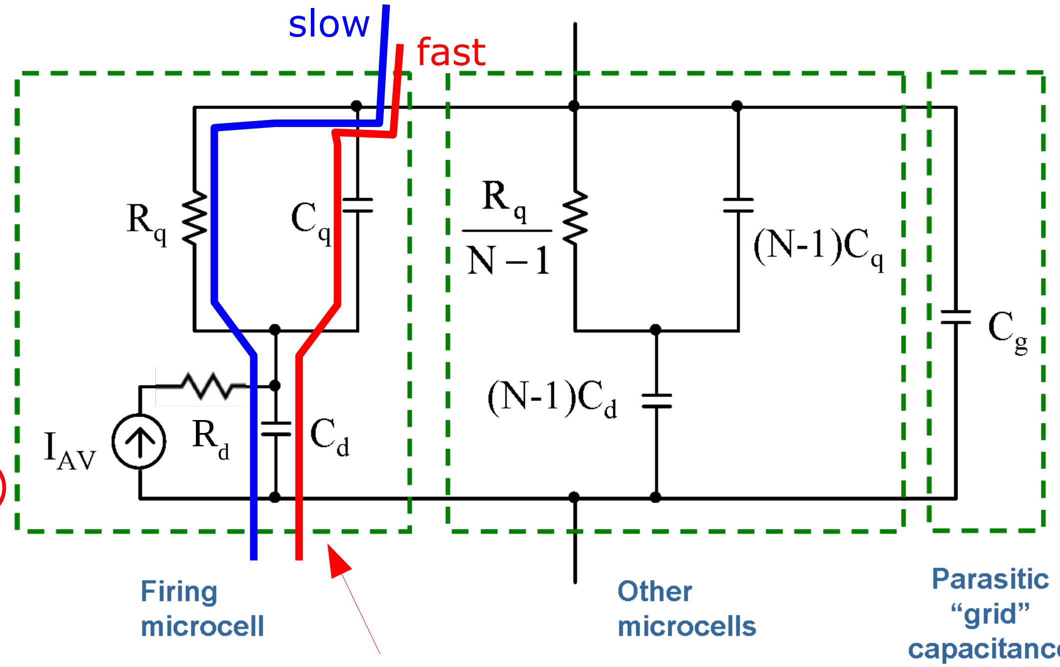

Cq → fast current supply path in the beginning of avalanche

Pulse shape

- Rise: Exponential
- Fall: Sum of 2 exponentials: transient + recovery

Sp.Charge Rd x Cd,q filtered by parasitic inductance, stray C, ... (Low Pass)

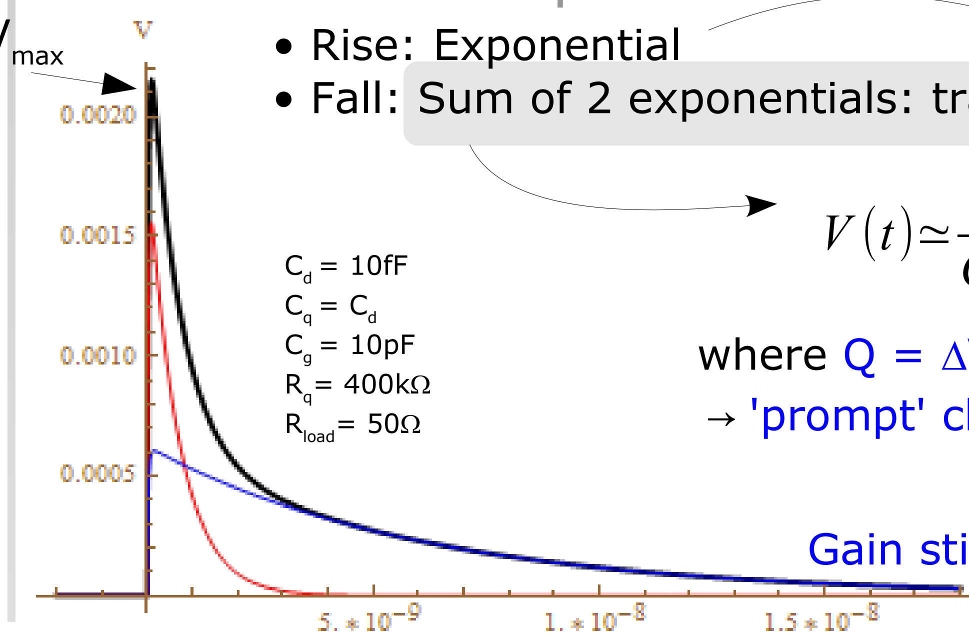

$$V(t) \simeq \frac{Q}{C_q+C_d}\left(\frac{C_q}{C_{tot}} e^{\frac{-t}{\tau_{FAST}}} + \frac{R_{load}}{R_q}\frac{C_d}{C_q+C_d} e^{\frac{-t}{\tau_{SLOW}}}\right) \text{ for } R_{load} << Rq$$

where $Q = \Delta V\ (C_q+C_d)$ is the total charge released by the cell

→ 'prompt' charge on C_{tot} is $Q_{fast} = Q\ C_q/(C_q+C_d)$

Gain still well defined: $$G = \int dt \frac{V(t)}{q_e R_{load}} = Q/q_e = \frac{\Delta V(C_d+C_q)}{q_e}$$

Optimizing signal shape for timing (SPTR)

→ peak height ratio $\frac{V_{fast}^{max}}{V_{slow}^{max}} \sim \frac{C_q^2 R_q}{C_d C_{tot} R_{load}}$

Enhancing C_q does improve timing performances

Hamamatsu test structures

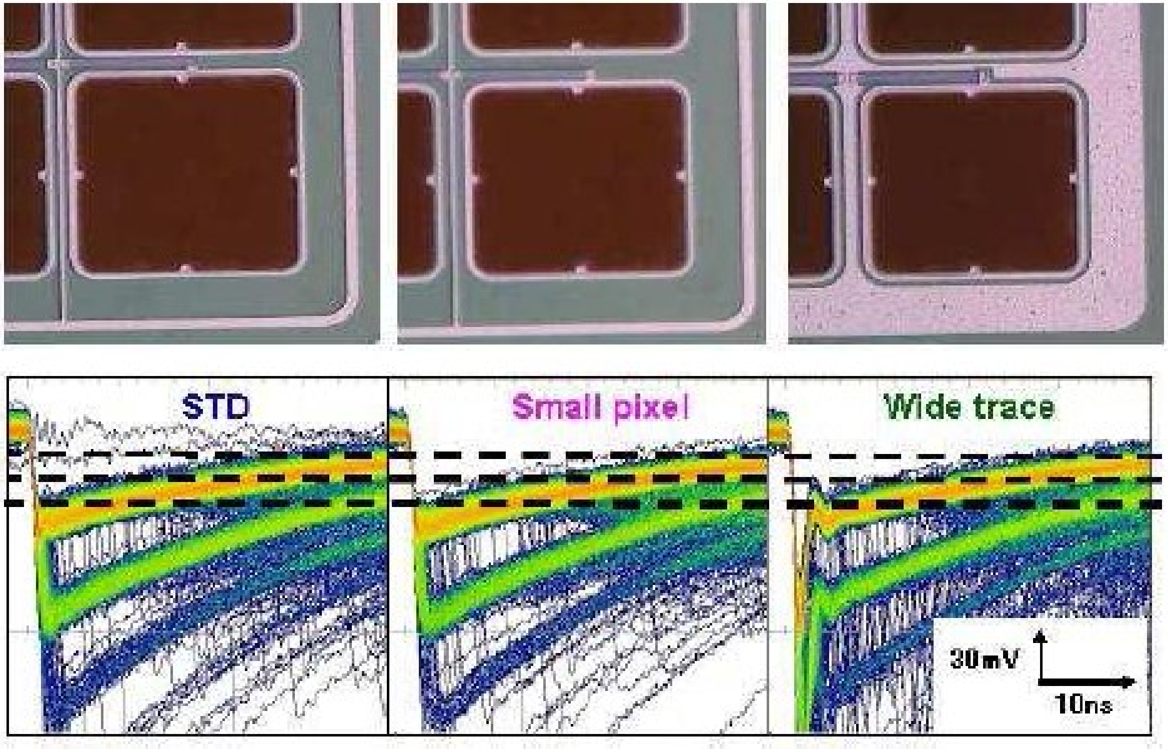

Yamamura et.al. at PD09

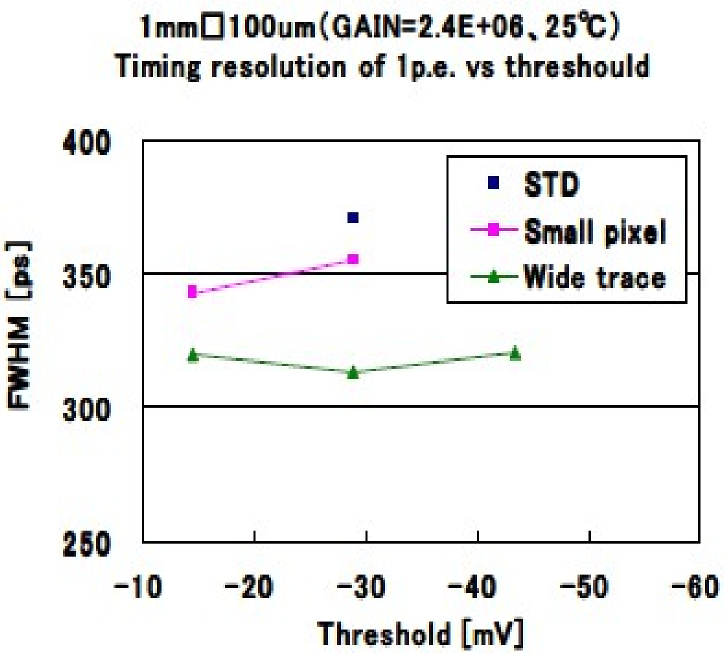

Analogous method for timing optimization proposed in C.Lee et al NIM A 650 (2010) 125 "Effect on MIM structured parallel quenching capacitor of SiPMs"

Note:
The steep falling front of the fast peak could be exploited too for optimum timing

$$\sigma_{time}^2 = \frac{\sigma_{amplitude}^2}{N_{samples} \int dt [f'(t)]^2}$$

Optimizing signal shape for timing

… and what about using just AC coupling ...

SiPM std architecture | **SensL new SiPM architecture for fast timing**

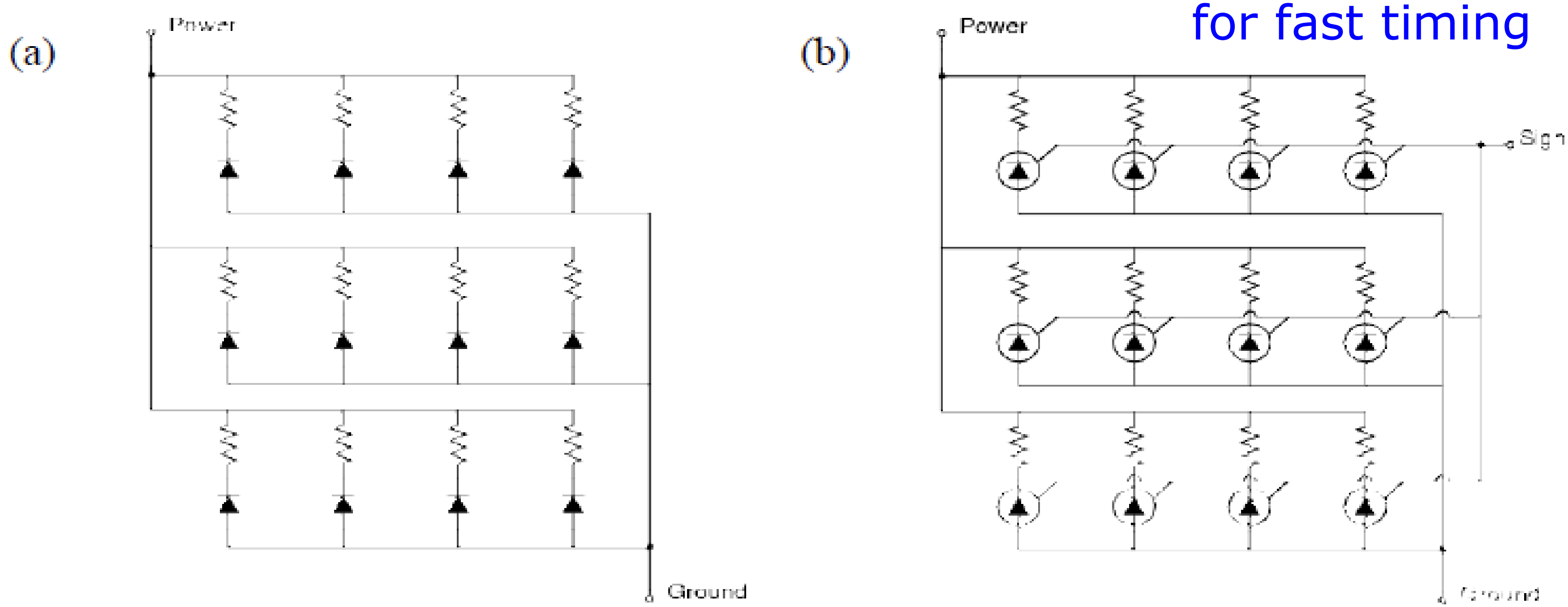

Figure 1: (a) traditional SPM architecture; (b) SPM architecture with inclusion of fast signal terminal.

The traditional SPM consists of a parallel array of avalanche photodiodes each in series with a quench resistor, as shown in Figure 1(a). In this configuration both bias and readout must occur on the same electrode. The introduction of a derivatively coupled electrode to each APD-resistor pair creates single-purpose signal line which delivers steeper rise-time pulses than the traditional SPM discharge which is inherently limited by the large output capacitance of each APD [3].

O'Neill et al " SensL New Fast Timing Silicon Photomultiplier " PhotoDet 2012 - proceedings

Comparisons

- SiPM vs APD

- Large Area devices → Hybrid

- Large Area devices → PMT/MCP

Single photon sensitivity

PMT (Hamamatsu R5600)

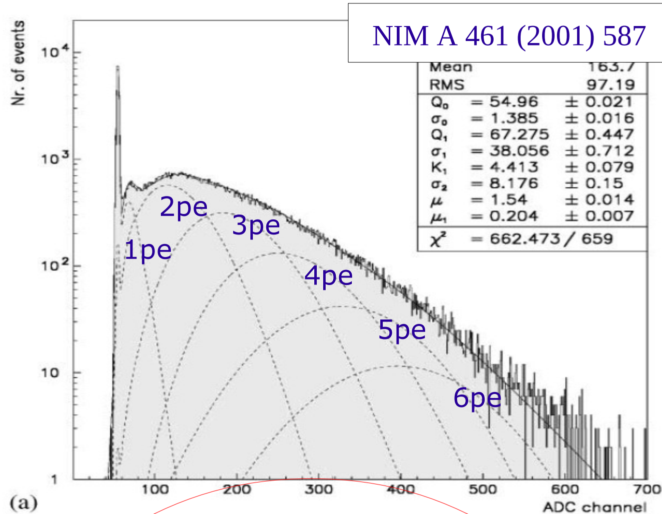

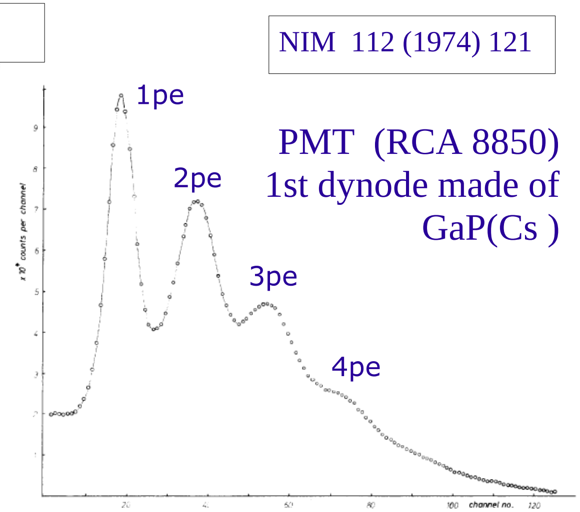

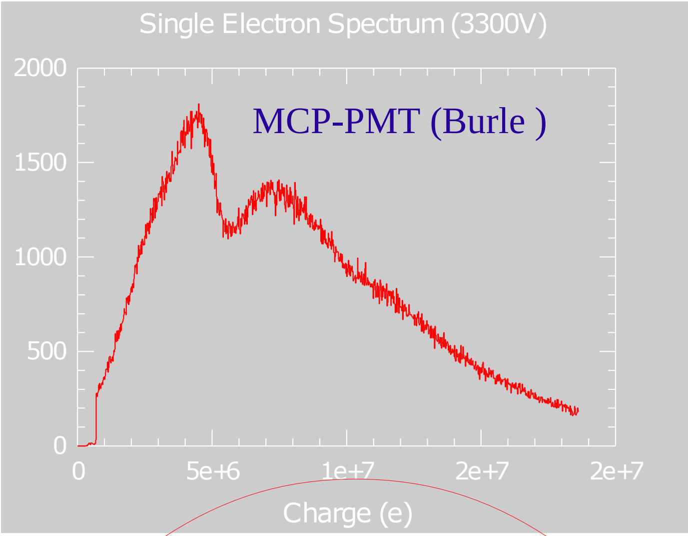

SiPM

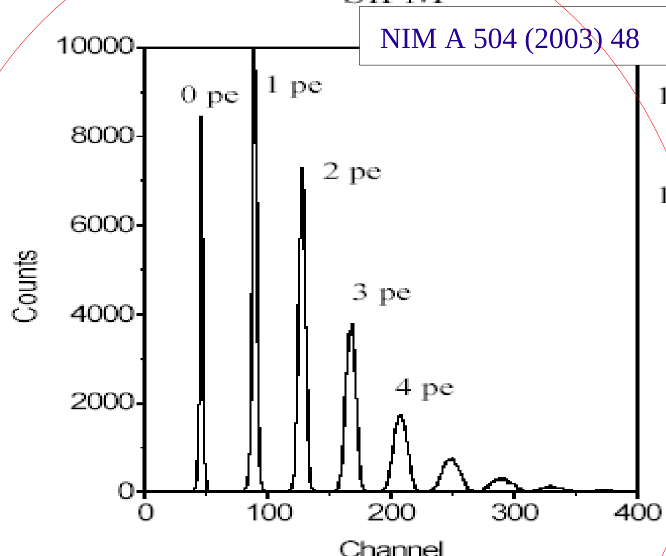

VLPC

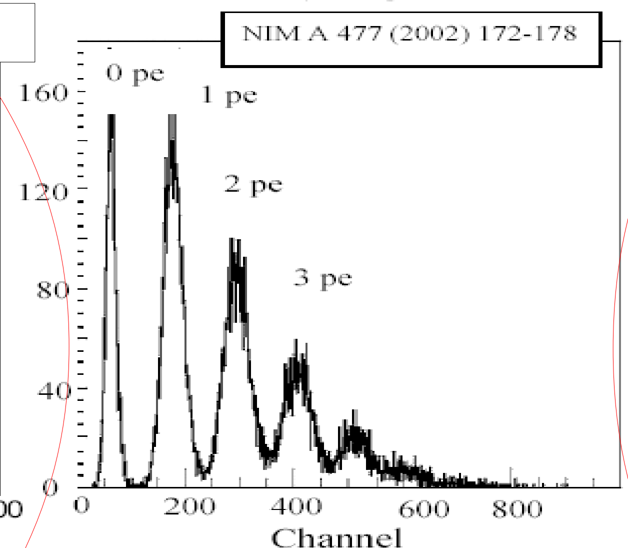

HPD

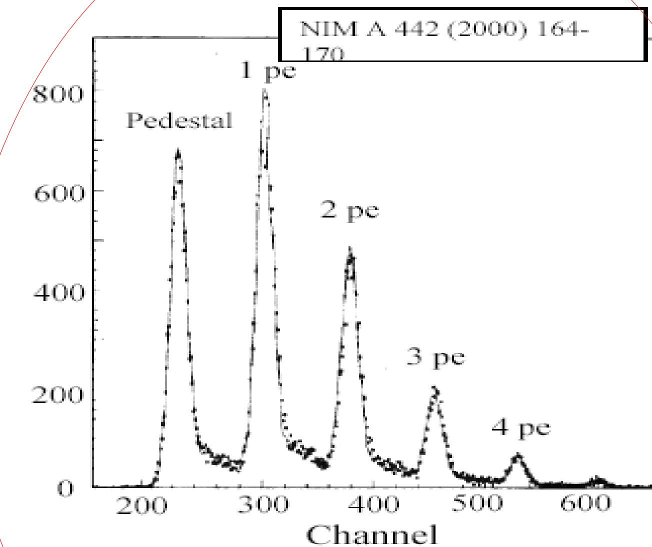

Silicon Photo-Multiplier
- room T
- V~50V

Visible Light Photon Counter
- T=6.5K
- V~5V

Hybrid Photo-Diode
- room T
- V~20000V

Large Area Photo-Detectors → HPD

Hybrid Photo Detectors

1) Photo-emission from photo-cathode
2) Photo-electron acceleration to **ΔV ~ 10-20kV**
3) charge multiplication in Si by ionization
→ **reduced fluctuations** due to Fano factor (F~0.12 in Si)

$$G = \frac{\Delta V - V_{thr.}}{W_{Si}}$$

$$\sigma_G = \sqrt{F \cdot G}$$

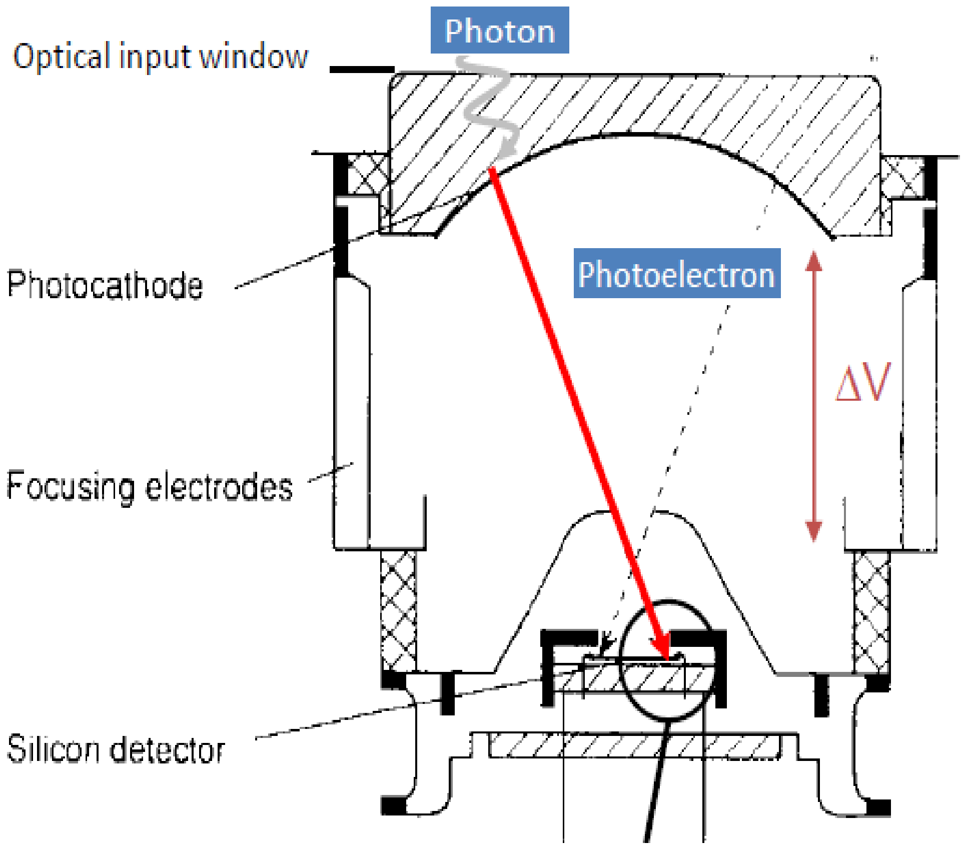

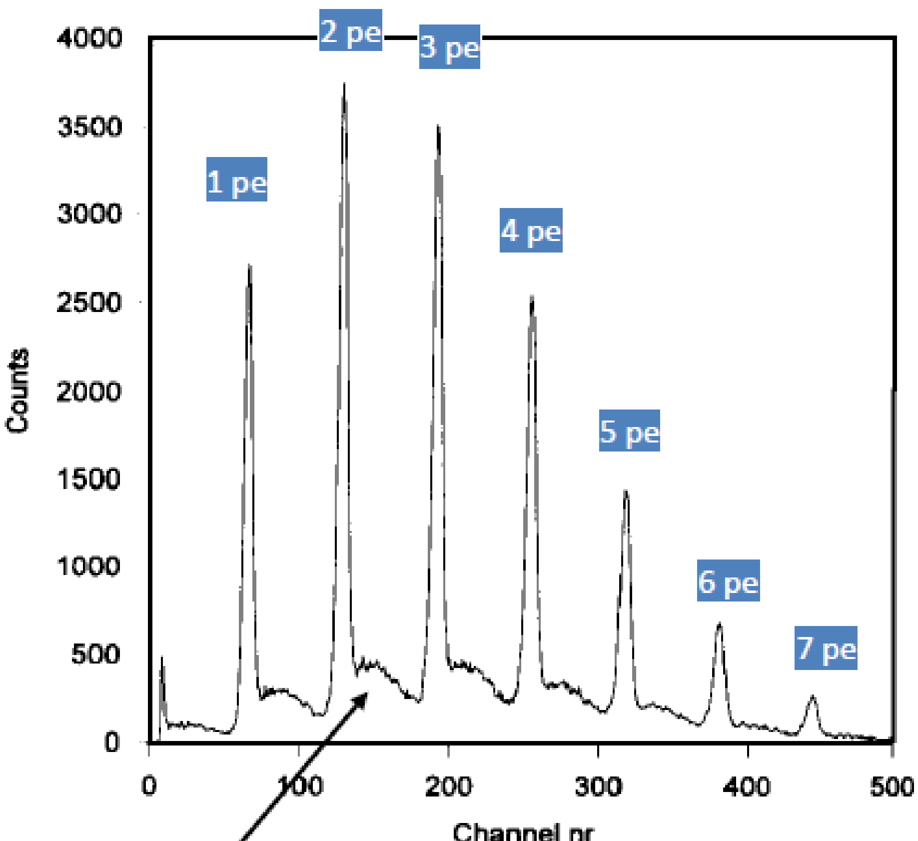

background from electron back-scattering at Si surface

EDIT 2011 School at CERN - photodetectors

Large Area Photo-Detectors → H-APD

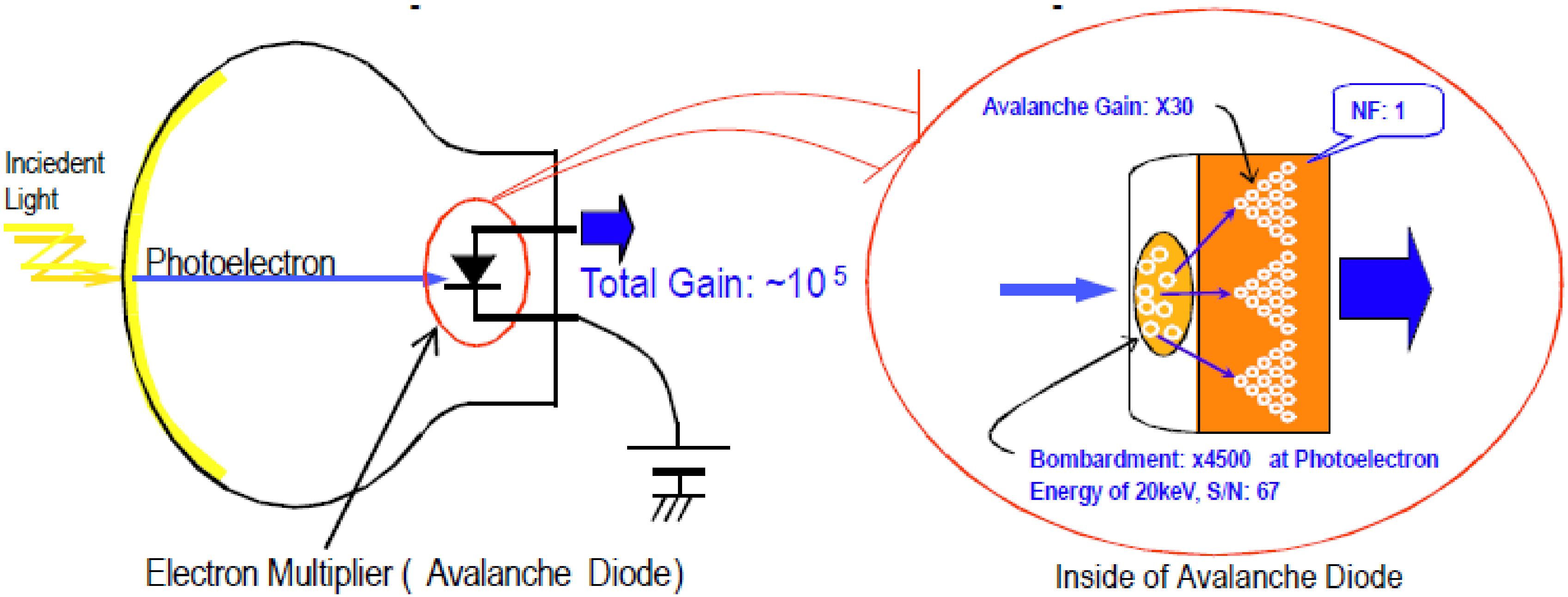

HPD

- ✓ has a simpler structure
- ✓ is expected to save production costs
- ✓ have better S/N but lower gain.

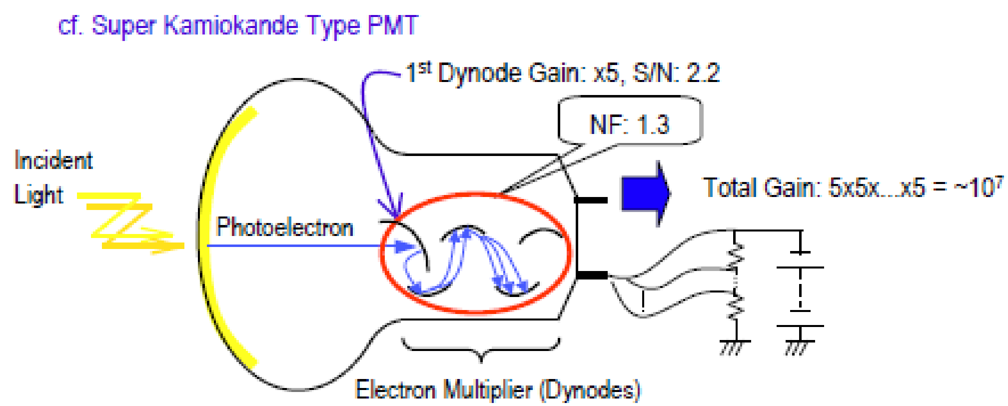

Developements (Hamamatsu) for various Cherenkov based detectors
→ Hyper-Kamiokande
→ Belle II ARICH

Large Area Photo-Detectors → HAPD

Total Gain ~ 7 10^5

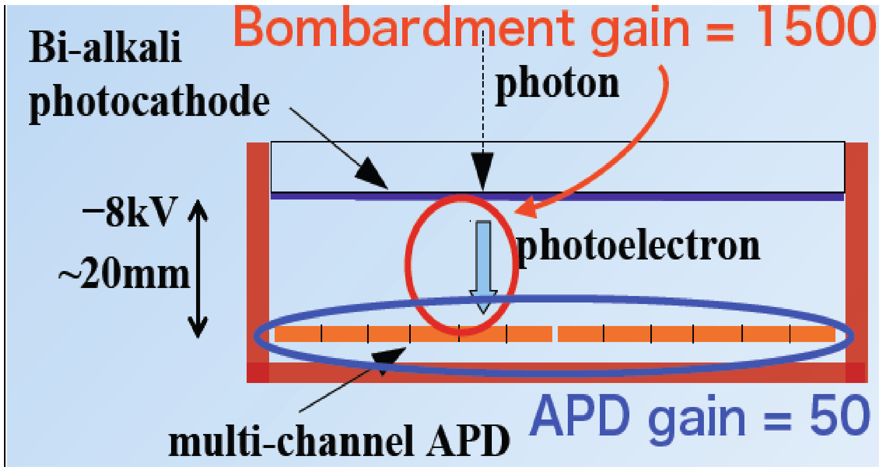

Single photon sensitivity

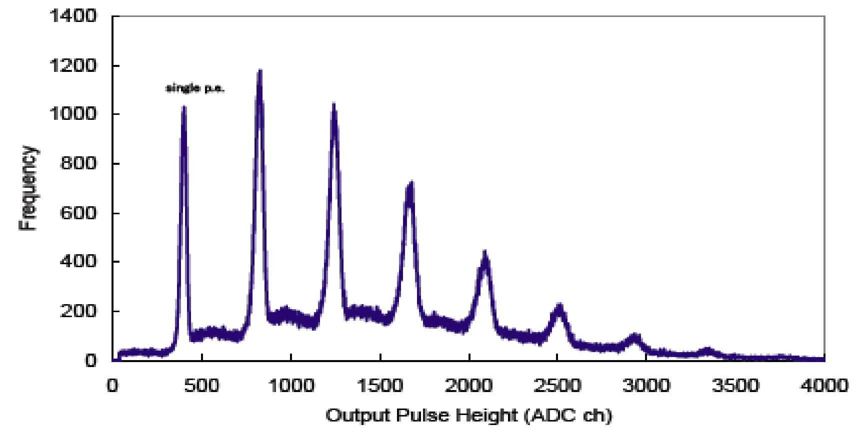

Dedicated APD layout for
- kinematic E threshold
- protection against alkali
- HV insulation

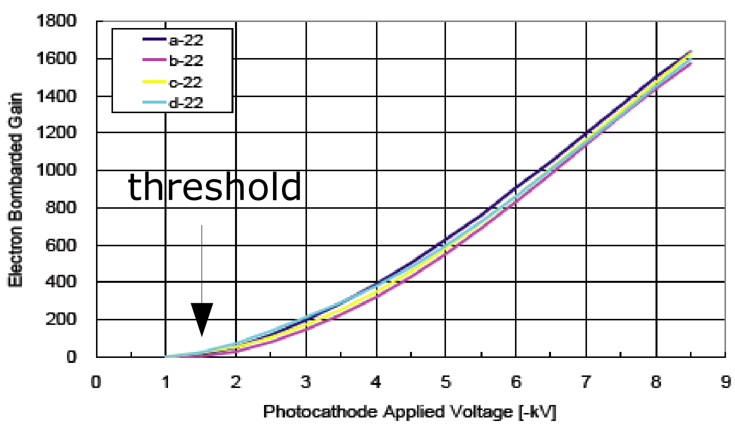

Use of Photo-cathode:
- limited PDE
- limited timing resolution

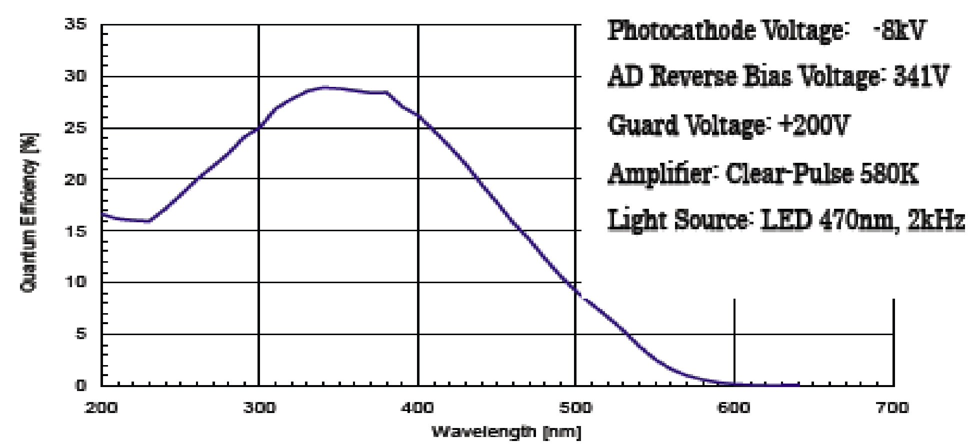

Y.Yusa at EPS 2013

Large Area Photo-Detectors → VSiPM

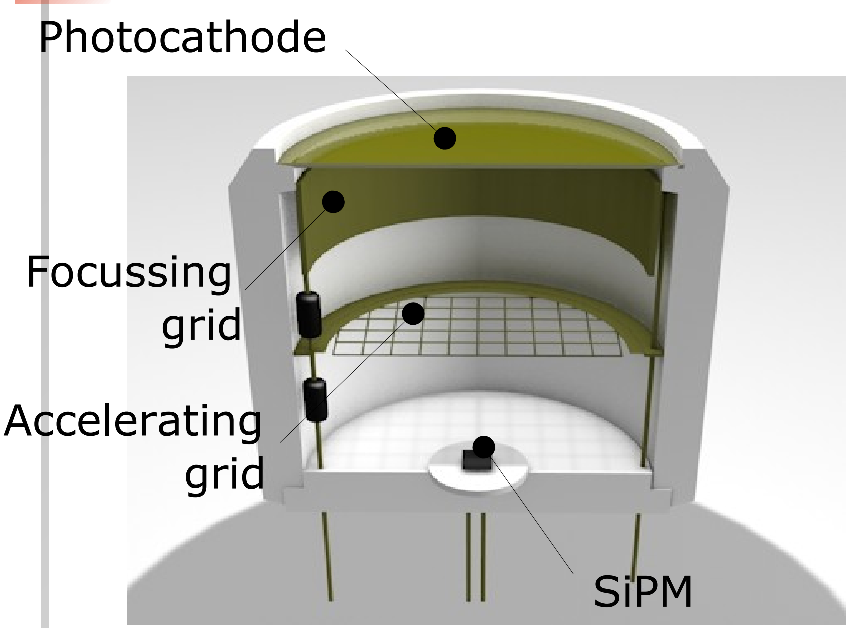

INFN Napoli – Barbarino et al
and Hamamatsu Collaboration

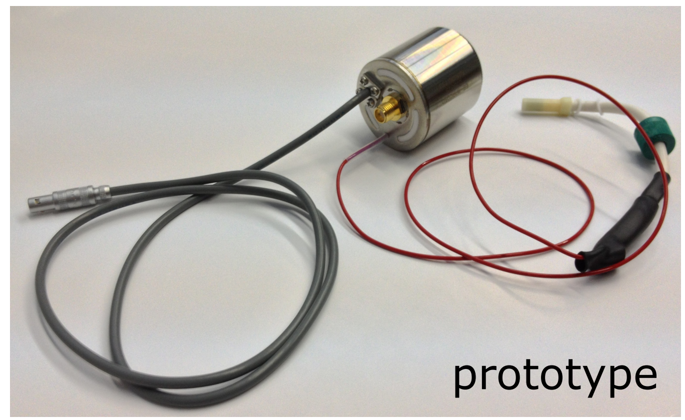

SiPM (Hamamatsu VUV)
- 1x1 mm^2
- No epoxy layer
- Thin SiO2 layer
- p-on-n structures

Photocathode
- NEA (GaAsP) (higher PDE, while SiPM noise dominates)
- 3x3 mm^2

Single photon sensitivity

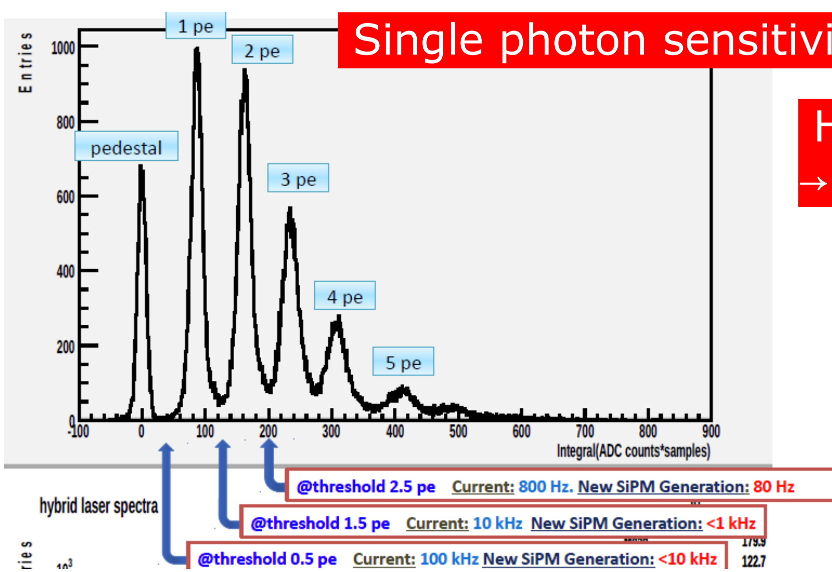

R.de Asmudis IPRD 2013

First measurements (2013)

Homogeneous PDE~0.2 over 7mm^2
→ surface enhancement x7

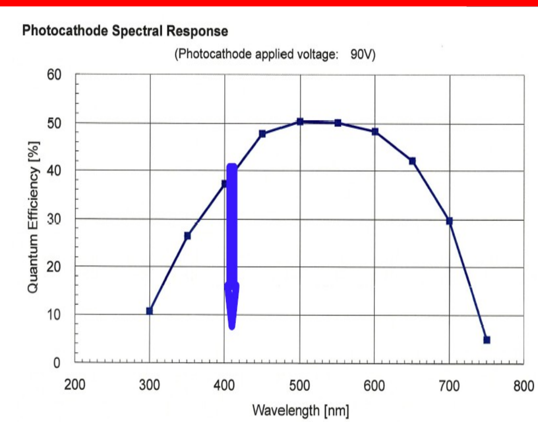

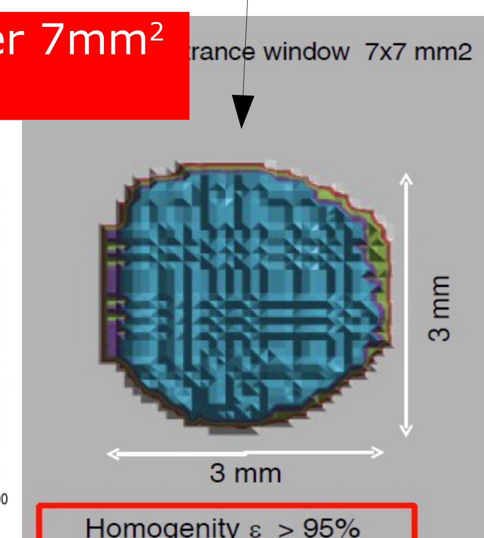

Large Area Photo-Detectors → hybrids

personal comments

Advantages of SiPM vs APD in hybrids

1) high gain in SiPM → no need for bombardment gain, just enough energy for photoelectrons to reach the active region → threshold ~ O(2-3kV)

2) gain stability
   - independent of HV stability
   - SiPM gain more stable than APD

3) less critical HV insulation

Note: can keep over-voltage lower than usual for SiPM (→ lower noise !)

Common disadvantages of hybrids

1) use of Photo-cathode
   - limited PDE
   - limited timing resolution
   - e^- backscattering

2) high vacuum needed
   - ion after-pulsing
   - high production cost (Photo-cathode + high vacuum)

A few examples of Cherenkov detectors base on SiPM

- Large Area with Light concentrators
  → FACT, Belle II, PANDA

- Proximity focusing
  → FARICH with dSIPM

FACT: First G-APD Cherenkov Telescope

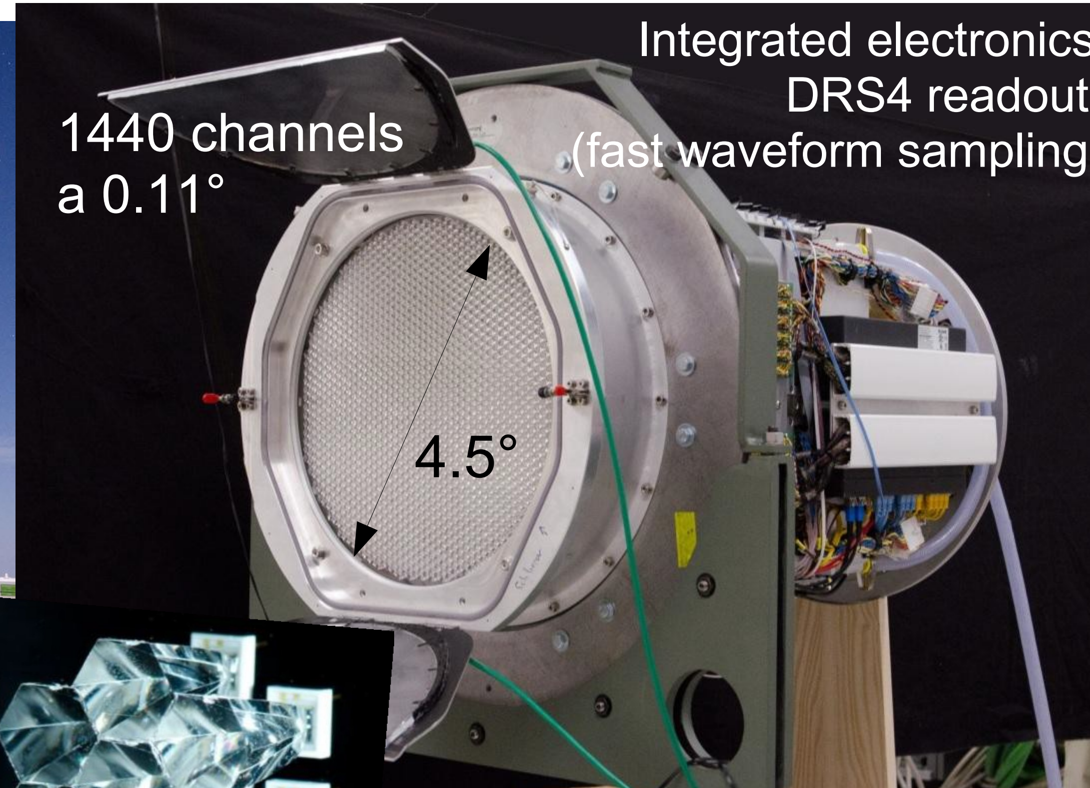

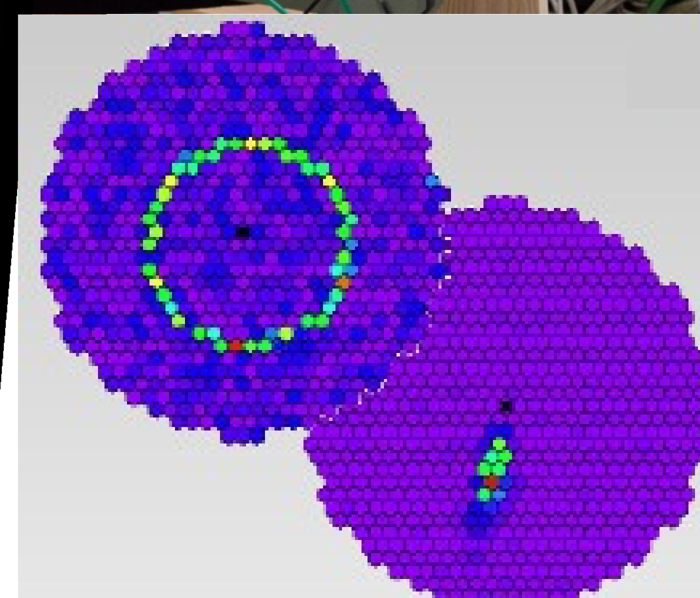

T.Krähenbühl at PhotoDet 2012

Electronics → fast sampling

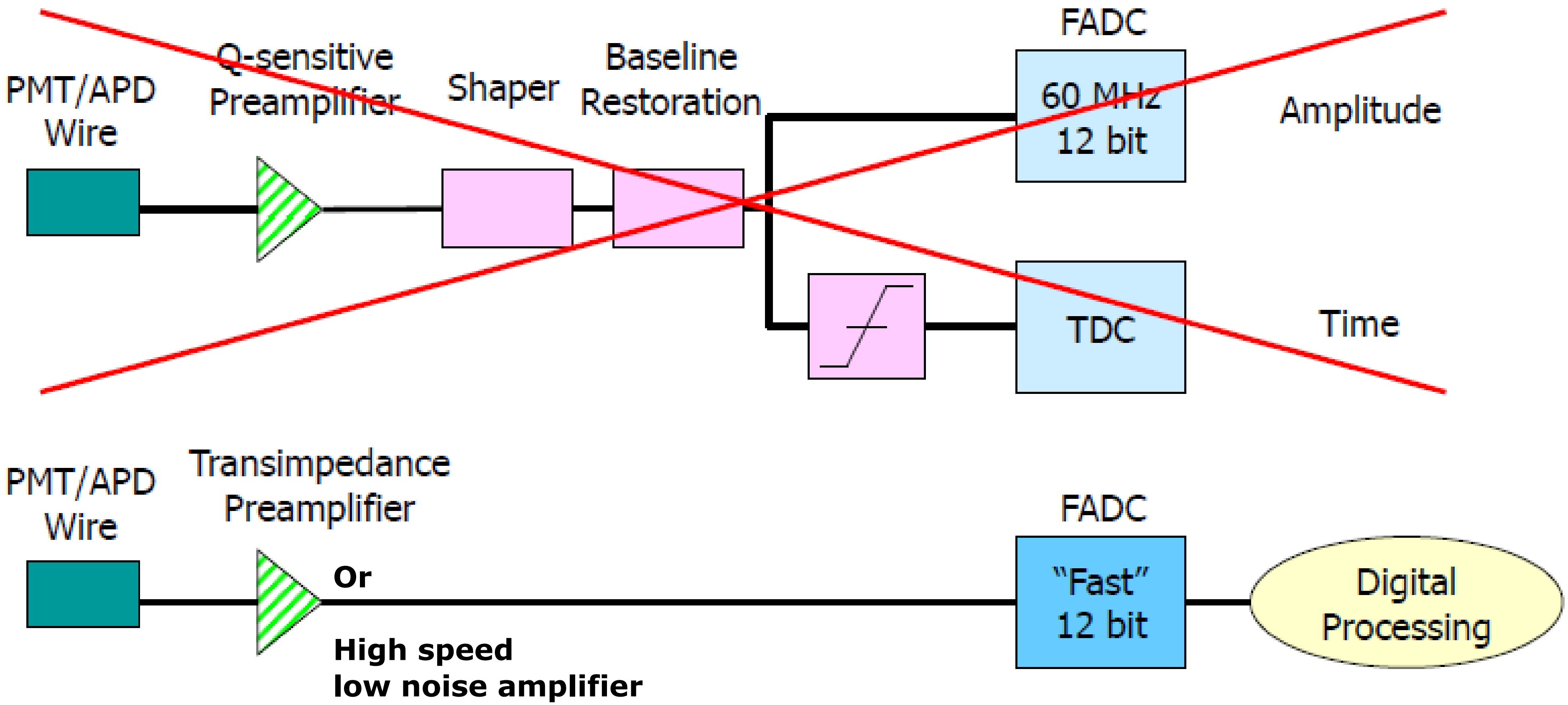

- Shaping stage can only remove information from the signal
- Shaping is unnecessary if FADC is "fast" enough
  = sampling speed 2x maximum frequency (Nyquist-Shannon)
- All operations (CFD, optimal filtering, integration) can be done digitally

PANDA: DIRC with SiPM

Light concentrator → Pyramid shaped funnels guide

→ cost effective — w.r.t. internal reflection
→ less light concentration — Winston cone

DIRC Principle

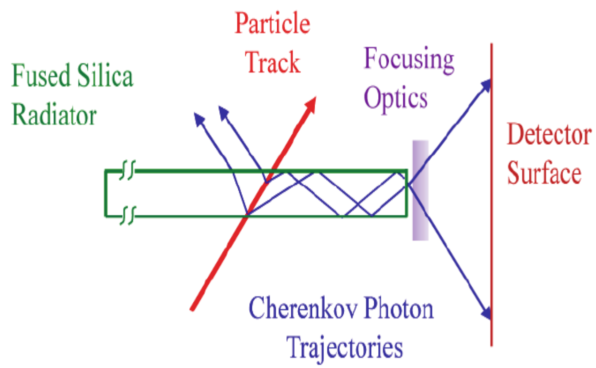

Schwiening, J. GSI

3D schematic of the detector

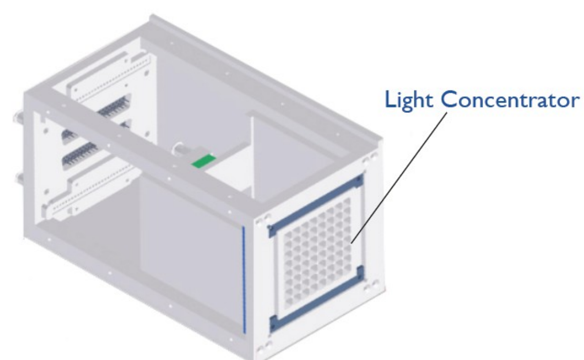

Silicon Photomultiplier (SiPM) Array

- 8x8 cells (Hamamatsu S10931-100P)
- active area of 3x3 mm² each
- pixel size of 100x100 μm²
- Space between SiPMs to fit with light conce-ntrator

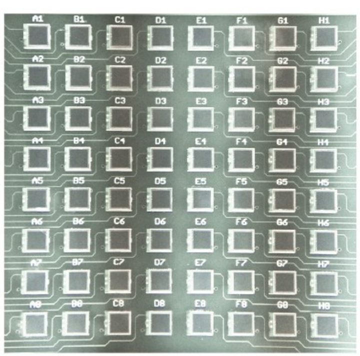

Light Concentrator

- 8x8 pyramid shaped funnels
- 7x7 mm² entrance area
- 3x3 mm² exit area
- Funnel length 4.5 mm
- Material: brass, funnels produced by electroerosion
- Coated with chrome and aluminum

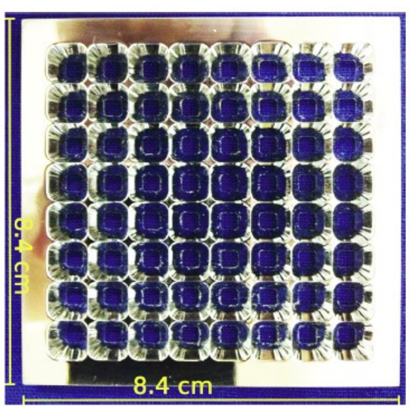

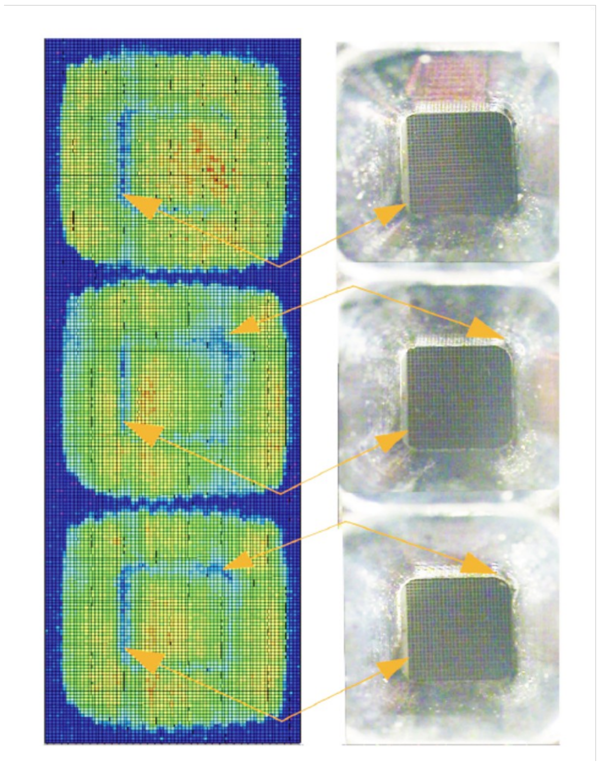

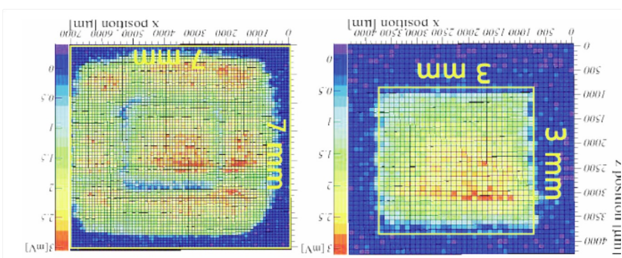

C(θ=0) < Sin/Sout x 80%

M.Rihl Vienna Conference on Instrumentation 2013

FARICH: Focusing Aerogel RICH with d-SiPM

Focusing Aerogel RICH for particle ID

→ Super Charm-Tau Factory (Novosibirsk): μ/π up to 1.7 GeV/c - 21m² detector area (SiPMs)
→ ALICE HMPID: π/K up to 10 GeV/c, K/p up to 15 GeV/c - 3m² area (SiPMs)
→ FWD Spectrometer PANDA: π/K/p up to 10 GeV/c - 3m² area (MaPMTs or SiPMs)

FARICH prototype

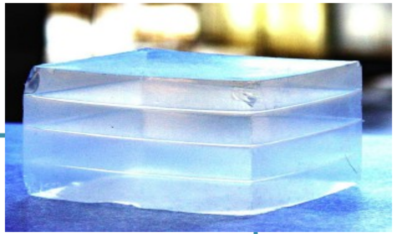

4-layer aerogel
- n_{max} = 1.046
- Thickness 37.5 mm
- Calculated focal distance 200 mm
- Hermetic container with plexiglass window to avoid moisture condensation on aerogel

Square matrix 20x20 cm²
- Sensors: DPC3200-22-44
- 3x3 modules = 6x6 tiles = 24x24 dies = 48x48 pixels in total
- 576 time channels
- 2304 amplitude (position) channels
- 4 levels of FPGA readout: tiles, modules, bus boards, test board

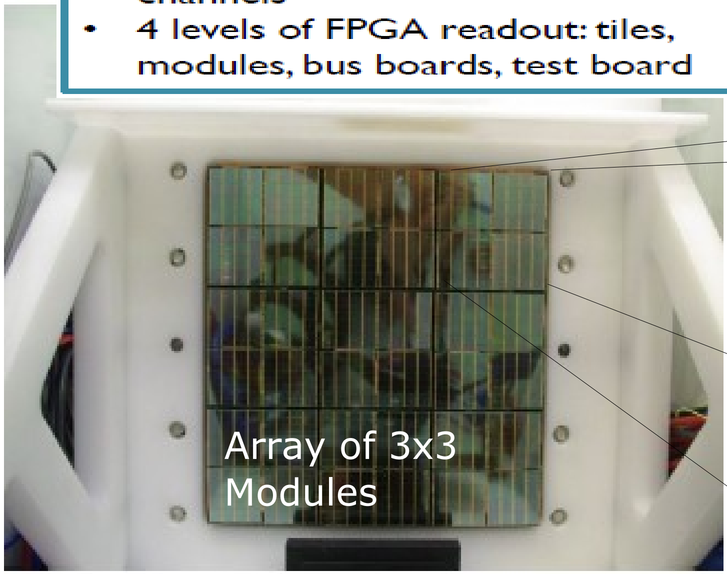

Module = Array of 8 x 8 dSiPMs

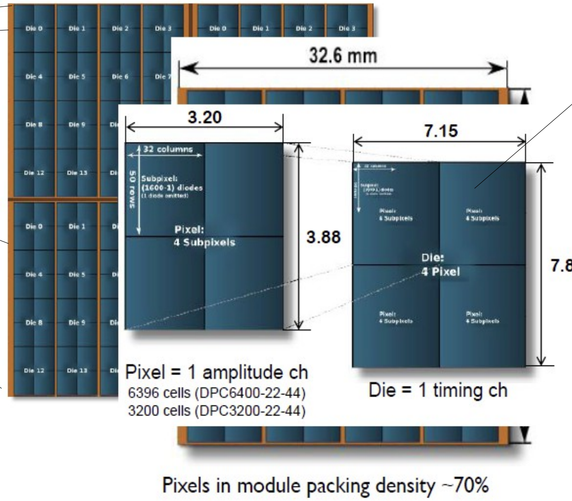

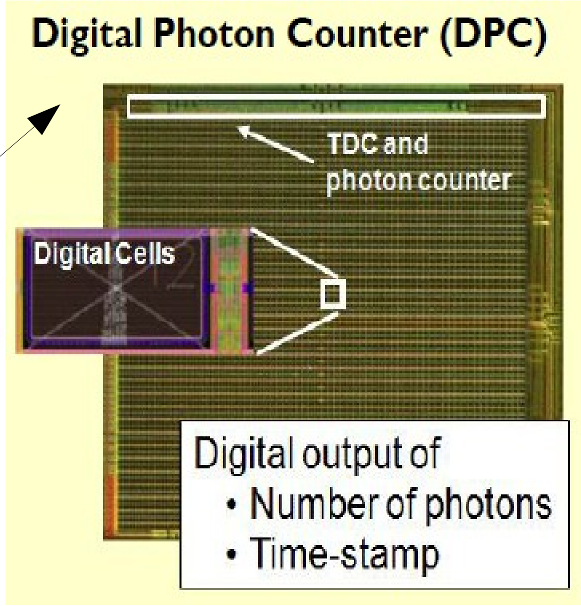

S.Kononov Vienna Conference on Instrumentation 2013

Digital SiPM 8x8 Array

DPC3200-22-44
DPC6400-22-44

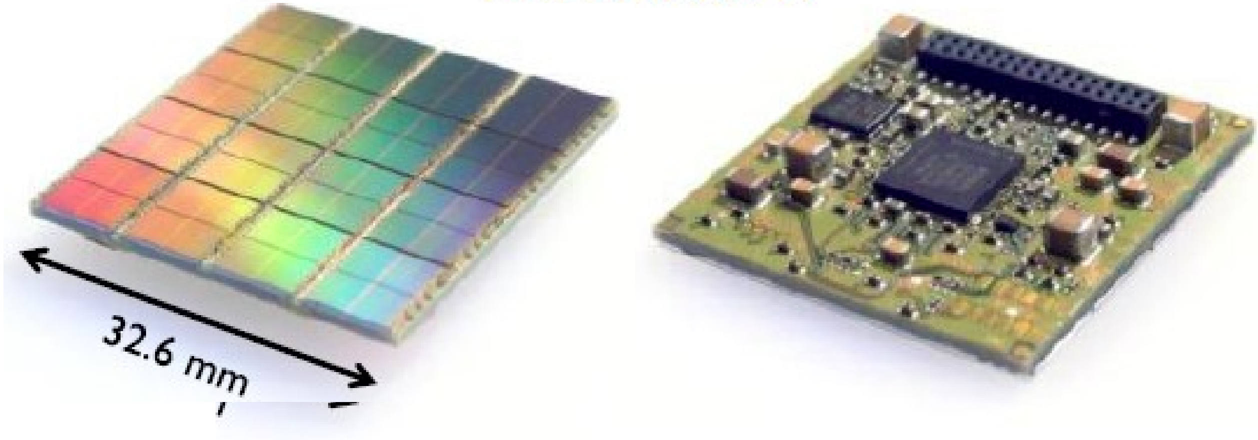

FPGA
- Clock distribution
- Data collection/concentration
- TDC linearization
- Saturation correction
- Skew correction

Flash
- FPGA firmware
- Configuration
- Inhibit memory maps

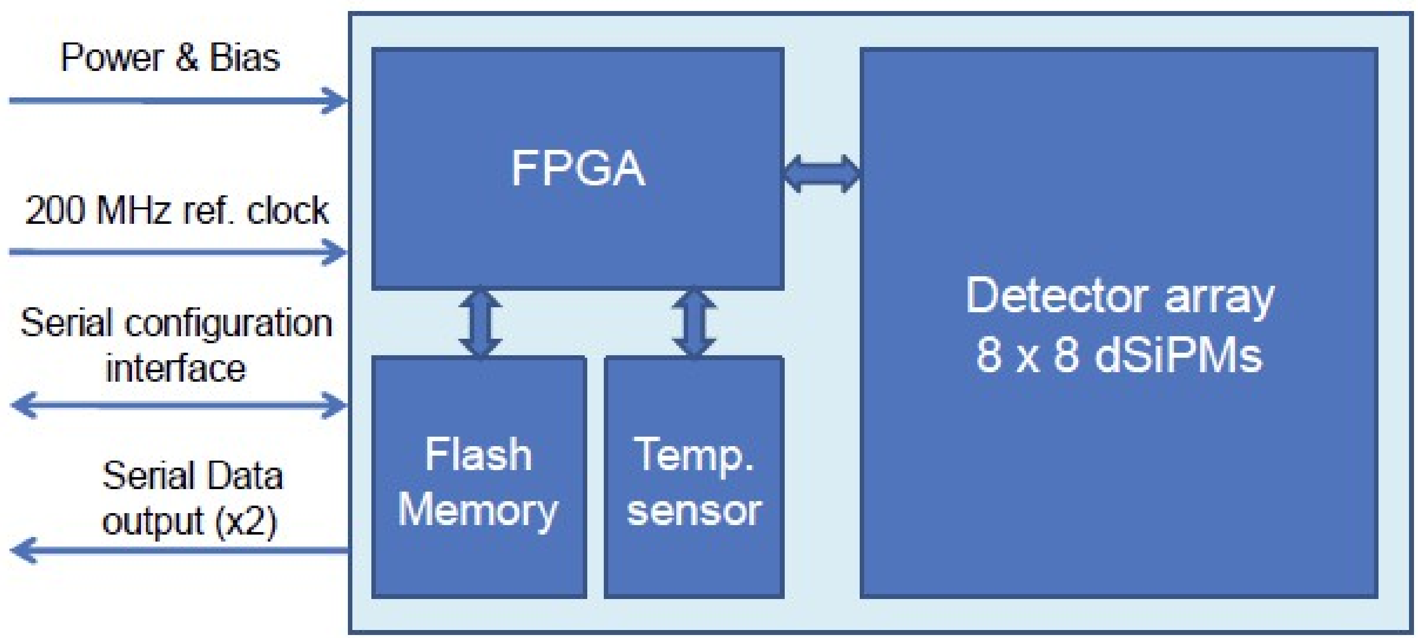

FARICH test beam at CERN T10

Test conditions

- Positive polarity

  $e^+, \mu^+, \pi^+, K^+, p$
- Momentum: 1 - 6 GeV/c
- Trigger: a pair of sc. counters 1.5×1.5 cm² in coincidence separated by ~3 m
- No external tracking, particle ID, precise timing of trigger
- Hardware hit selection in a programmable time window to fit in data bandwidth

Pixel hit map

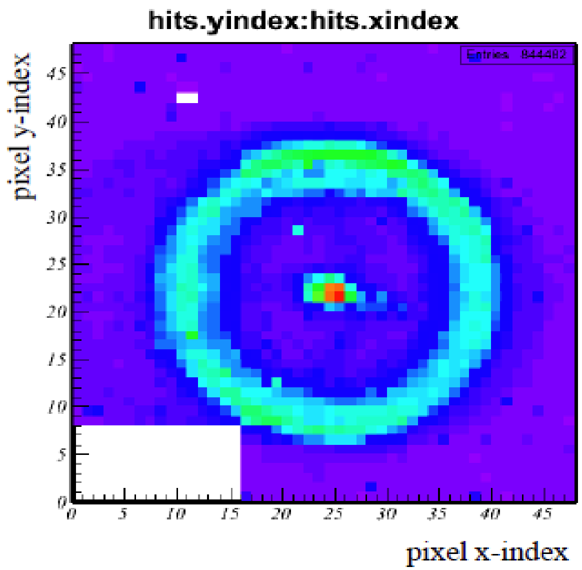

Event by Event ring fit

Hit selection and ring fit:

- Reject central hits
- Select hits in 4 ns time window
- More than 3 selected hits per event
- 4 parameters fitted: X_{center}, Y_{center}, R, t_0

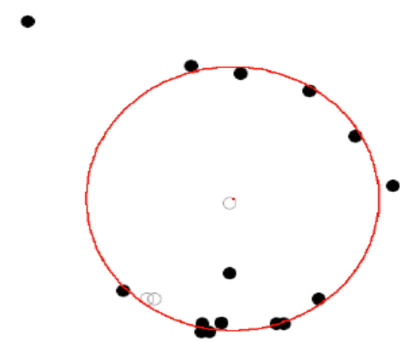

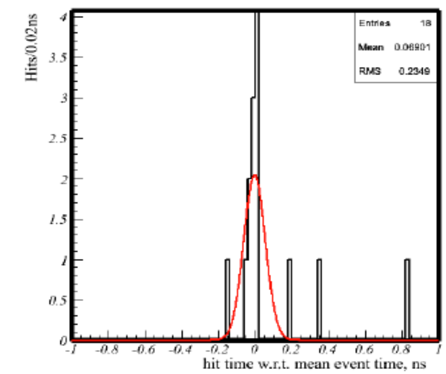

Timing resolution for Cherenkov hits

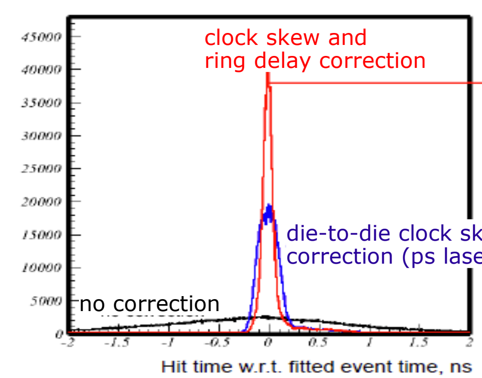

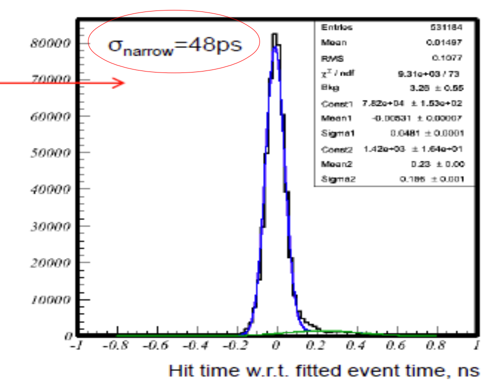

Fit two gaussians plus constant. 90% of area is contained in the narrow gaussian.

FARICH: Momentum dependence

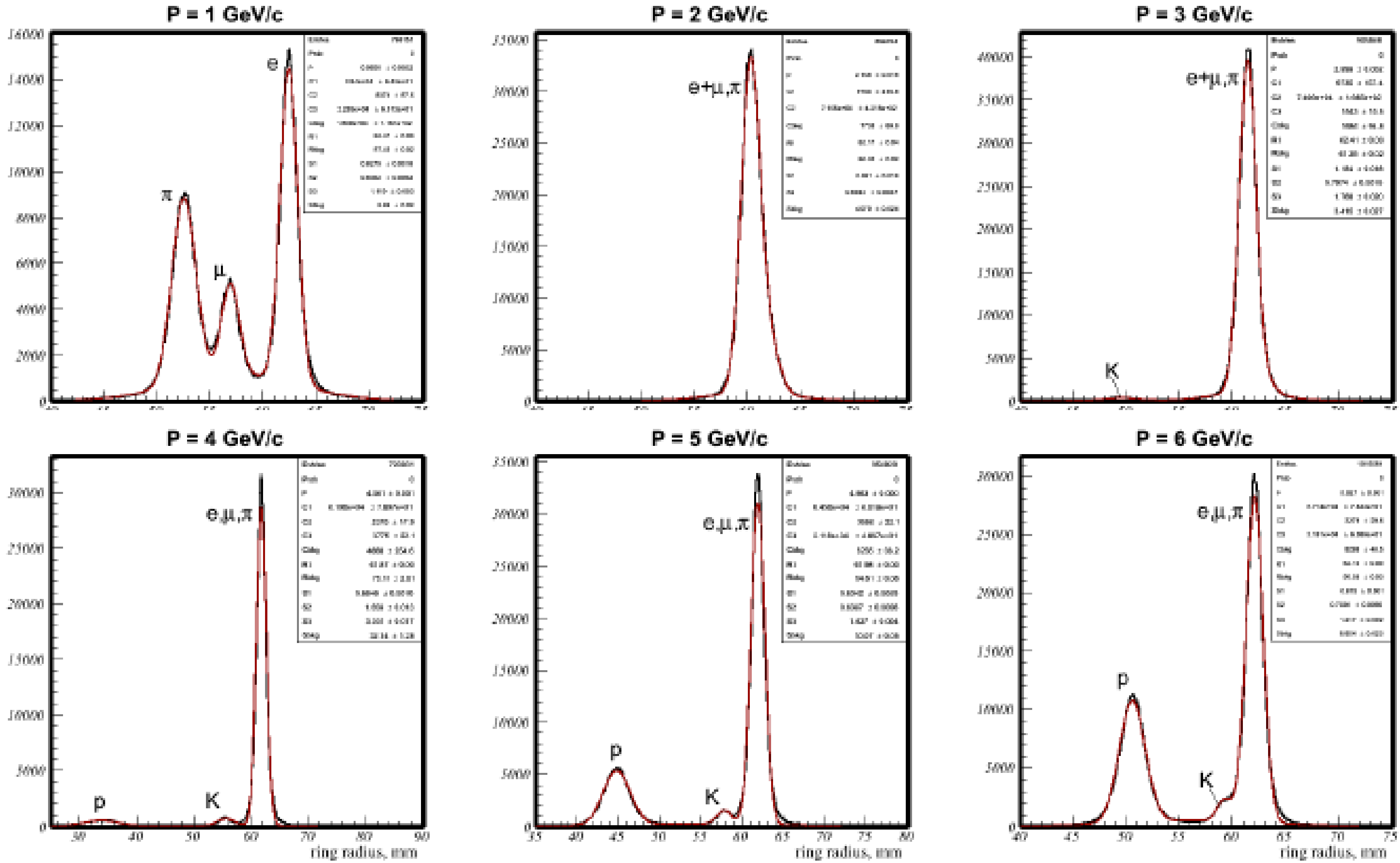

S.Kononov Vienna Conference on Instrumentation 2013

FARICH: Particle separation

$$S = 2\frac{R_\pi - R_K}{(\sigma_\pi + \sigma_K)}$$

S.Kononov Vienna Conference on Instrumentation 2013

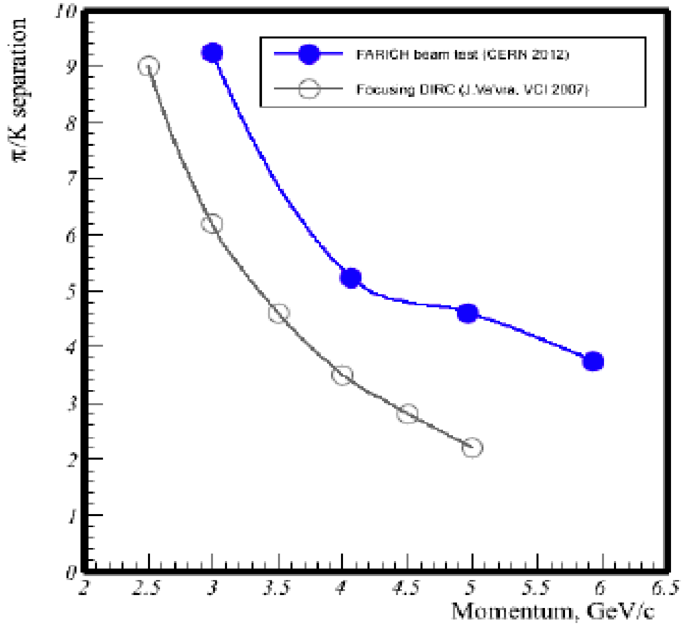

π /K: 3.8σ @ 6GeV/c
μ/π: 4.5σ @ 1 GeV/c

Rather idealized simulation for P=6 GeV/c gives
N_{pe} (π) = 24
π/K separation = 9 σ
Experimental results are far from simulated values, but there are reasons:

- Seems to be lower PDE than measured by PDPC previously (needs to be checked)
- Resolution deterioration due to pixel crosstalk
- No tracking (simulation relies on it)
- Probably: focusing aerogel tested gives wider ring than expected

PDE improvement expected for next generation dSiPM

Impressive anyway !!!

Cross-Talk between dSiPM pairs (same die)

Crosstalk distribution of pixel pairs

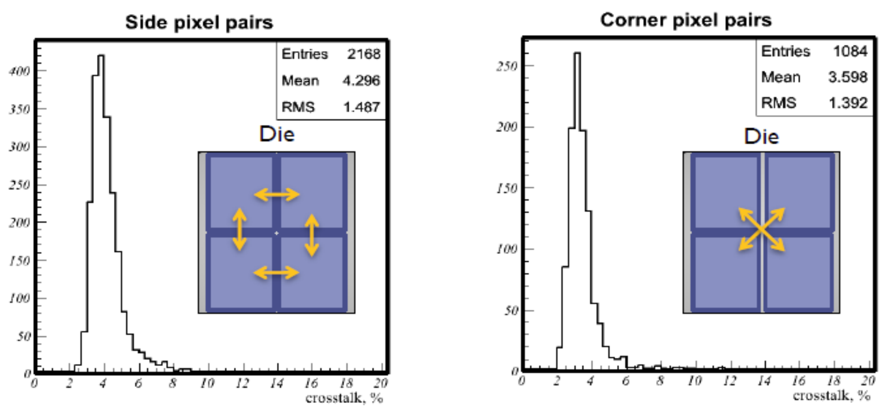

~4% crosstalk probability between pixels of one die → ring radius resolution deterioration

Note (G.C.) : after-pulsing and cross-talk between diodes are kept at very low level by active quenching/reset

Conclusions

PIN photo-diode: No single photon sensitivity

Avalanche photo-diode: massive use in big experiments (CMS at LHC)

- Internal multiplication: S/N improved → still >5 p.e. detectable
- Gain limited by the excess noise due to **avalanche multiplication noise**
- Practical use for single photon only in Hybrid photo-det. (H-APD)

GM-APD based PM: technology of **SiPM** is mature
→ many flavours of SiPM → w/ external ("analog") or integrated electronics
→ candidates for more and more experimental setups including Cherenkov det.
→ price decreasing to 10\$/cm^2 (analog SiPM) ← competition

- **Dark noise (DC)** still the most limiting factor → **limited active area**
  → **large area hybrid detectors** demonstrated feasible (VSiPM or H-GMAPD)

- **Correlated noises (AP,CT)** under control → lower gain (small cells) desirable

… → **tiny cells (low gain)** for reducing noises (DC,AP,CT)
and mitigating radiation damage impact on performances too
→ **active quenching** (Digital-SiPM) is alternative solution those issues ...

- **Low T**: SiPM perform ideally in the range 100K < T < 200K
  → best candidates for applications (superior to PMT also for radio-purity)

Development of GM-APD new directions:
- ultra-fast timing specific SiPM → relatively easy, but still missing
- position sensitive → relatively easy but still missing
- DUV/VUV sensitive devices → can be done with Si, just started
- IR/NIR sensitive devices → possibly based on different semiconductors
- charge particle detection → just started

Thanks for your attention

Additional material →

Photo-detection in two steps

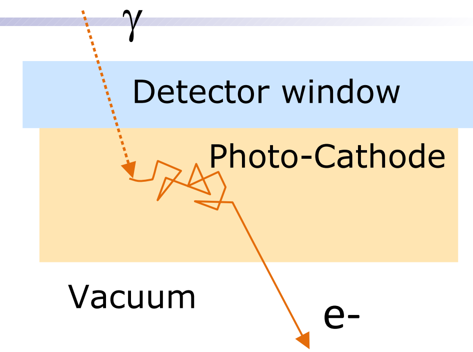

1. Photo-electric conversion with or without emission in vacuum

→ "external" photo-emission

→ "internal" photo-emission

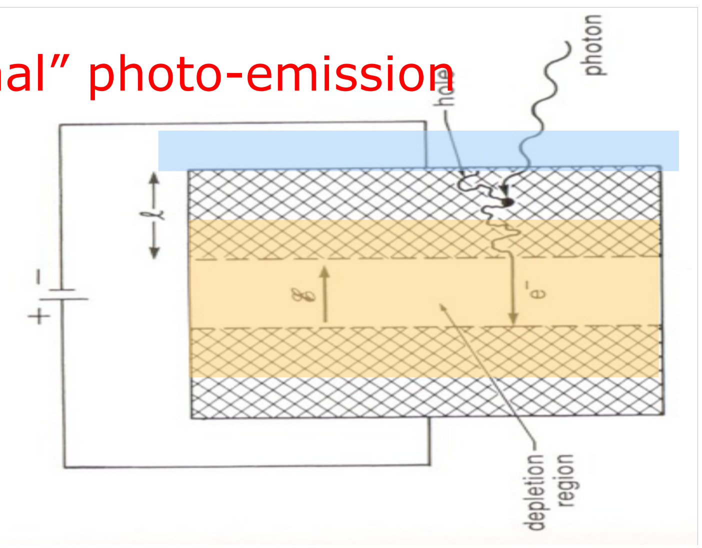

Emission in vacuum implies

→ low detection efficiency

→ low dark count rate

...source of differences between vacuum and solid state devices including multiplication mechanisms...

2. Internal charge multiplication implies

→ better Signal/Noise ratio

→ intrinsic fluctuations in amplitude and timing (depending on the multiplication mechanism)

Photo-detector family tree

Gas
External photoemission

gas photoionization
(TMAE, TEA, …)

and/or

multiplication in gas
by avalanche
(MWPC, GEM, …)

Vacuum devices
External photoemission

secondary electron multiplication

Dynodes:
- discrete (PMT)
- continuous dynode (channeltron, MCP)

Anode:
- multi-anode
- strip lines RF

hybrid
photocathode +

- multiplication by **ionization in Si** (HPD, HAPD, …)

or

- multiplication by **luminescent anodes** (light amplifiers: SMART/Quasar, X-HPD, …)

Solid state
Internal photoemission

- Photo-Diode (PD)
- Avalanche PD (APD)
- GM-APD (SPAD, SiPM)

- Imaging CMOS, CCD

- Quantum well detectors
- Supercond. Tunnel Junc.

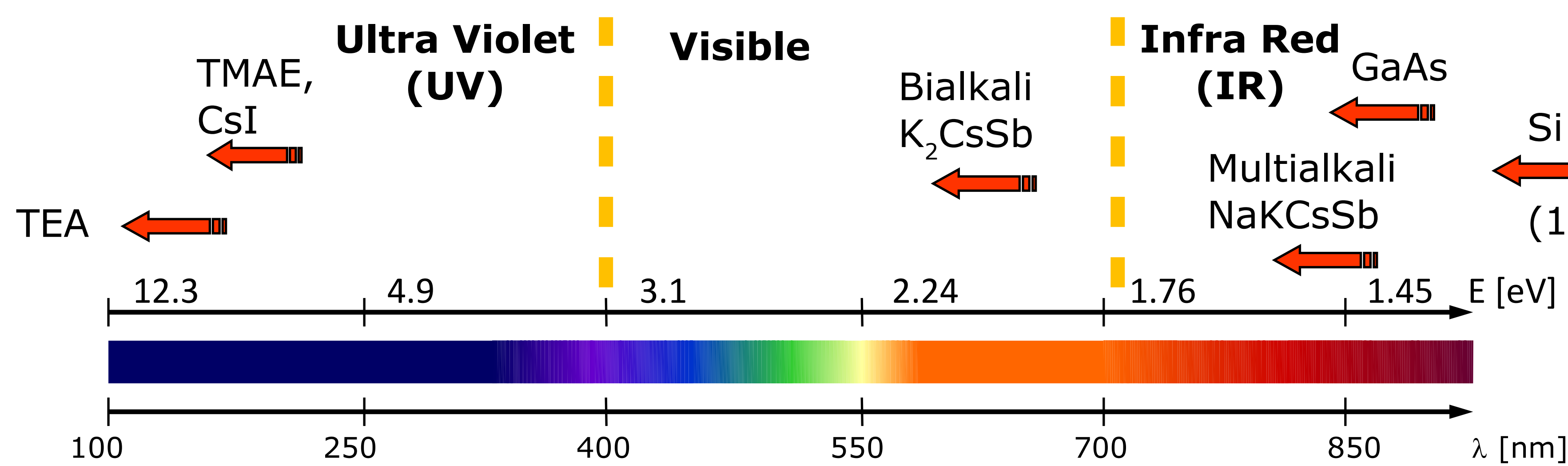

Geiger Mode APD → SPAD

· Two types of implementation (→ arrays)

planar -

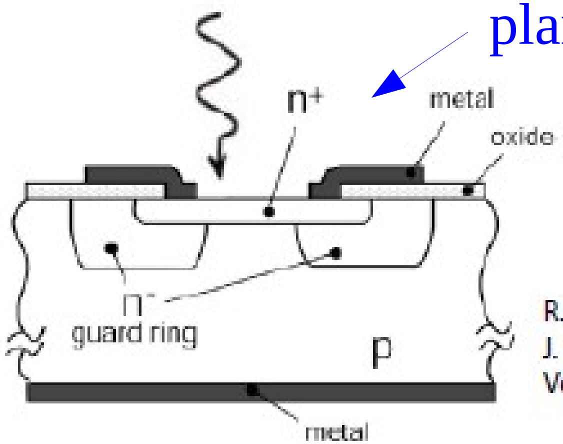

R.H. Haitz
J. Appl. Phys.,
Vol. 36, No. 10 (1965) 3123

- reach through

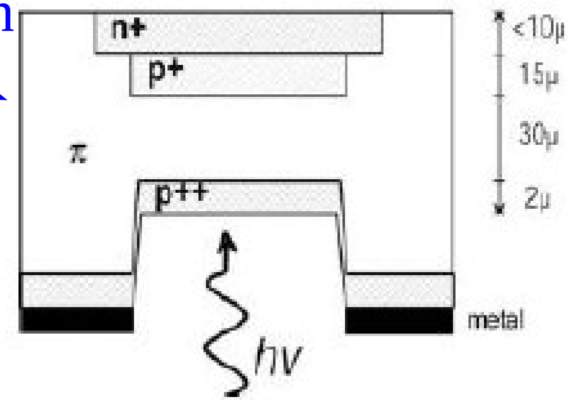

J.R. McIntire
IEEE Trans. Elec. Dev.
ED-13 (1966) 164

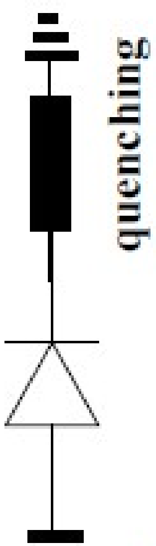

$-V_{bias}$

- Quenching mechanisms
  - Passive quenching: large resistance
  - Active quenching: analog circuits

S. Cova & al., App. Opt. 35 (1996) 1956-1976

Standard output signal
$Q = 10^5\text{-}10^6 e$

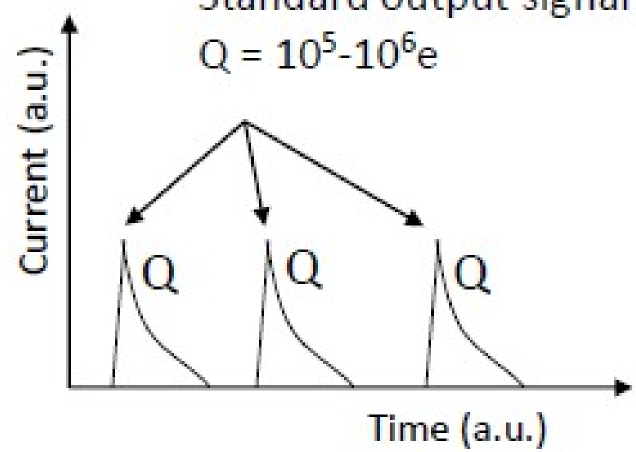

Binary device

- If one or more simultaneous photons fire the GM-APD, the output is anytime a standard signal: $Q \sim C(V_{bias} - V_{BD})$
- GM-APD does not give information on the light intensity

Today

Many institutes/companies involved in SiPM development/production

- **CPTA**, Moscow, Russia
- **MePhi/Pulsar** Enterprise, Moscow, Russia
- **Zecotek,** Vancouver, Canada
- **Hamamatsu HPK**, Hamamatsu, Japan
- **FBK-AdvanSiD**, Trento, Italy
- **ST Microelectronics**, Catania, Italy
- **Amplification Technologies** Orlando, USA
- **SensL**, Cork, Ireland
- **MPI-HLL**, Munich, Germany
- **RMD**, Boston, USA
- **Philips**, Aachen, Germany
- **Excelitas** tech. (formerly Perkin-Elmer)
- **KETEK**, Munich, Germany
- **National Nano Fab Center**, Korea
- **Novel Device Laboratory** (**NDL**), Bejing, China
- **E2V**
- **CSEM**

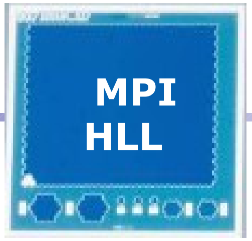

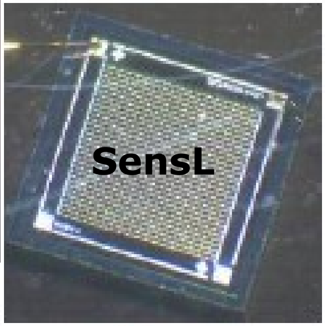

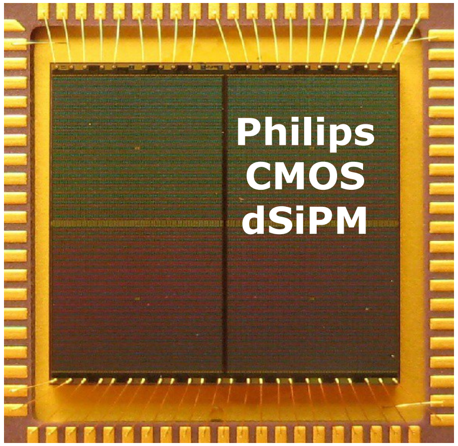

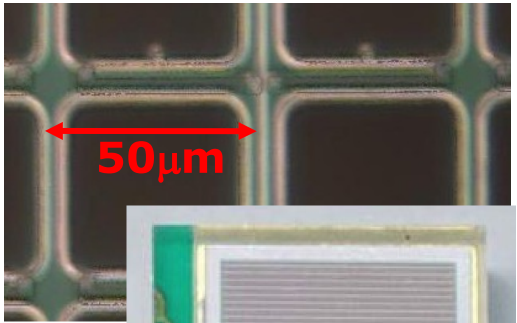

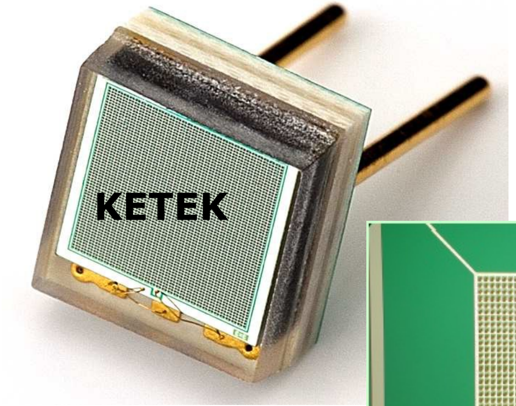

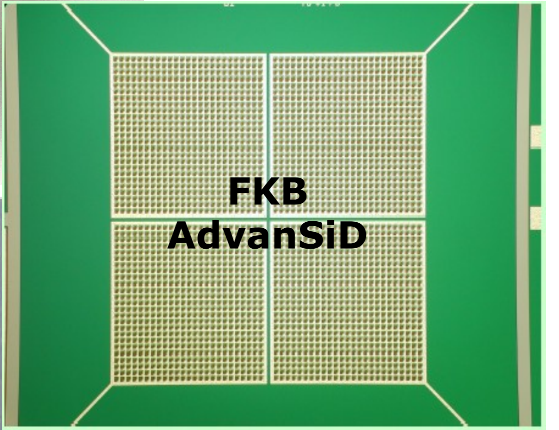

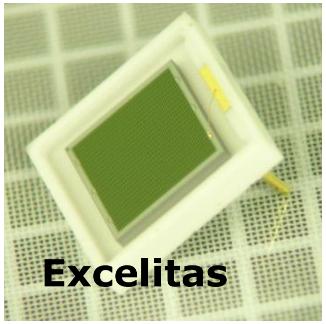

Amplification Technologies (DAPD)

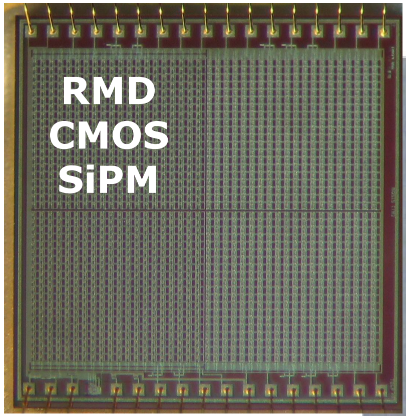

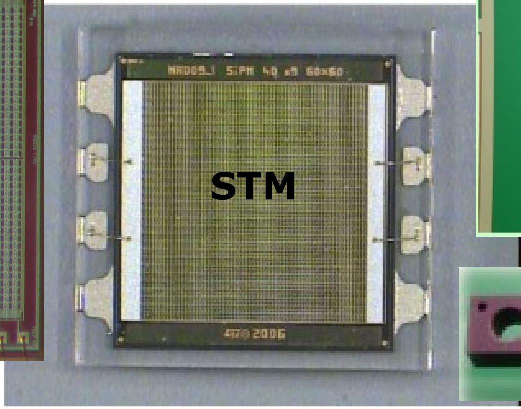

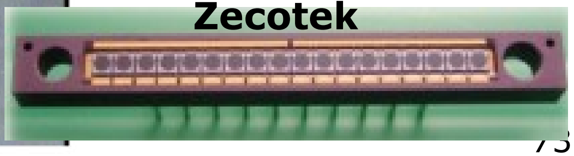

Discrete arrays

Producer	Device ID	Picture	Total area (mm^2)	SiPM area (mm^2/channel)	Nr. channels	µcell size
Hamamatsu	S11064-025P S11064-050P	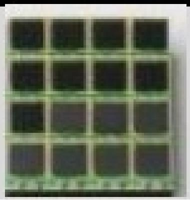	18 x 16.2	3x3	16(4x4) ch	25x25 µm 50x50 µm
Hamamatsu	C11206-0404DF	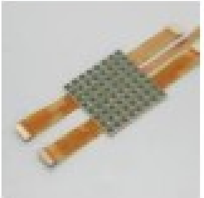		3x3	64(8x8) ch	
Hamamatsu	S11834-3388DF		72x64.8	3x3	256(16x16)ch	
FBK AdvanSiD	ASD-SiPM4s-P-4x4T-50 ASD-SiPM4s-P-4x4T-69	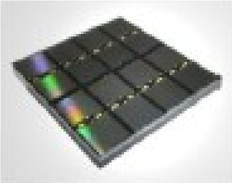	8.2 x 8.2	4x4	16(4x4) ch	50x50 µm 69x69 µm
FBK AdvanSiD	SiPM tile	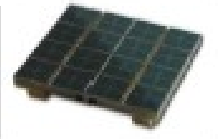	32.7x32.7	4x4	64(8x8) ch	
SensL	ArraySM-4P9 ArraySB-4P9 (blue sensitive)		46.3 x 47.8	3x3	144(12x12) ch (based on monolithic Array SM4)	35x35 µm

Monolithic Arrays

Producer	Device ID	Picture	Effective area (mm^2)	SiPM area/channel (mm^2)	Nr. channels	µcell size
Hamamatsu	S10984-025P S10984-050P S10984-100P	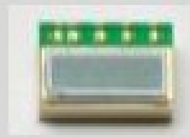	1 x 4	1x1	4(1x4) ch	25x25 µm 50x50 µm 100 x 100 µm
Hamamatsu	S10985-025C S10985-050C S10985-100C	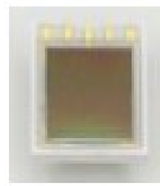	6 x 6	3x3	4(2x2) ch	25x25 µm 50x50 µm 100 x 100 µm
Hamamatsu	S11828-3344M	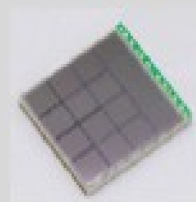	12 x 12	3x3	16(4x4) ch	50x50 µm
FBK AdvanSiD	ASD-SiPM1.5s-P-8X8A	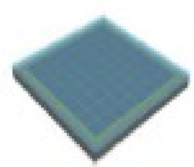	11.6 x 11.6	1.45x1.45	64(8x8) ch	50x50 µm
FBK AdvanSiD	ASD-SiPM3S-P-4X4A	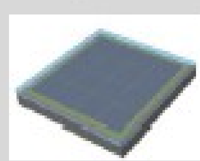	11.8 x 11.8	2.95x2.95	16(4x4) ch	50x50 µm
SensL	Array SM-4 Array SB-4 (blue sensitive)	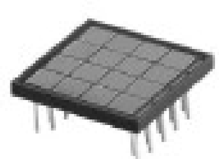	12 x 12	3x3	16(4x4) ch	35x35 µm

Technologies around the world

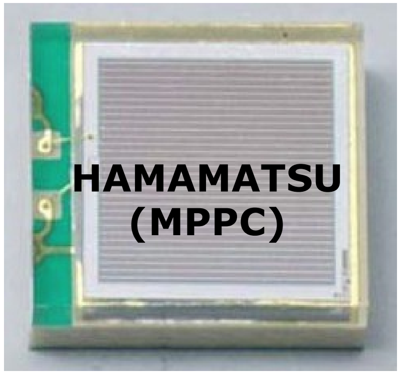

Pioneering work in '90s by Russian institutes

- **CPTA**, Moscow
- **JINR**, Dubna

Metal-Resistive-Semiconductor

- **MePhi/Pulsar** Enterprise, Moscow **Poly-silicon resistor**

+ Metal resistor
+ VUV technology

Today many players involved

- **Hamamatsu HPK**, Hamamatsu
- **FBK-AdvanSiD**, Trento
- **SensL**, Cork
- **ST Microelectronics**, Catania
- **Excelitas** techn. (formerly Perkin-Elmer)
- **National Nano Fab Center**, Korea
- **Novel Device Laboratory** (**NDL**), Bejing

+ SiPM Matrixes,
both p-on-n and n-on-p
+ vias to avoid bonding

Poly-silicon resistor

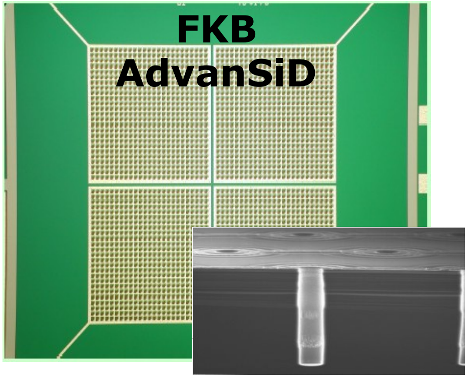

- **MPI-HLL**, Munich — **Resistor embedded in the bulk**
- **RMD**, Boston — **CMOS process**
- **Philips**, Aachen — **Digital SiPM (CMOS)**
- **Zecotek,** Vancouver — **Quenching with floating wells**
- **Amplification Technologies**, Orlando

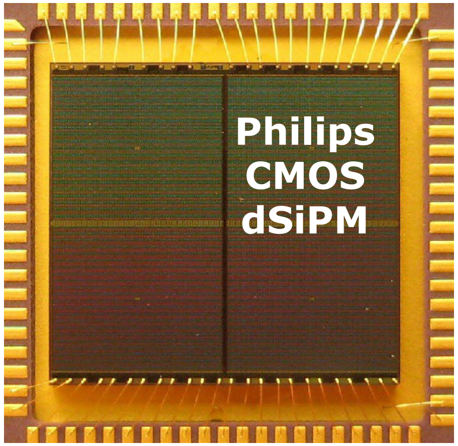

Some are commercially available, other are prototypes

Passive Quenching: tread-off τ_{quench} vs $\tau_{recovery}$

If R_Q is high enough the internal current is so low that statistical fluctuations may quench the avalanche

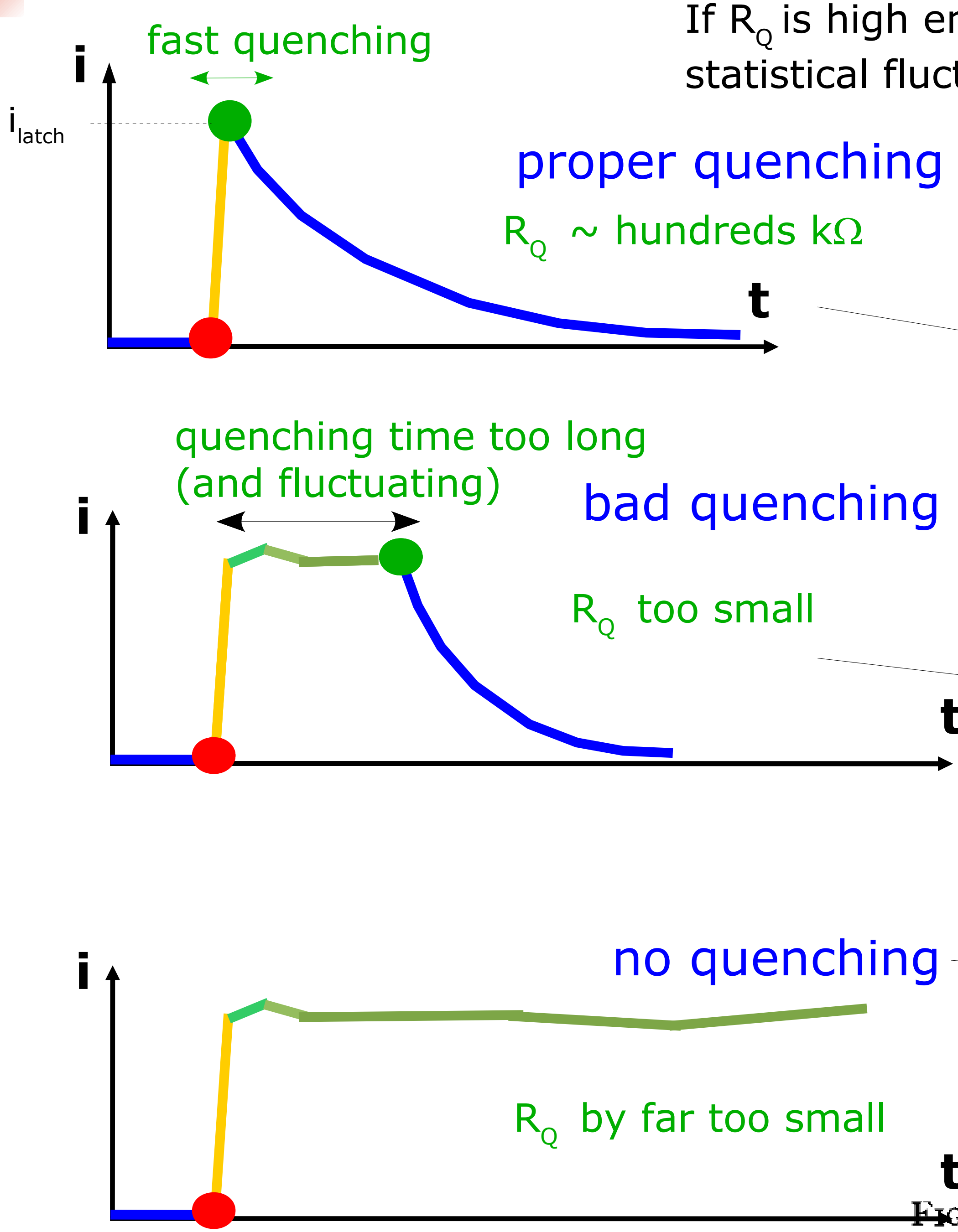

Haitz JAP 35 (1964)

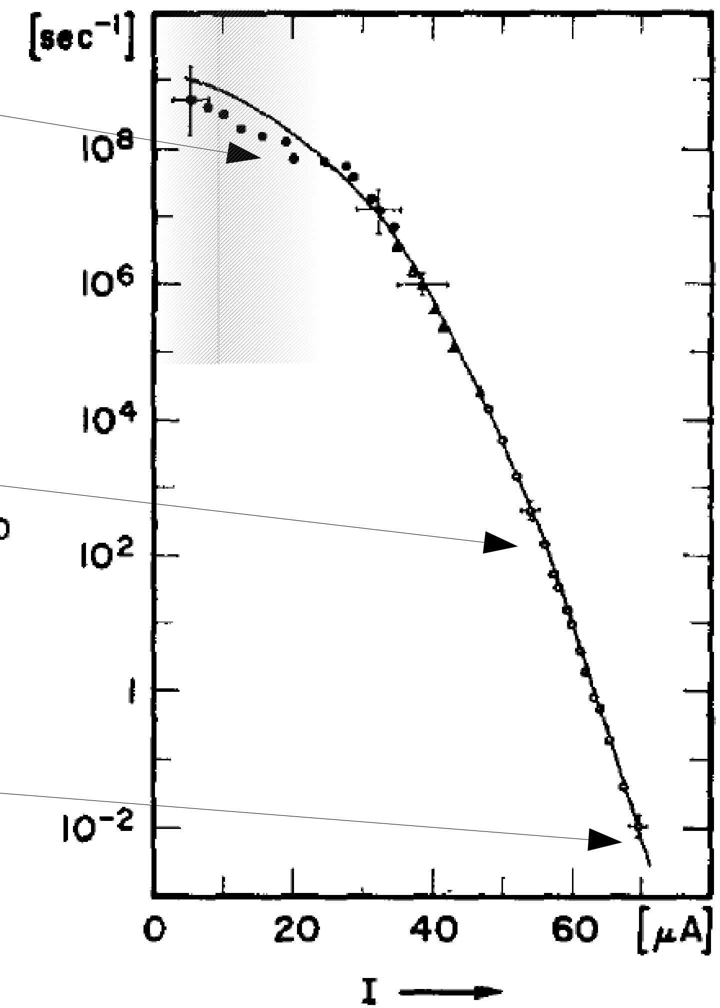

FIG. 2. Turnoff probability per second as function of pulse cu

Quenching resistor

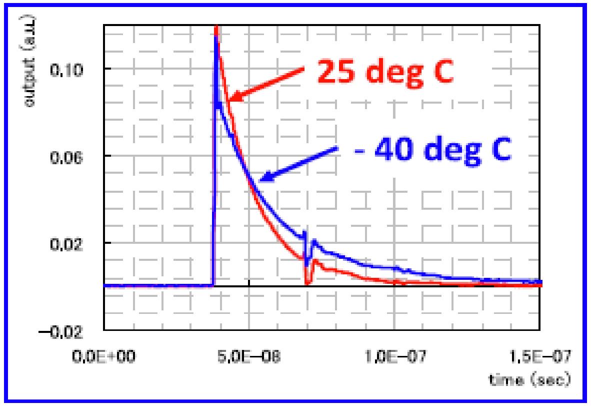

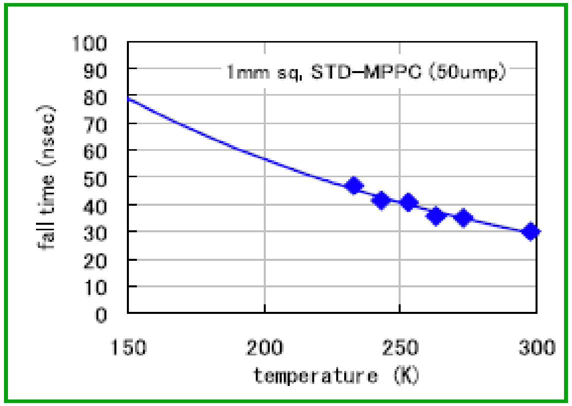

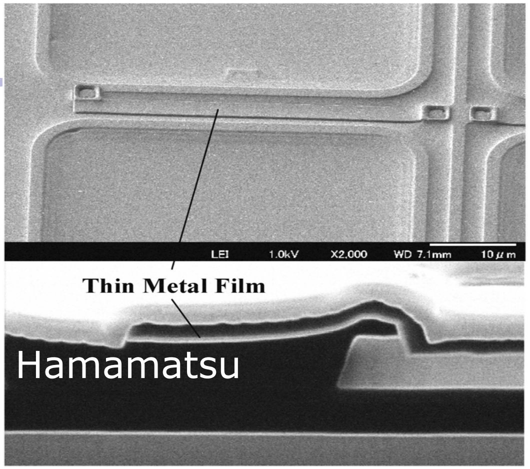

Adopting metal quenching resistor

The quenching resistor value increases as environmental temperature decreases. The larger resistor makes the pulse amplitude lower and the tail longer.

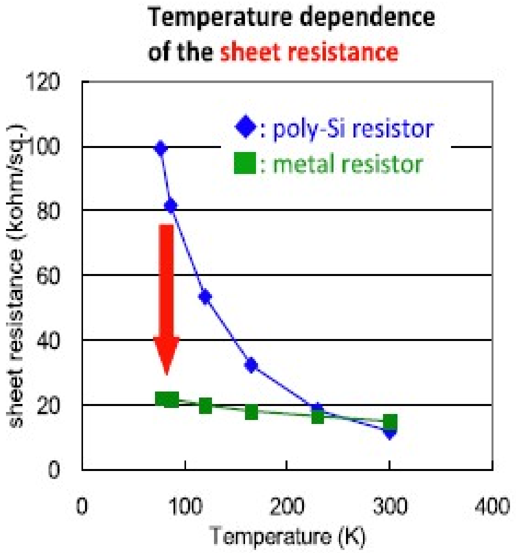

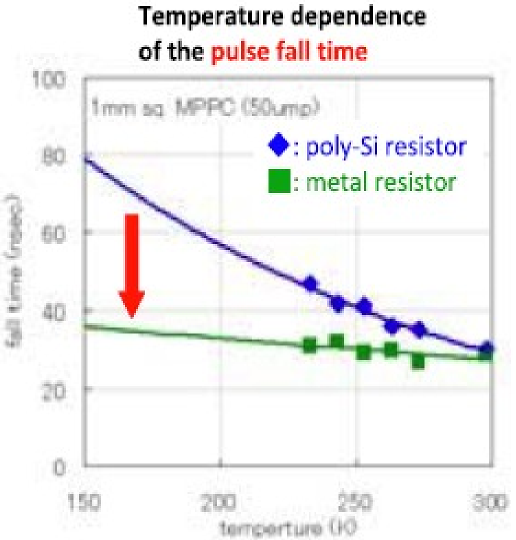

Improved temperature stability

Recent progresses of Hamamatsu devices

Metal quenching resistor achieved 1/5 temperature dependence

Pulse shape: dependence on Temperature

The two current components behave differently with Temperature
→ fast component is independent of T because C_{tot} couples to external R_{load}
→ slow component is dependent on T because $C_{d,q}$ couple to $R_q(T)$

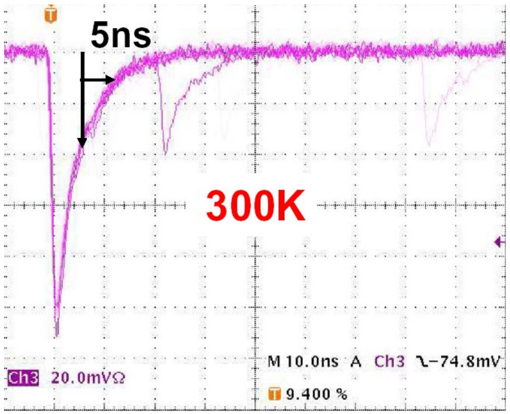

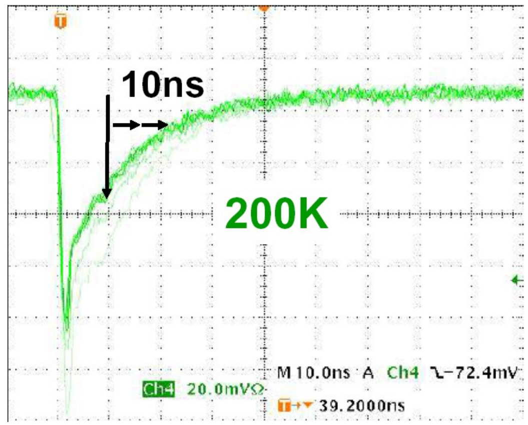

HPK MPPC

H.Otono, et al. PD07

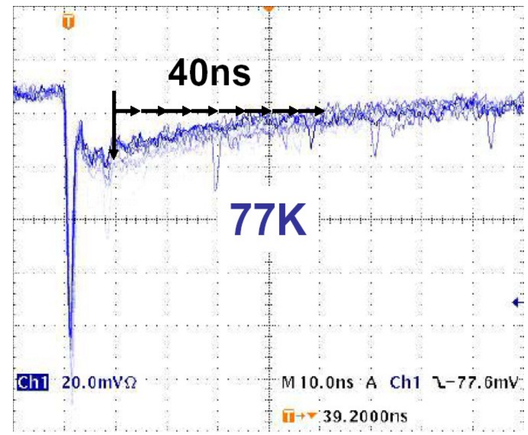

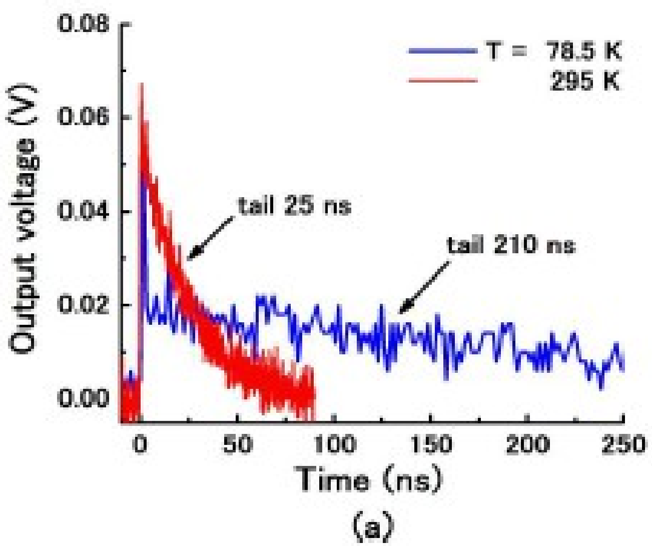

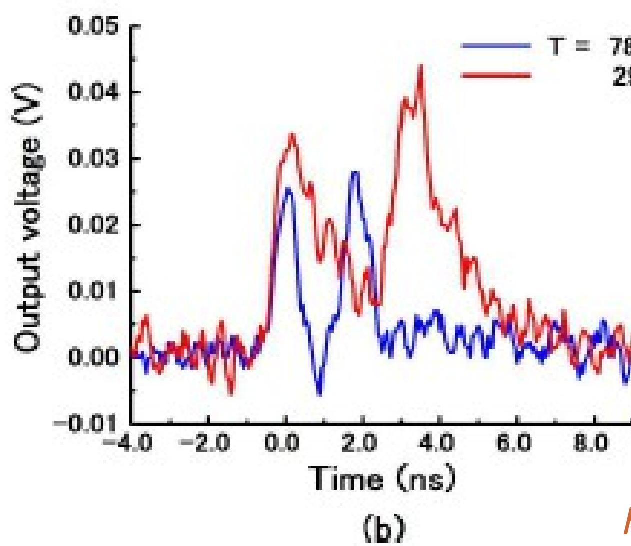

high pass filter / shaping
→ recover fast signals

HPK MPPC

Fig. 2. (a) Output signals from the MPPC when no high-pass filter is used, and (b) output signals from the high-pass filter when two pulses were generated successively.

Akiba et al Optics Express 17 (2009) 16885

Passive / Active quenching and recharge

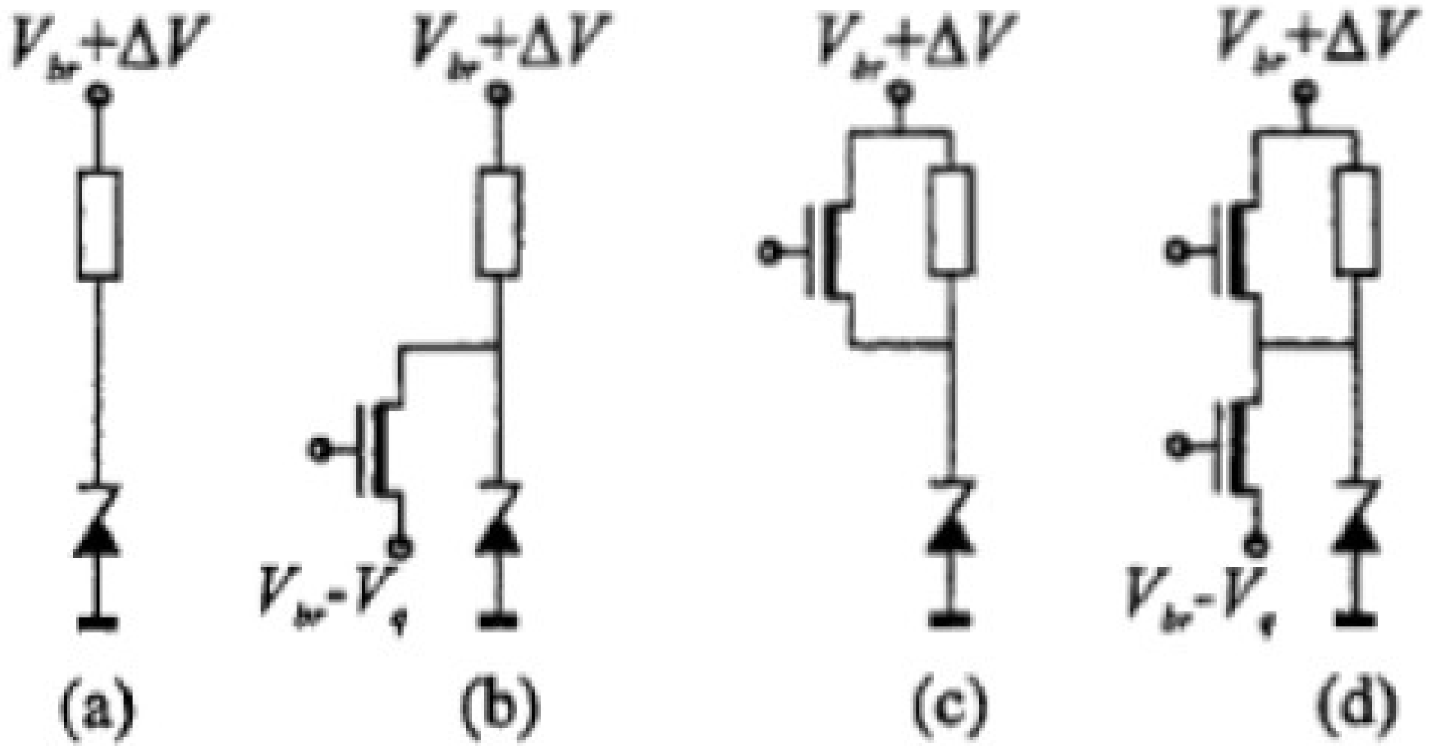

Figure 3 – Four Quenching Circuit Schematics: (a) passive quench; (b) active quench; (c) active recharge; (d) active quench and recharge (Kindt and de Langen 1998)

Reverse I-V

→ Dark Current behavior
and V_{bd} measurement

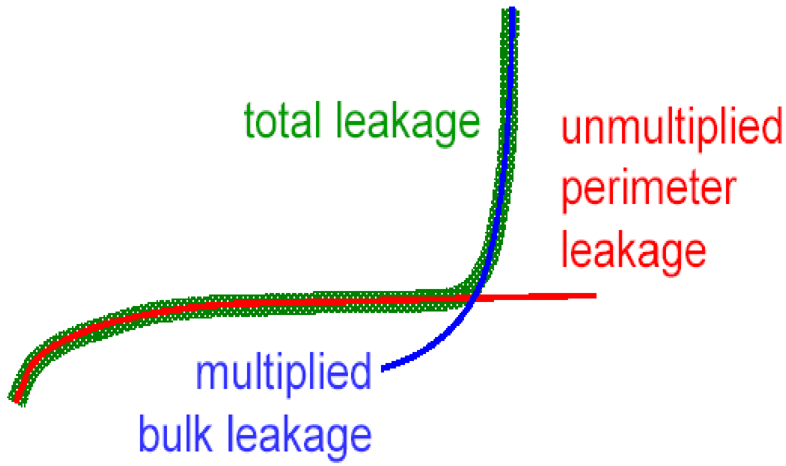

~ linear with Vbias → linear with ΔV (overvoltage)

~q · Gain (G) · Dark Count Rate (DCR)
~ q · ΔV · ΔV → quadratic with ΔV

Note:
- G is linear with ΔV
- Dark Count Rate is ~PDE which is linear with ΔV
  (at least for few volts)

Reverse I-V characteristics at fixed T

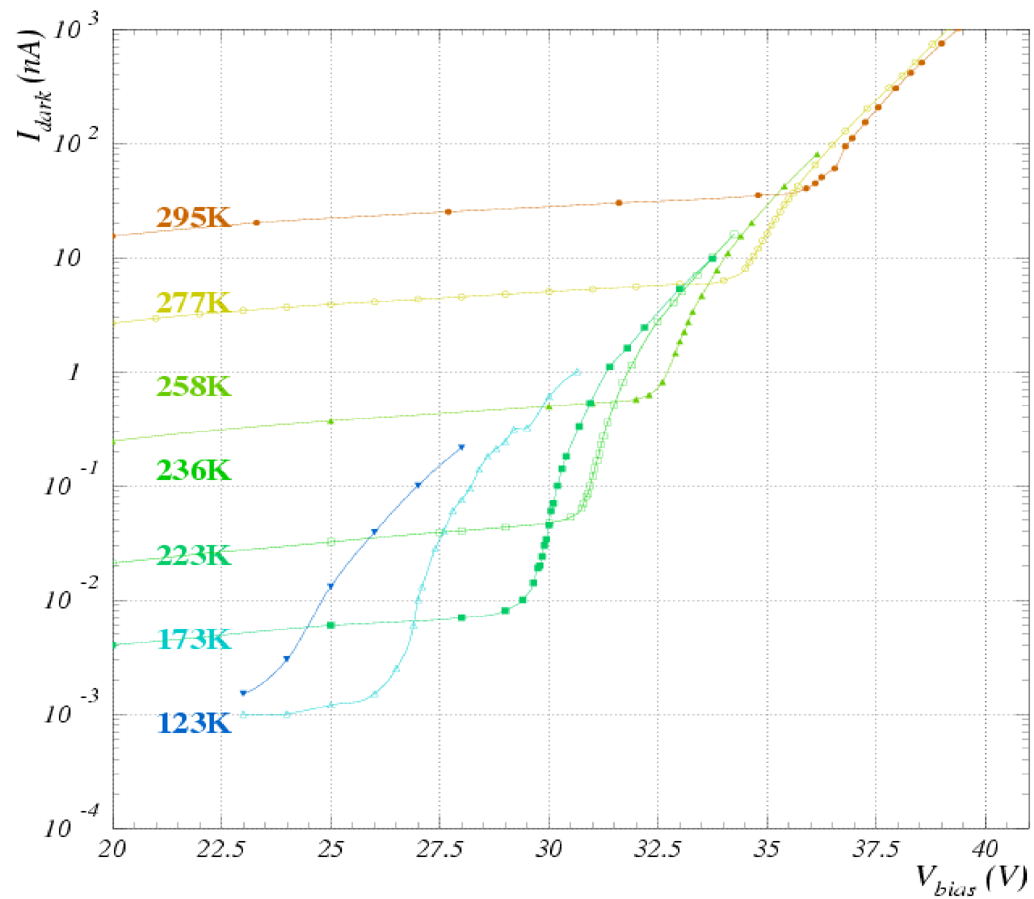

Improved V_{bd} temperature coefficient

Engineering high electric field & depletion/drift layer profiles

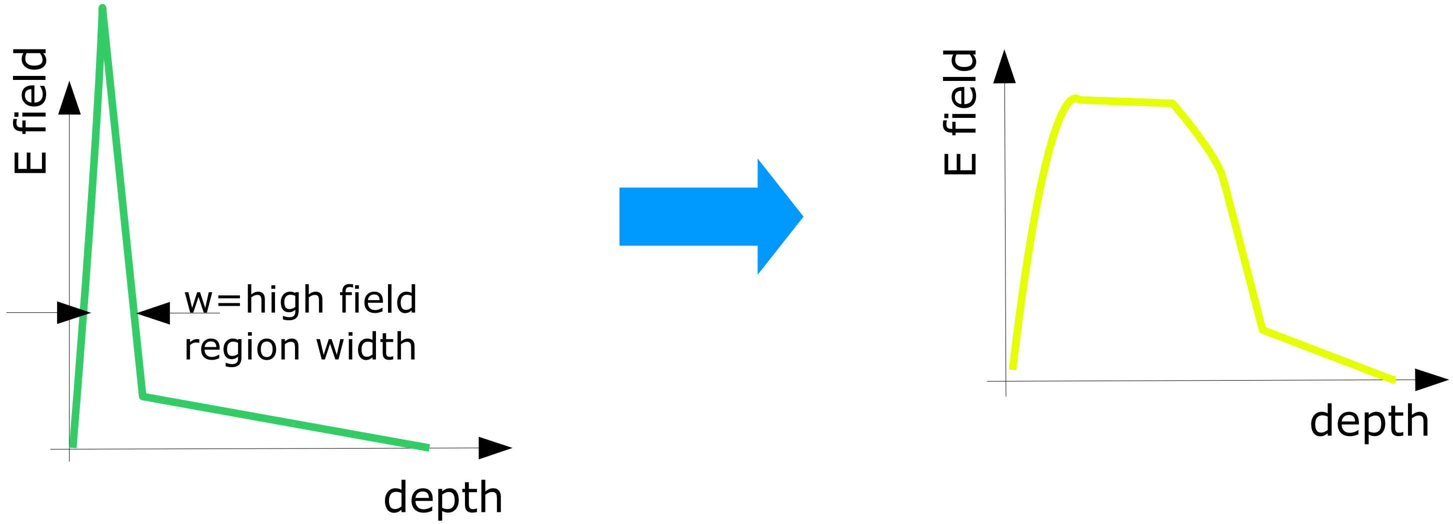

→ Improved stability & working over-voltage range

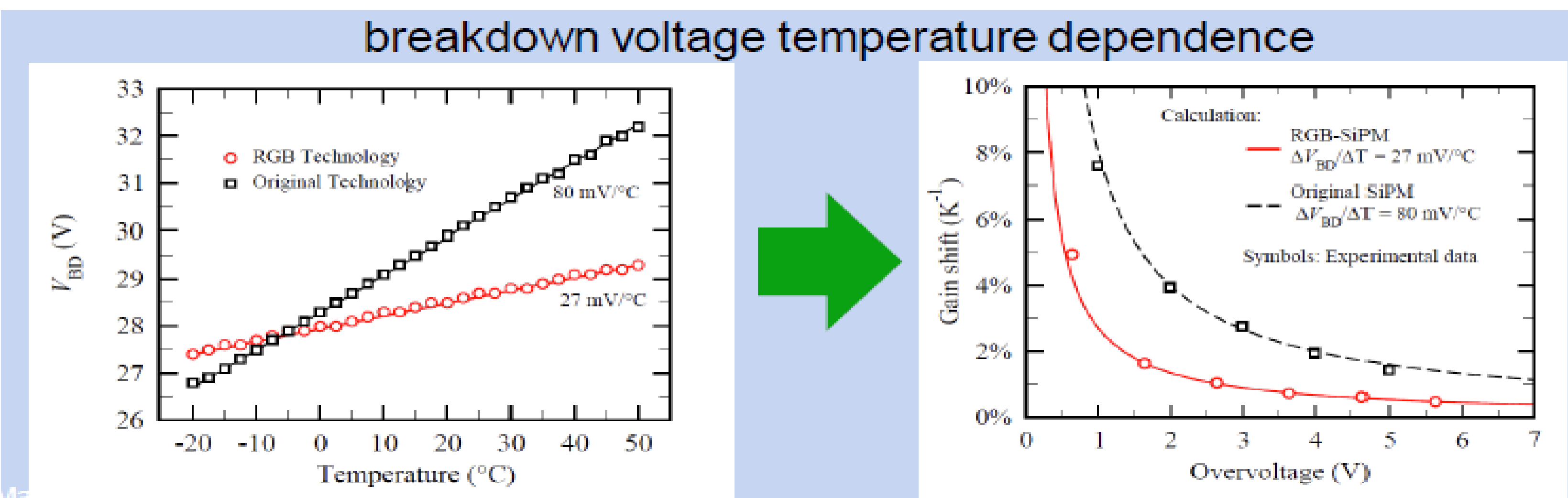

Recent progresses in FBK-Advansid devices

N.Serra: "Characterization of new FBK SiPM technology for visible light detection", JINST 2013 JINST 8 P03019

V_{bd} vs T → T coefficient (ΔV stability)

Breakdown Voltage

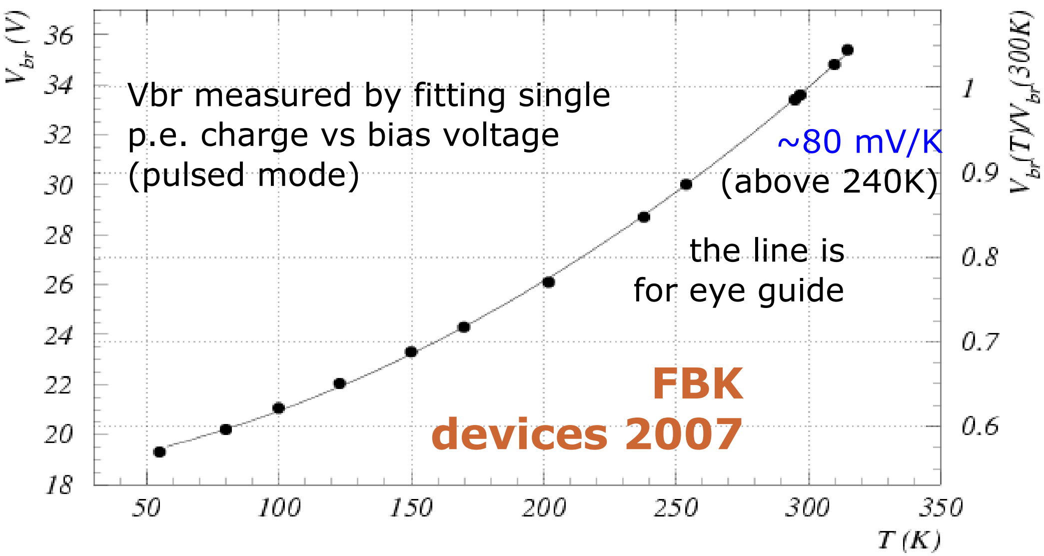

G.C. et al NIM A628 (2011) 389

Temperature coefficient

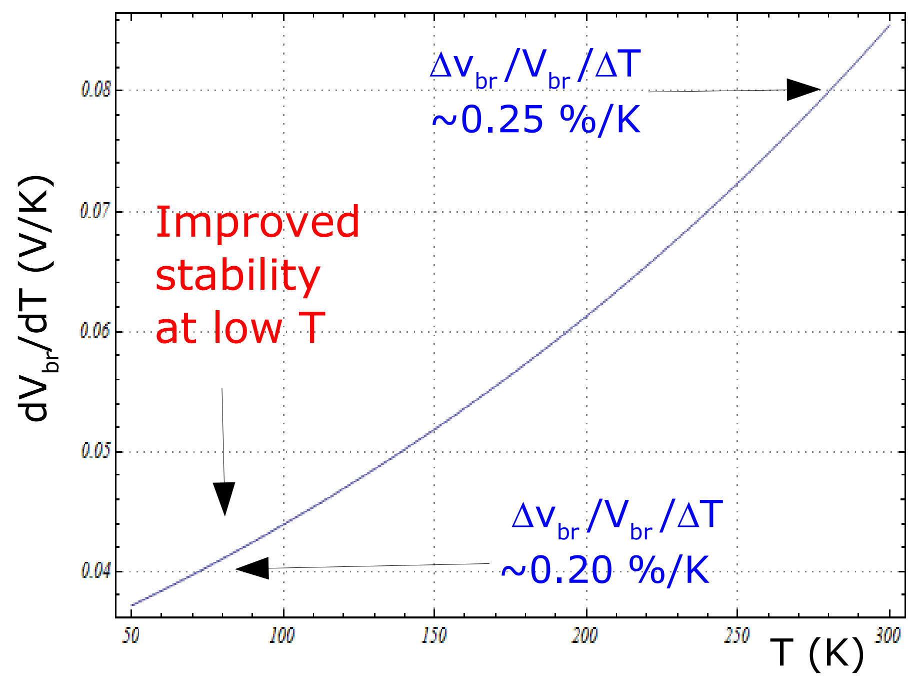

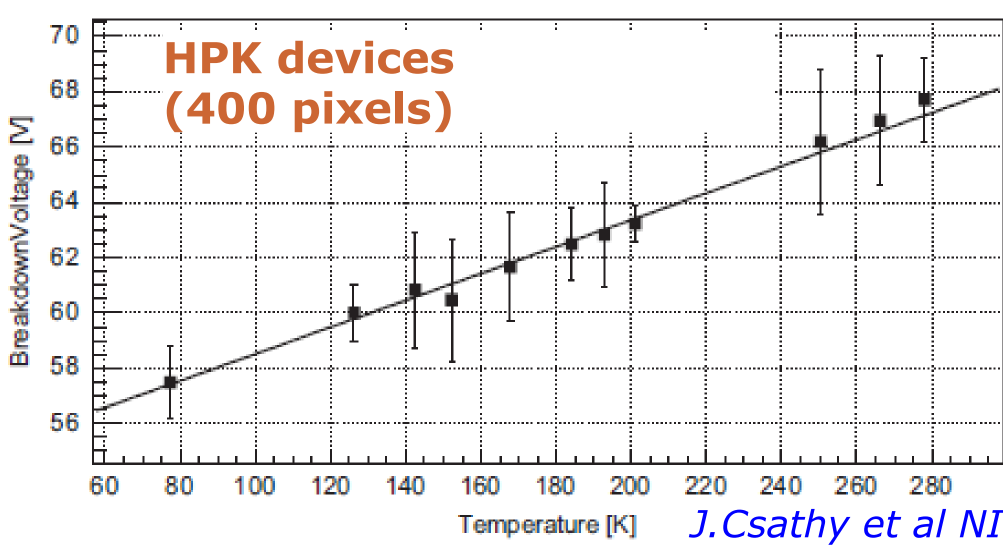

J.Csathy et al NIM A 654 (2011) 225

Fig. 6. Breakdown voltage as a function of temperature of the MPPC with 400 pixels.

Amplitude fluctuations

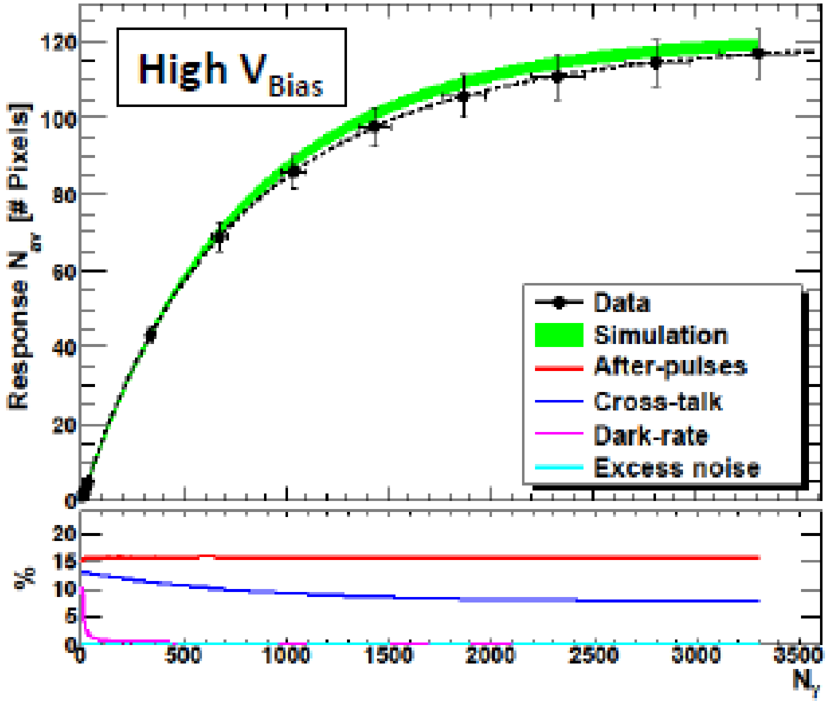

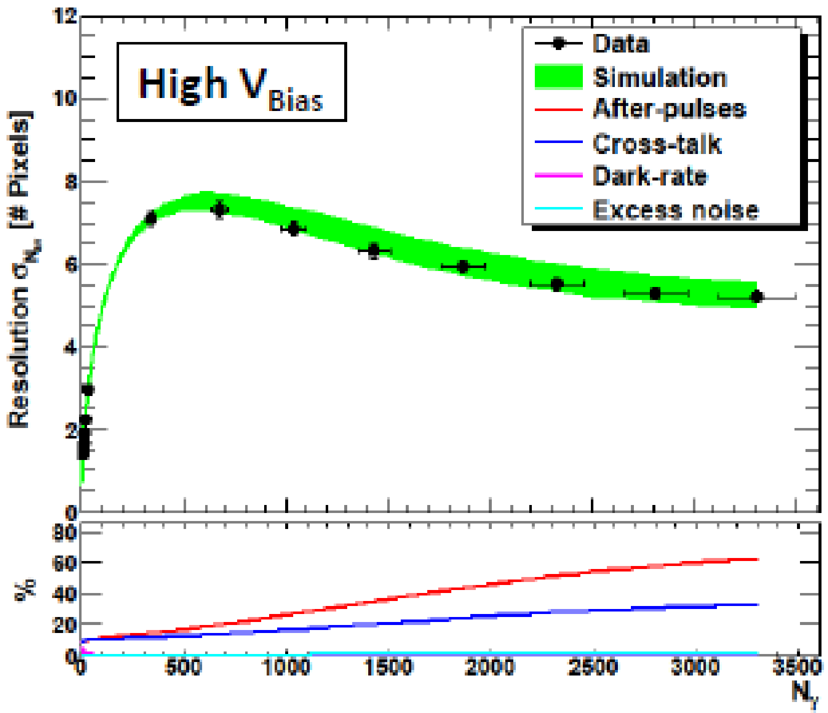

finite number of pixels: constraint
→ limit in resolving the number of photons

Eckert et al, Procs. of PhotoDet 2012

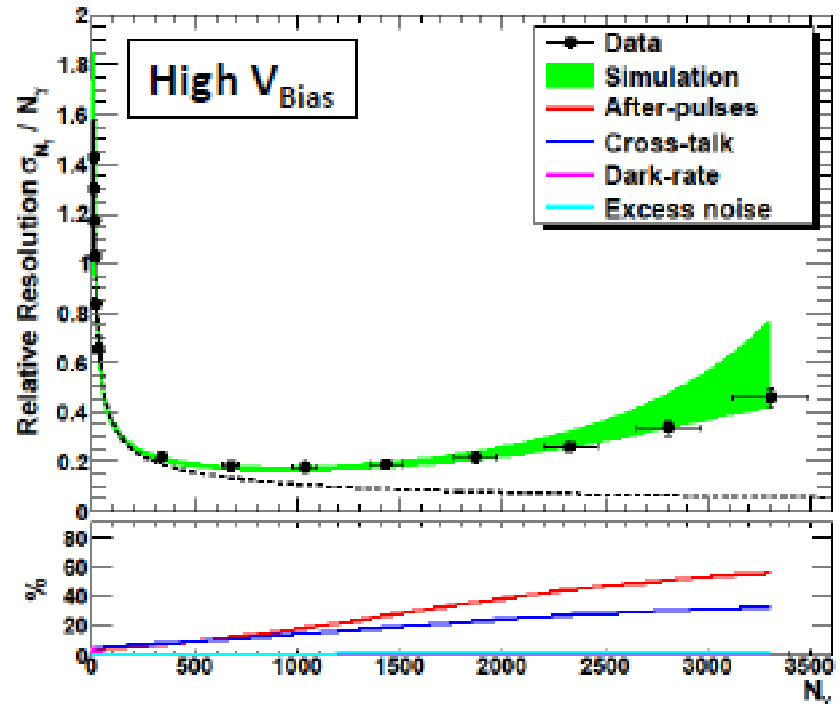

$$\frac{\Delta N_\gamma}{N_\gamma} \approx \overset{\text{DR}}{\frac{a}{N_\gamma}} \oplus \overset{\text{PDE, CT, AP}}{\frac{b}{\sqrt{N_\gamma}}}$$

see also Musienko et al JINST 2 2007 P0600

After-Pulses vs T (constant ΔV)

Measurement by waveform analysis:
- trigger on single carrier pulses (with no preceding pulses within $\Delta t = 5\mu s$), **count subsequent pulses** within $\Delta t = 5\mu s$ (find the after-pulsing rate r_{AP})
- Subtract dark count contribution
- extract **after-pulsing probability P_{AP}**
corrected for after-pulsing cascade •

$$P_{AP} = \frac{r_{AP}}{1 + r_{AP}}$$

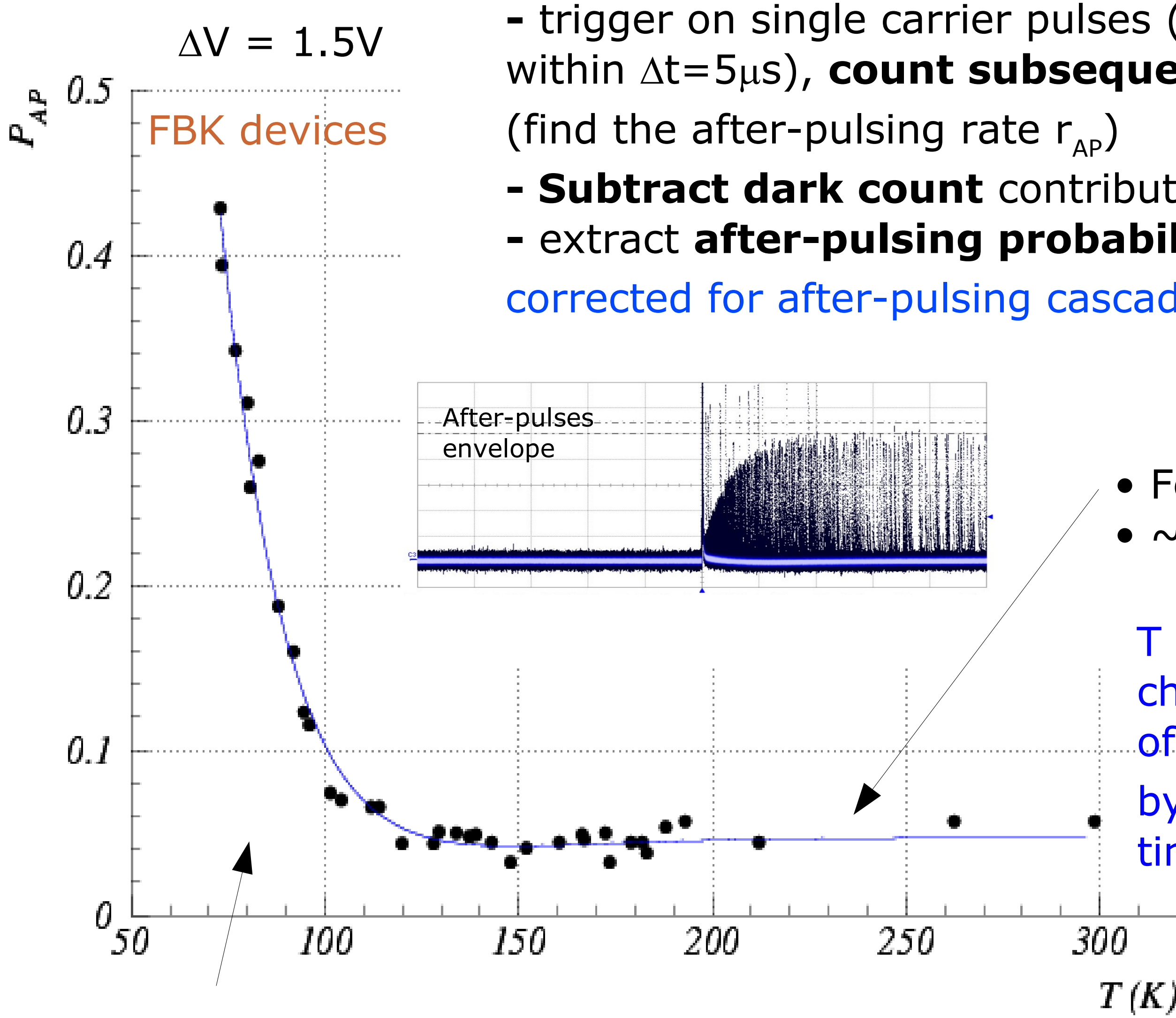

- Few % at room T
- ~constant down to ~120K

T decreasing: increase of characteristic time constants of traps (τ_{traps}) compensated by increasing cell recovery time (R_q)

- several % below 100K

T<100K: additional trapping centers activated possibly (?) related to onset of carriers freeze-out

→ Analysis of life-time evolution vs T of the various traps (at least 3 types at T_{room})

G.C. et al NIM A628 (2011) 389

Disentangling noise components

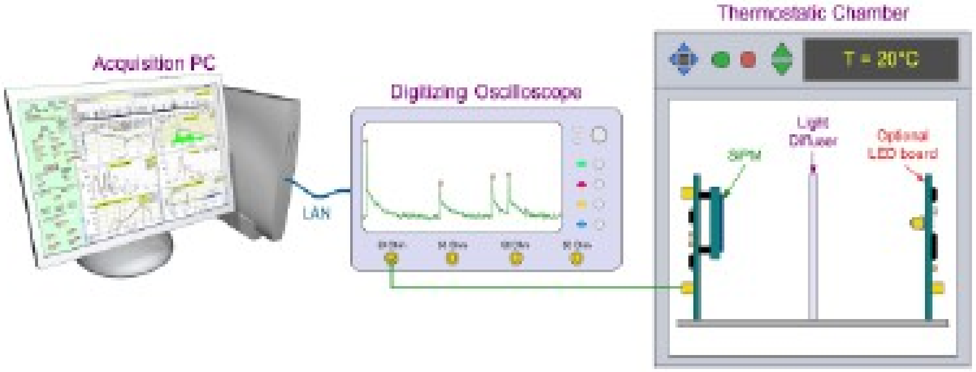

We acquire ms-long waveforms

Signal filtered to reduce pulse length

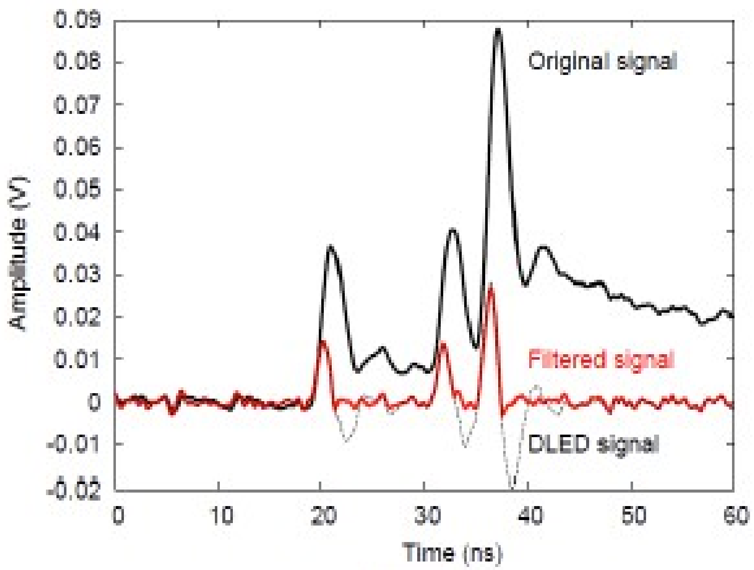

→ time delay array
→ amplitude array

Disentangling noise components

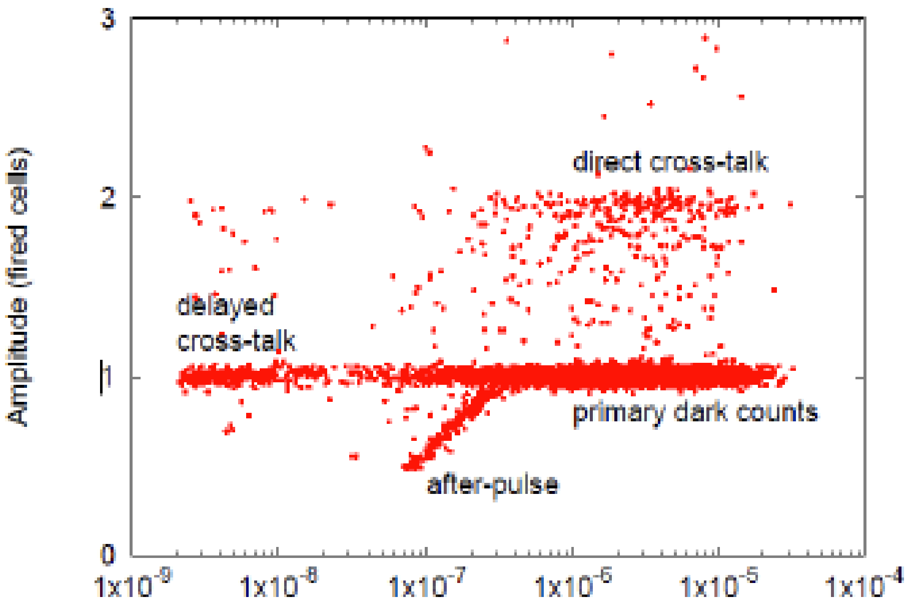

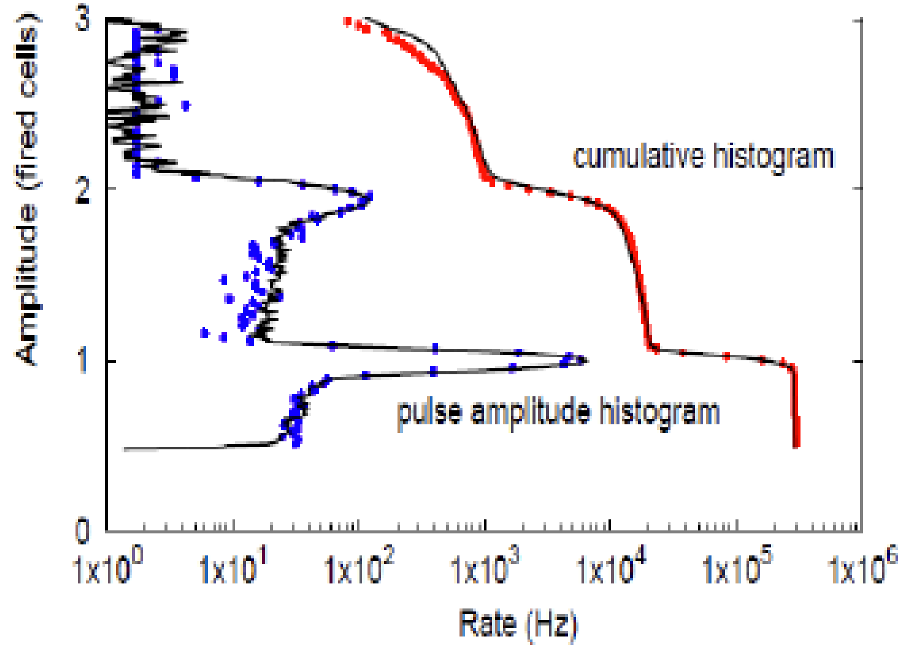

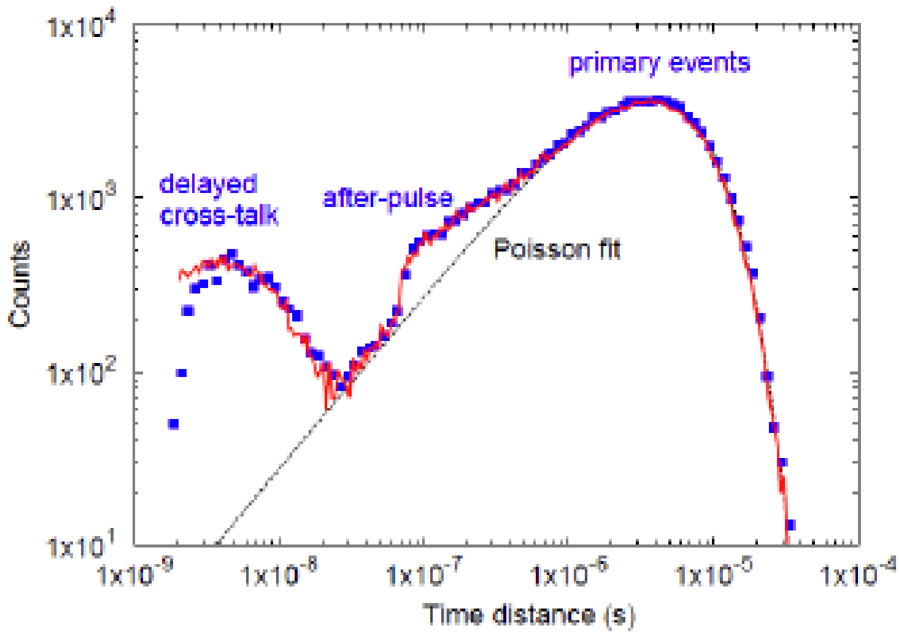

→ primary dark rate (DCR)
→ direct cross-talk
→ delayed correlated components

PDE

Improving PDE by E field engineering

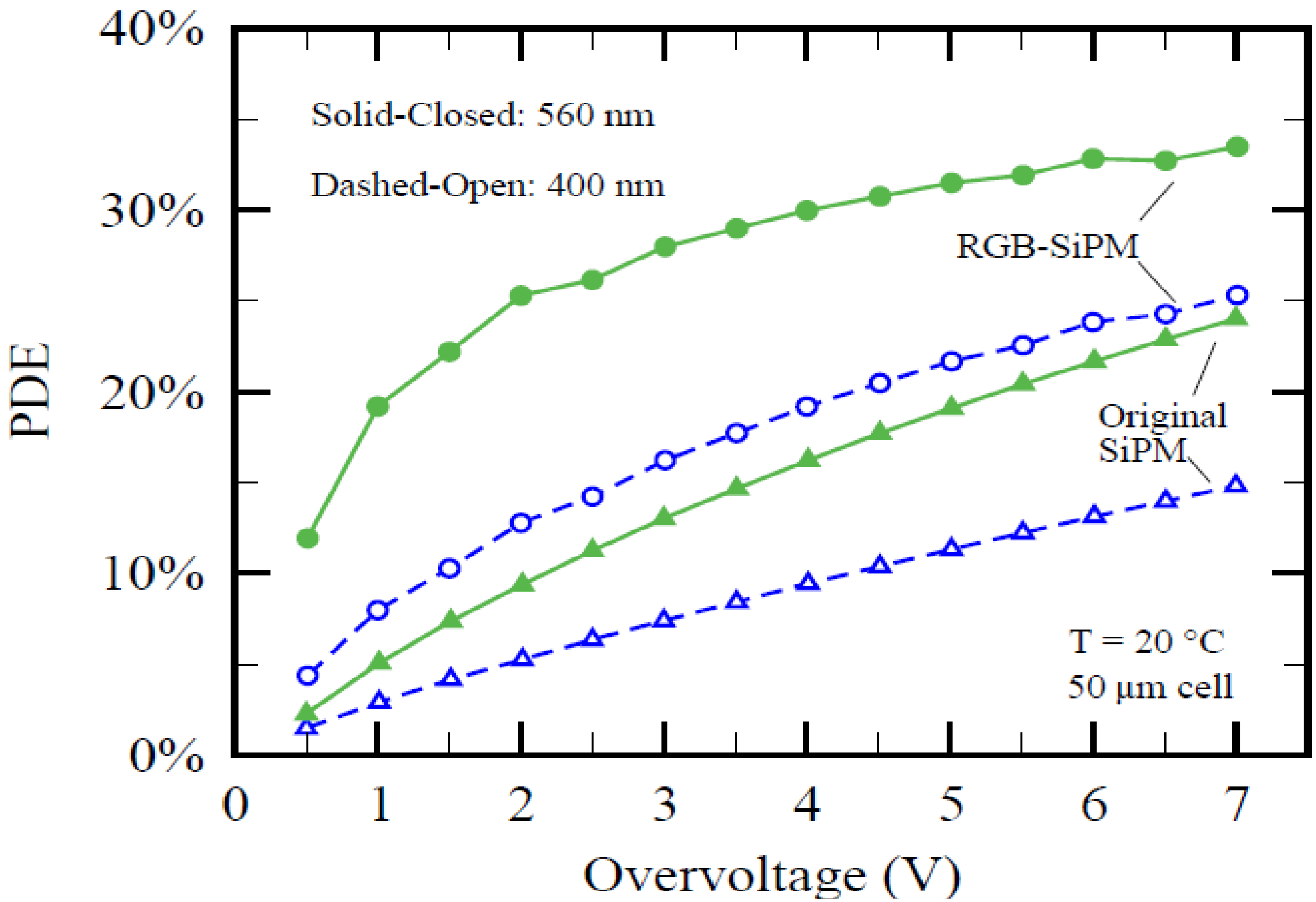

Latest "RGB" FBK devices vs older devices

N.Serra et al
JINST 8 (2013) P03019

Table 1. Main properties of the fabricated RGB-SiPMs.

FBK n-on-p RGB-SiPMs.			
SiPM size (mm^2)	1×1, 3×3, 4×4	Gain (1)	$4\cdot10^6$
Cell pitch (μm)	25-50-70-100	R quenching (at 20°C)	500 kΩ
Fill-factor (%)	21-45-58-72	Cell capacitance (1)	170 fF
V_{BD} (at 20°C)	28.5 V	Rise time (1)(2)	5.6 ns
Dark count rate (1)	480 kHz	Recovery time (1)(2)	350 ns

(1) 1×1 mm^2 SiPM, 50 μm cell at 20°C, OV=4 V; (2) Single-cell pulse, see figure 2.

PDE vs Temperature (ΔV constant)

When T decreases:

1) silicon E_{gap} increasing
→ larger attenuation length
→ lower QE (for larger λ)

2) mobility increasing
→ larger impact ionization
→ larger trigg. avalanche P_{01}

3) carriers freeze-out
onset below 120K
→ loss of carriers

G.C. et al NIM A628 (2011) 389

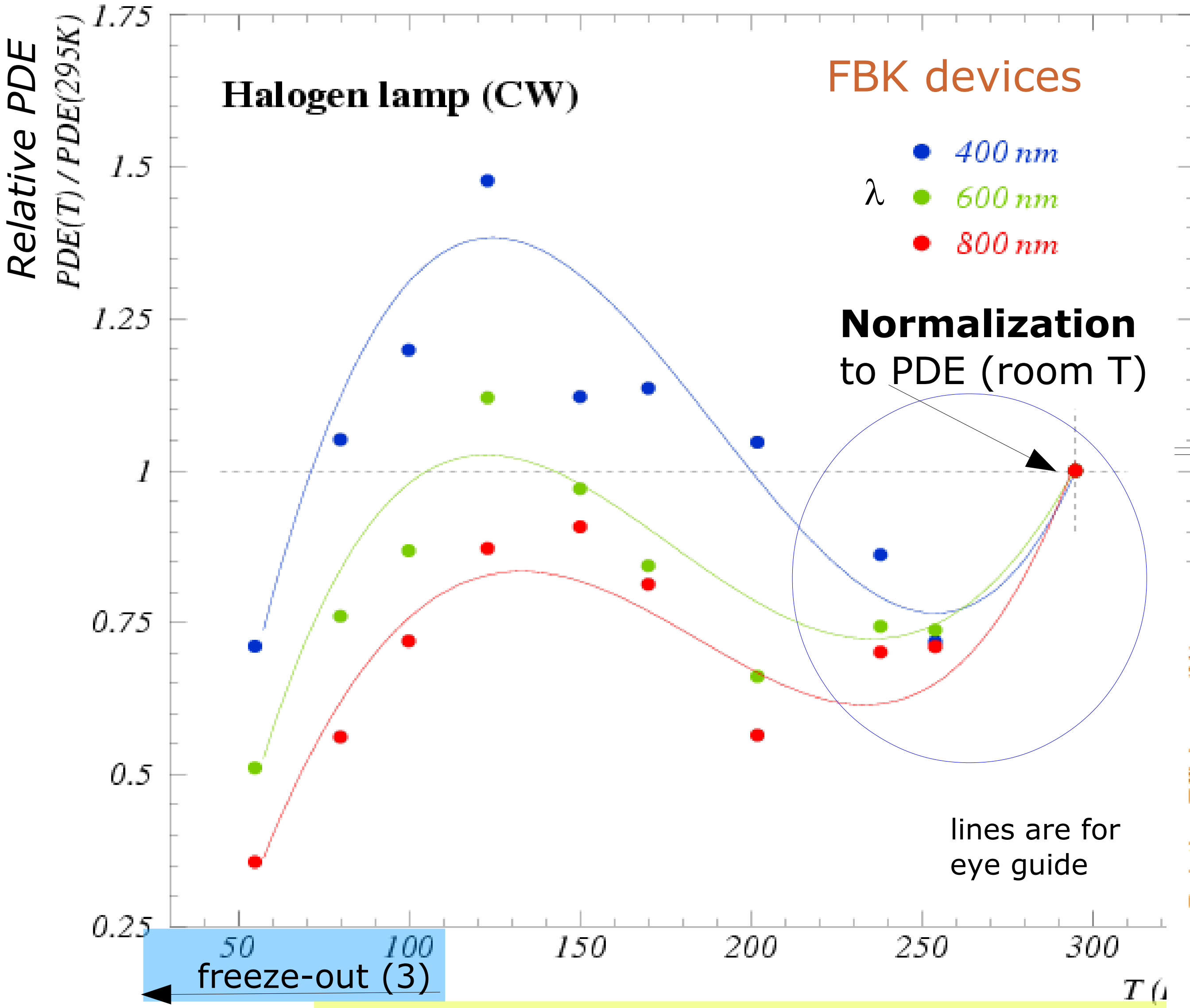

freeze-out (3)

??? interplay between (1) and (2): modulation
… drop in 250<T<300 not well understood
(common feature with APDs')

RMD APD at 400nm < λ < 700nm
Johnson et al, IEEE NSS 2009

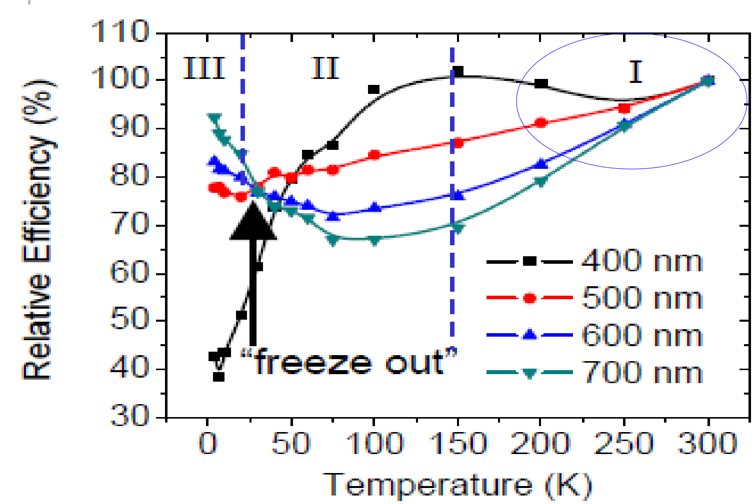

Additional effects in APD
(depletion region depends on T, ...)

Timing

Single Photon Time Resolution = gaussian + tails

Time resolution of SiPM is not just a gaussian, but gaussian + tails
(in particular at long wavelengths)

G.C. et al NIMA 581 (2007) 461

Data at λ**=400nm**

A simple **gaussian component** fits fairly

Data at λ**=800nm**

fit gives reasonable χ^2 in case of an **additional exponential term** $\exp(-|\Delta t|/\tau)$ summed with a weight

- **$\tau \sim$ 0.2÷0.8ns** (depending on device) in rough agreement with diffusion tail lifetime: $\tau \sim L^2 / \pi^2 D$ where L is the diffusion length
- Weight of the **exp. tail ~ 10%÷30%** (depending on device)

Gaussian + Tails (long λ)

rms ~ 50-100 ps

~ exp (-t / O(ns))
contrib. several %
for long wavelengths

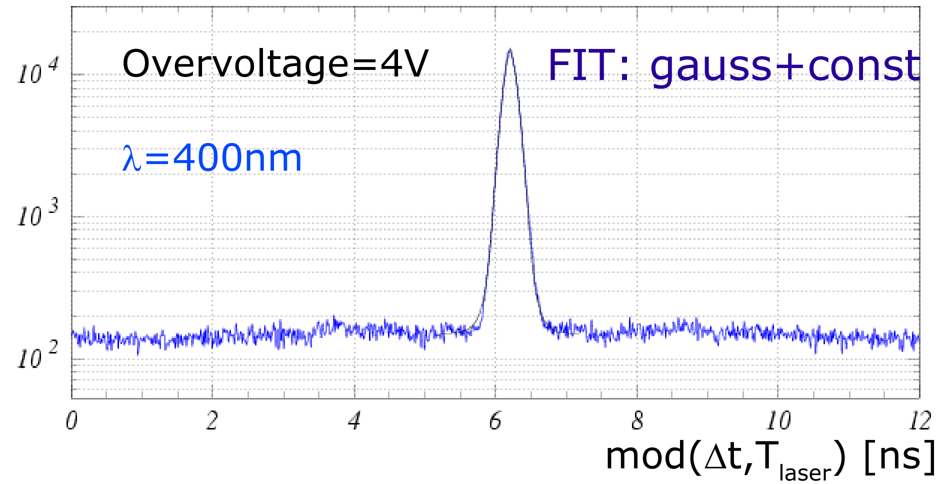

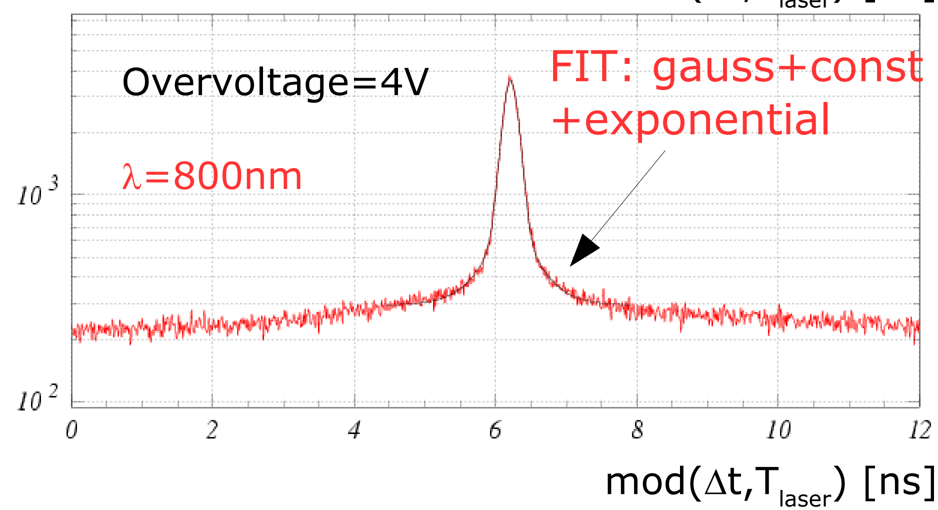

Distributions of the difference in time between successive peaks

PDE vs timing trade off / optimization

C.H.Tan et al IEEE J.Quantum Electronics 13 (4) (2007) 906

k=ratio of hole (β) to electron (α) ionization coefficient (increasing with E field)

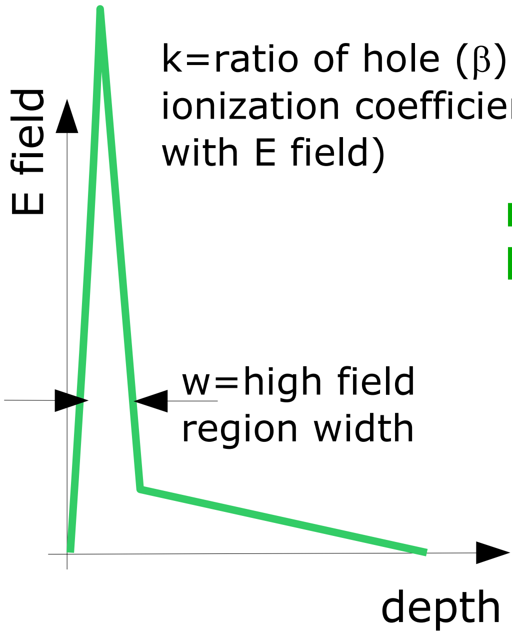

narrow avalanche region, high E:
- **small w**
- **high k = β / α**

better for **TIMING**

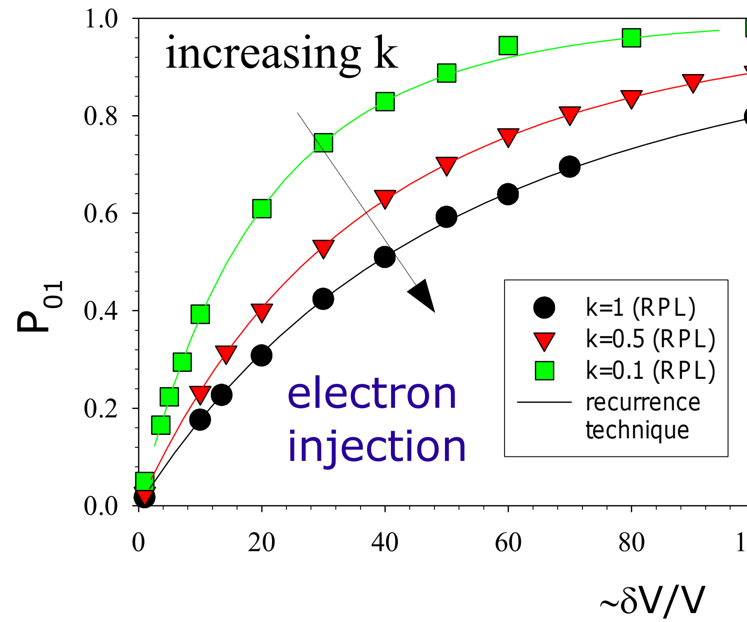

better for **PDE**

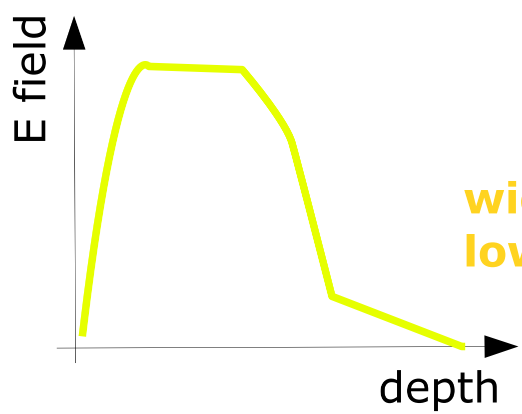

wide avalanche region, low E:
- **wide w**
- **small k = β / α**

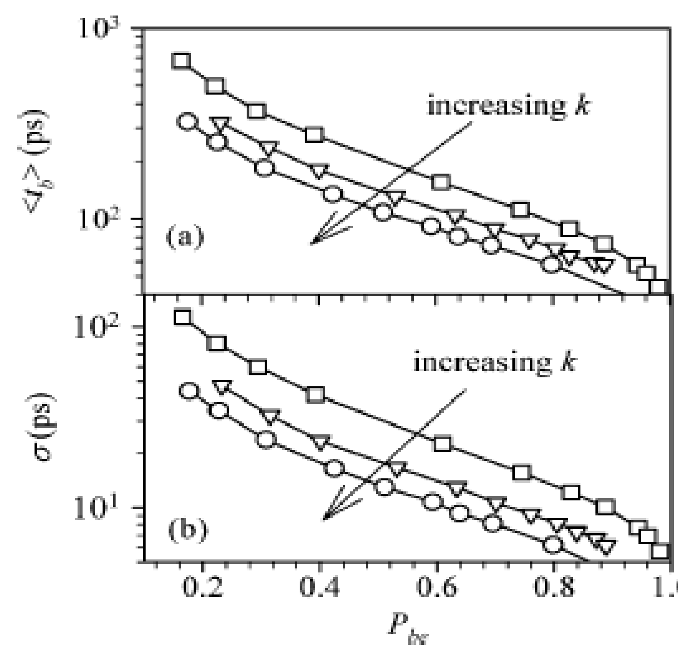

Radiation damage

Radiation damage: two types

- Bulk damage due to Non Ionizing Energy Loss (NIEL) ← neutrons, protons
- Surface damage due to Ionizing Energy Loss (IEL) ← γ rays
  (accumulation of charge in the oxide (SiO2) and the Si/SiO2 interface)

Assumption: damage scales linearly with the amount of Non Ionizing Energy Loss (NIEL hypothesis)

G.Lindstrom et al. NIM A426(1999)1-15

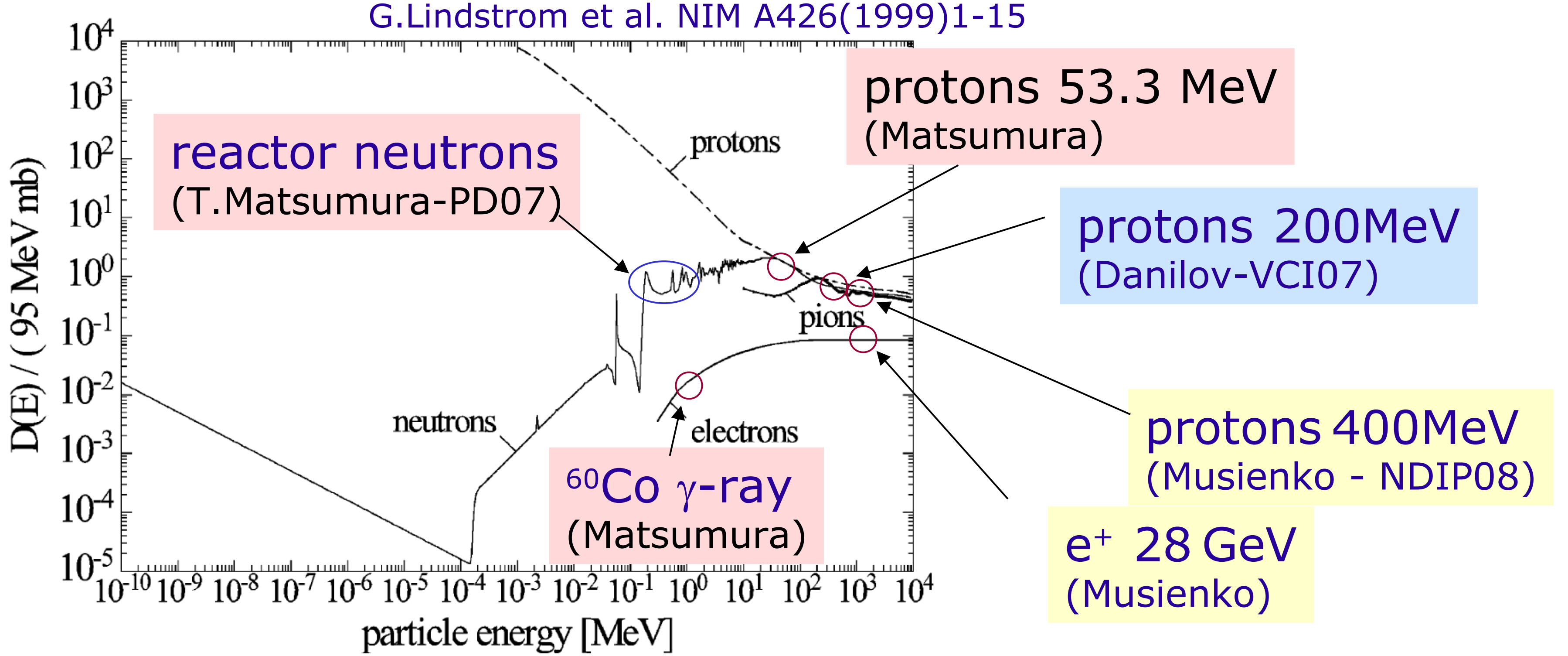

Examples of radiation tolerances for HEP and space physics
ATLAS inner detector ... 3×10^{14} hadrons/cm^2/10 year
~ 10^4 hadrons/mm^2/s
General satellites ... ~ 10 Gy/year

Expectations:
protons / γ-ray ~ 100
protons / neutrons ~ 2~10

Radiation damage: effects on SiPM

1) Increase of dark count rate due to introduction of generation centers

Increase (ΔR_{DC}) of the dark rate:
$\Delta R_{DC} \sim P_{01}\ \alpha\ \Phi_{eq}\ Vol_{eff}\ /q_e$
where $\alpha \sim 3 \times 10^{-17}$ A/cm is a typical value of the radiation damage parameter for low E hadrons and $Vol_{eff} \sim Area_{SiPM} \times \varepsilon_{geom} \times W_{epi}$

NOTE:
The effect is the same as in normal junctions:
- independent of the substrate type
- dependent on particle type and energy (NIEL)
- proportional to fluence

2) Increase of after-pulse rate due to introduction of trapping centers

→ loss of single cell resolution → no photon counting capability

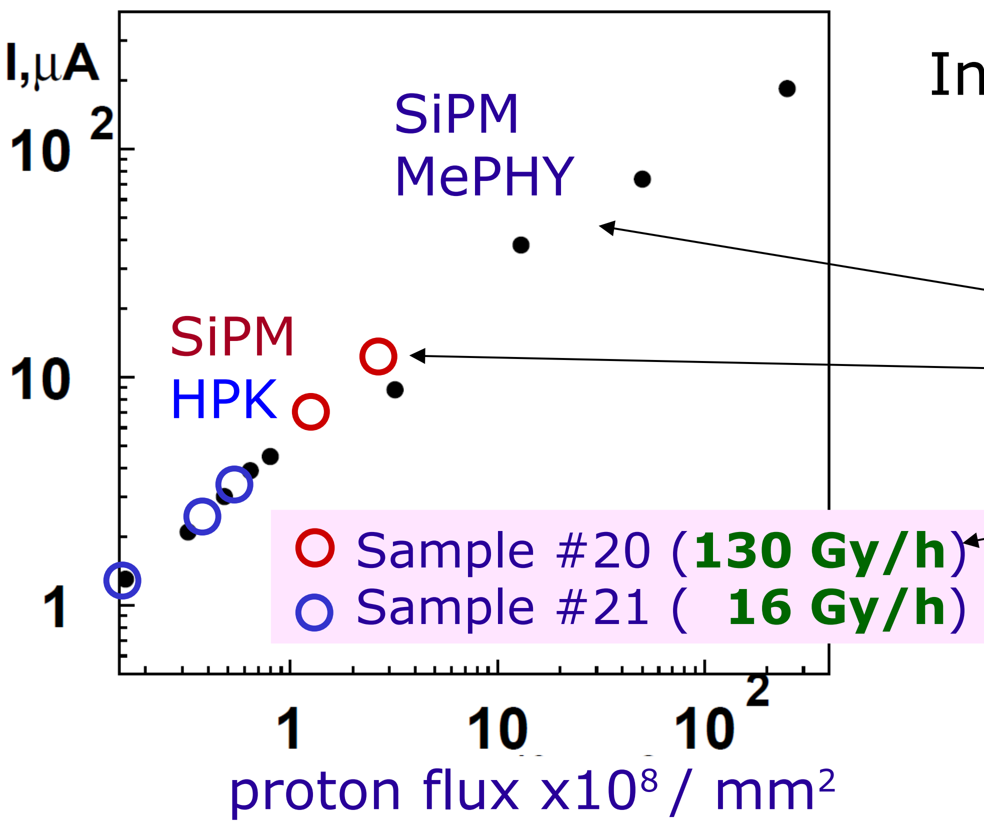

Indications from measurements:

1) no dependence on the device
similar effects found for SiPM from MePHY (Danilov) and HPK (Matsumura)
(normaliz. to active volume)

2) no dependence on dose-rate
HPK (Matsumura)

3) n similar damage than p

4) p x10^1-10^2 more damage than γ

Damage comparison

2.3×10^5 p/mm²/s (130 Gy/h)

I_{leak} @ (V_{op}, 1.4×10^8 p/mm²) = 6.7 μA

Damage effect …
almost the same for protons and neutrons

HPK devices
T.Matsumura – PD07

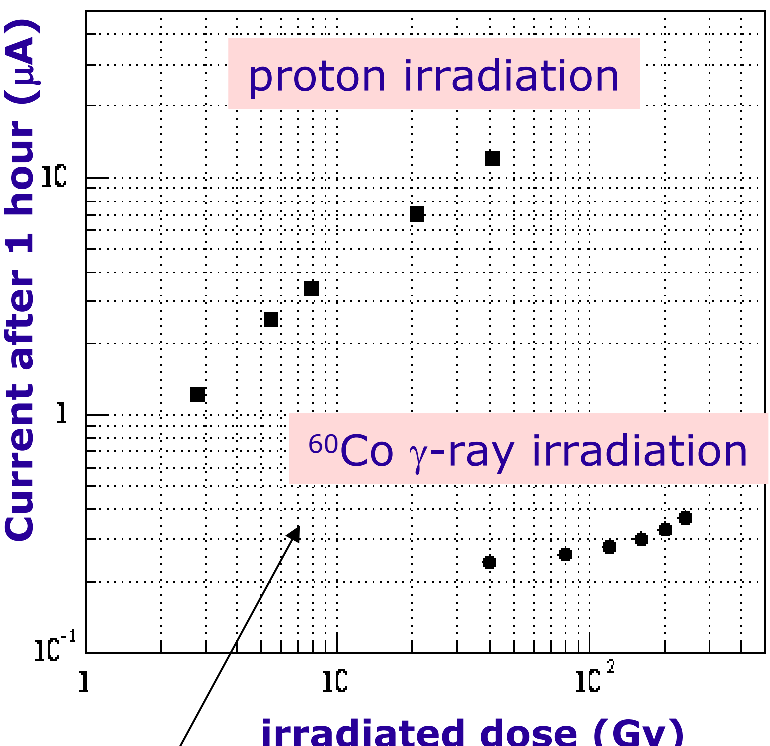

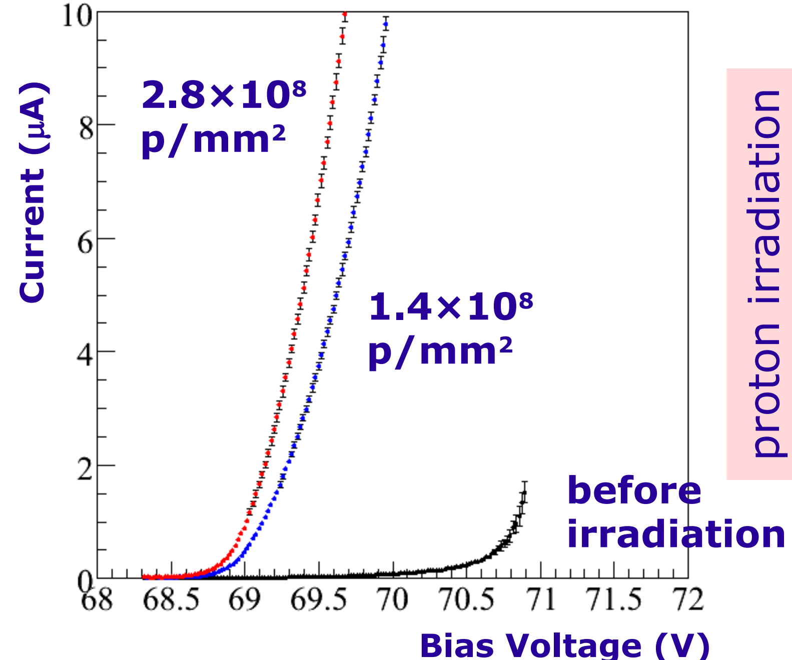

4.2×10^5 n/mm²/s

I_{leak} @ (V_{op}, 1.0×10^8 n/mm²) = 8.5 μA

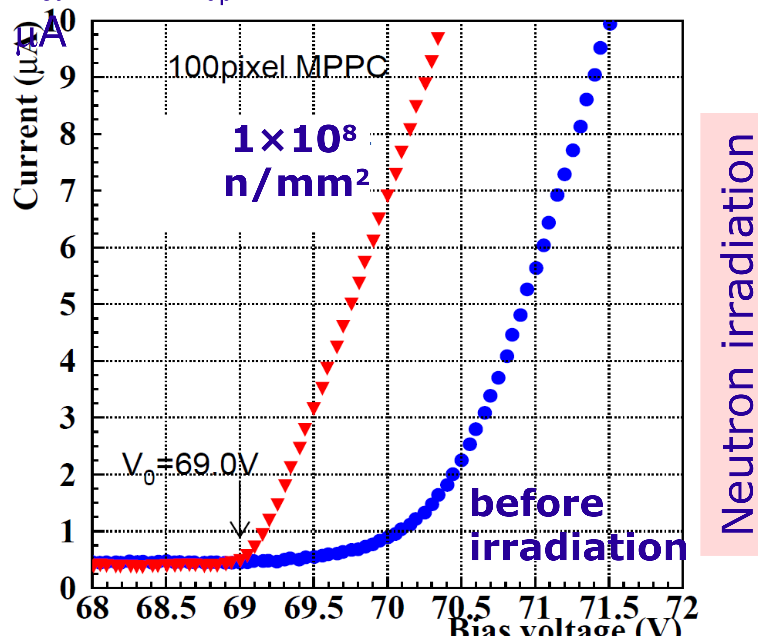

T.Matsumura – PD07

Damage effect …
1~2 orders larger with protons than γ-ray irradiation

Radiation damage: neutrons (0.1 -1 MeV)

8.3×10^{4} n/mm² | 3.3×10^{5} n/mm² | 1.0×10^{8} n/mm²

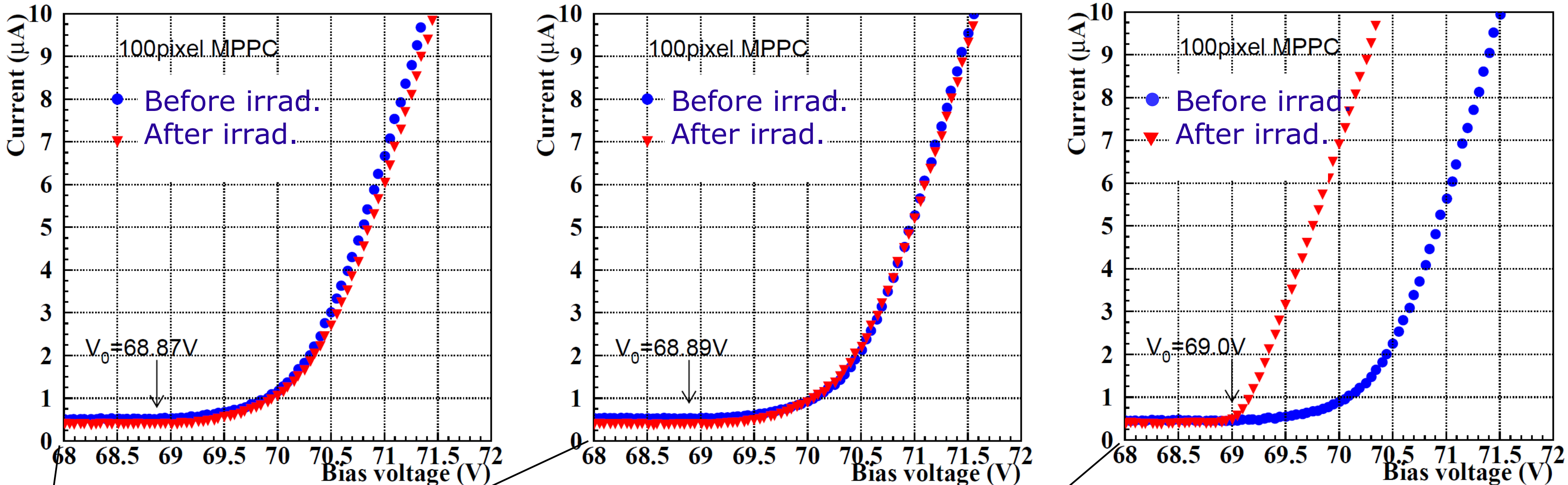

T.Matsumura – PD07

10^{5} n/mm² 10^{6} n/mm² 10^{7} n/mm² 10^{8} n/mm² 10^{9} n/mm² 10^{10} n/mm²

n dose

No significant change

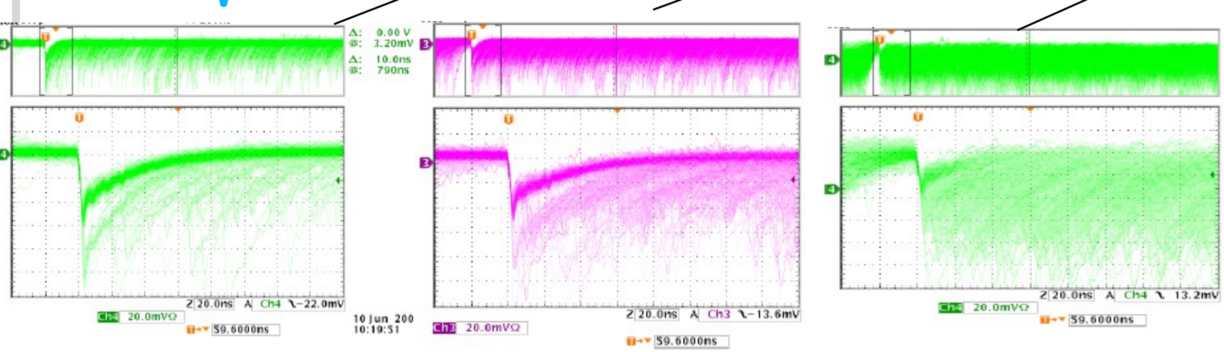

I-V drastically change.
Signal pulse is still there,
but continuous pulse height.
(No photon-counting capability)

No signal

Nakamura at NDIP08

Radiation damage: neutrons 1 MeV E_{eq}

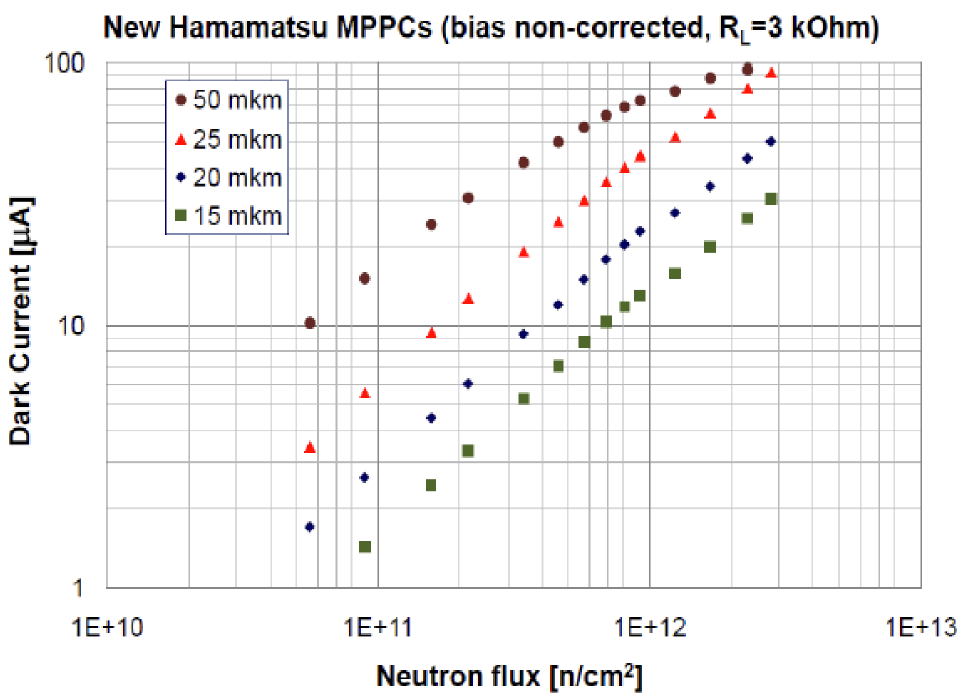

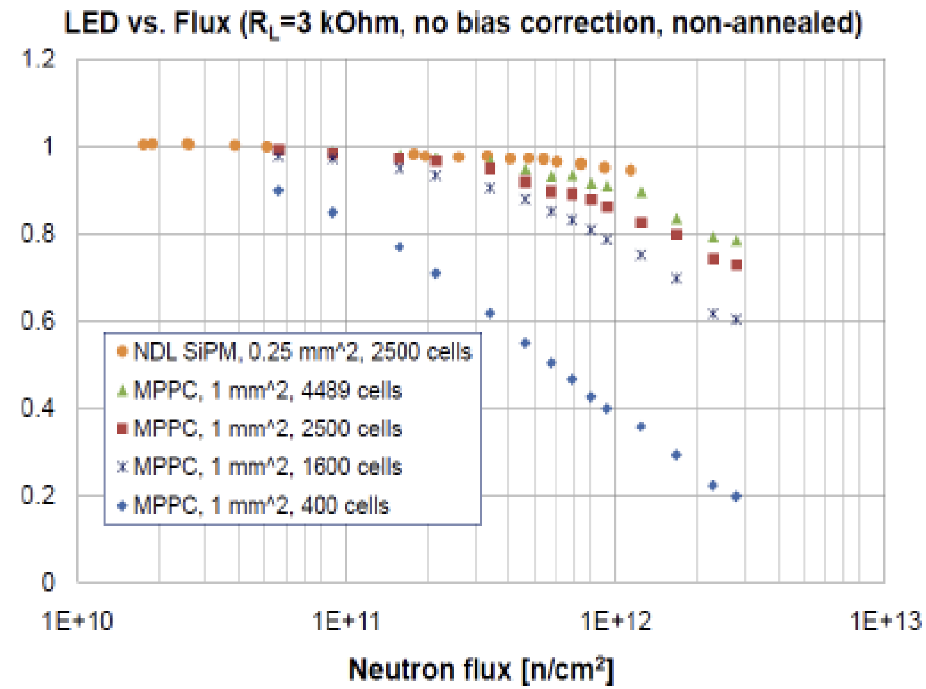

- No change of V_{bd} (within 50mV accuracy)
- No change of R_q (within 5% accuracy)
- I_{dark} and DCR significantly increase

SiPMs with high cell density and fast recovery time can operate up to $3*10^{12}$ n/cm^2 ($\delta G < 25\%$)

Y.Musienko at SiPM workshop CERN 2011

Radiation damage effects are mitigated by using devices with:
→ **small cells** → smaller charge flow (smaller gain → charge)
→ thin epi-layer

Comparison

SiPM vs APD for single photon

APD biased for **low gain** M < 1/k

- fast exponential growing due to only electrons
- high number of carriers in high field region at given time: variations of impact ionization induce
  → small gain fluctuations
- Timing fluctuations are small limited by the length of depletion region
  → time resolution limited by electronics
  (high Amplification for low light signals)

Hayat et al J. Lightwave Tech. 24 (2006) 755
Fox et al Rev. Sci. Instr. 70 (1999) 1951

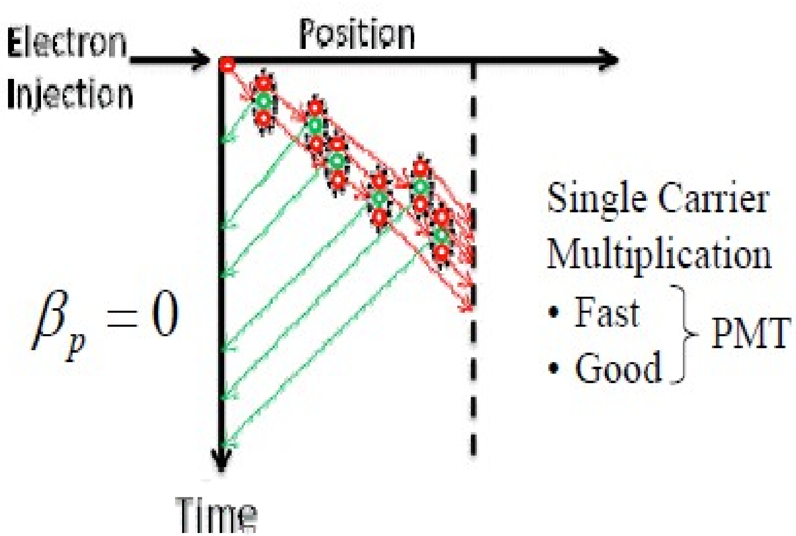

APD biased for **high gain** M > 1/k

- hole ionization events contribute
  → increase of gain is the result of small numbers of large pulses that are due to one or more hole ionization initiated secondary avalanches
- low number of carriers in high field region at given time and hole ionization near cathode result in larger pulses
  → large gain fluctuations
- **slow buildup** and long pulse due to many carriers over long time
  → large timing fluctuations

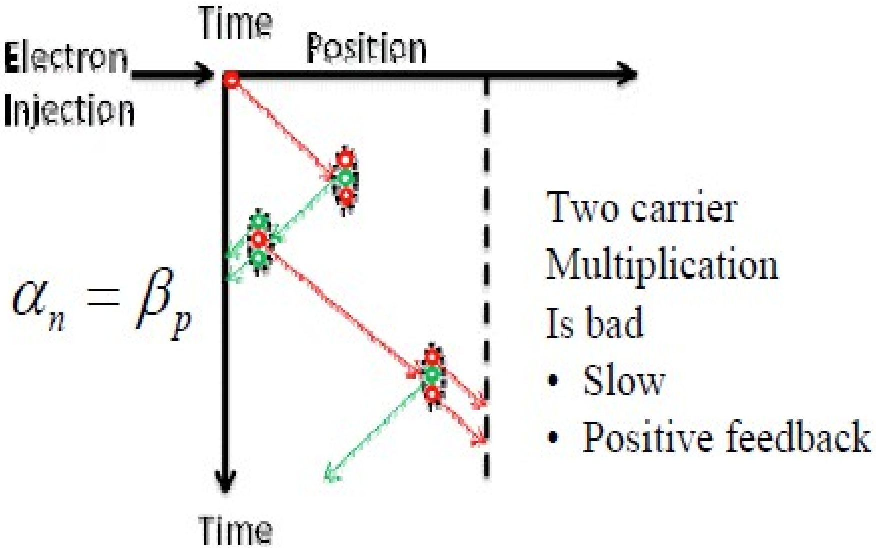

SiPM vs APD for single photon

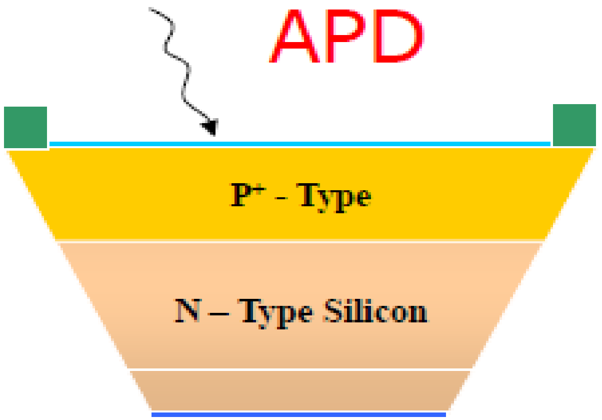

→ ENF increases with increasing gain
→ Temperature coefficient also increases with gain (… gain stability)

Devices with high multiplication noise are not good for single photon counting

Single photon counting is possible, but at **low temperature (T~77K)** and with slow electronics (and PDE~20%)

A. Dorokhovet.al.,JournalMod.Opt. v51 2004 p.1351

Reminder about SiPM correlated noise

1) no multiplication (excess) noise in SER

2) SER width due to intrinsic fluctuations in doping densities and variations among cells

3) Correlated noise is there, namely After-Pulsing and Cross-Talk
"excess charge factor (ECF)"
It does not prevent clean single photon

Vacuum based PD

PMT: 80 years old... still the most used sensor for low-level light detection

matrices of

Features
- sensitivity from DUV to NIR
- **high gain**
- **low noise**
  - → single photon sensitivity
  - → large area at low cost
  - → low capacitance
- imaging capabilities (large pixels)
- high frequency response
  - → fast speed
- stability

Issues
- intrinsic **limit QE < 40%**
- broad SER
- high voltage, bulky, fragile
- influenced by B, E fields
- damaged by high-level light
- ageing (eg. He)
- radiopurity

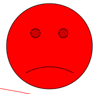

Developement

→ photocathodes: new materials and geometries → high QE

mm^2

→ ultra-fast, large area, imaging MCP based PMTs

→ hybrids (eg photocathode + SiPM) → narrow SER

Recovery Time

Fast Timing & Imaging devices

	Multi-anodes PMTs Dynodes	matrices of Silicon-PMTs [10] Quenched Geiger in Silicon	Micro-Channel Plates [1] Micro-Pores
		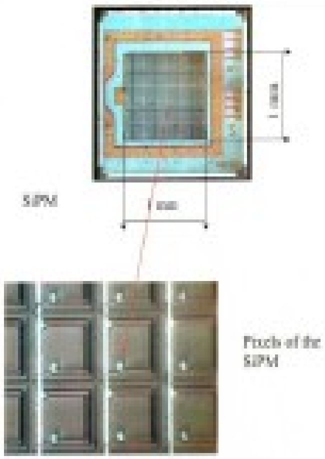	
Quantum Eff.	30%	90%	30%
Collection Eff.	90%	70%	70%
Rise-time	0.5-1ns	250ps	50-500ps
Timing resolution (1PE)	150ps	100ps	20-30ps
Pixel size	$2x2mm^2$	$50x50\mu m^2$	$1.5x1.5mm^2$
Dark counts	1-10Hz	$1\text{-}10MHz/mm^2$	$1Hz\text{-}1kHz/cm^2$
Dead time	5ns	100-500ns	$1\mu s$
Magnetic field	no	yes	15kG
Radiation hardness		1kRad=noisex10	good (a-Si, Al_2O_3)

Recovery Time

J.F.Genat, LAPPD Electronics Workshop (2012)

Large Area Pico-second MCP Photo-detectors

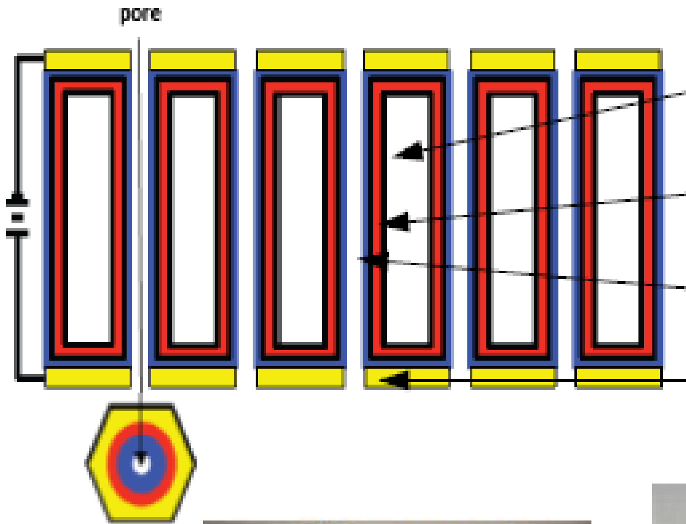

Porous glass

Resistive coating ~100nm (ALD)

Emissive coating ~ 20nm (ALD)

Conductive coating
(thermal evaporation or sputtering

Incom glass substrate

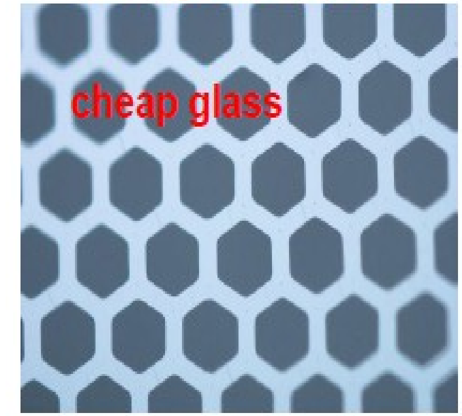

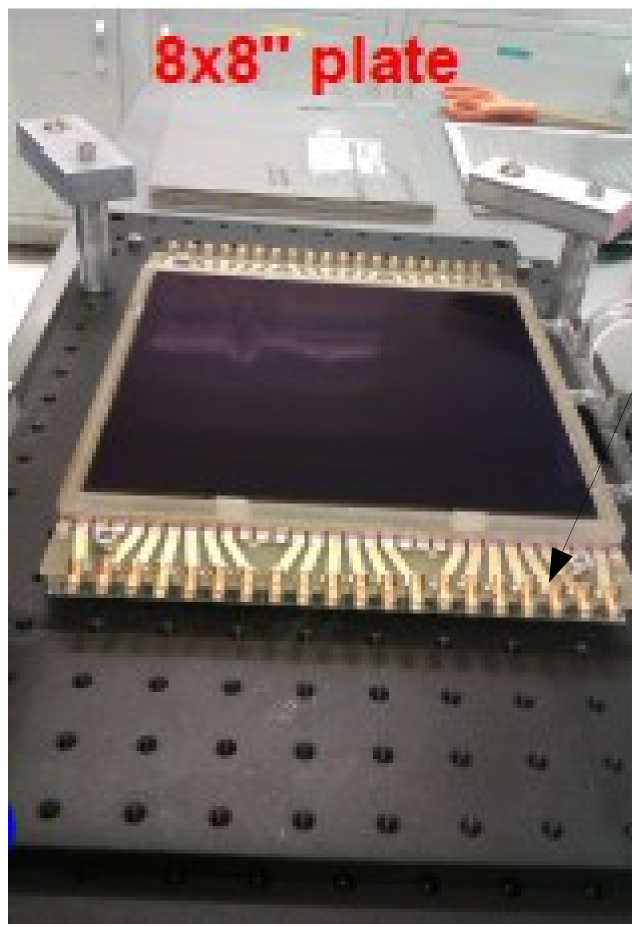

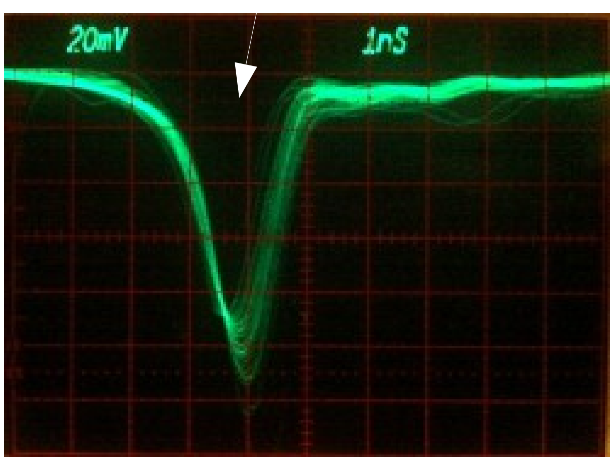

RF strip-line anodes

- 50 Ω impedance
- 1.6-0.4GHz bandwidth

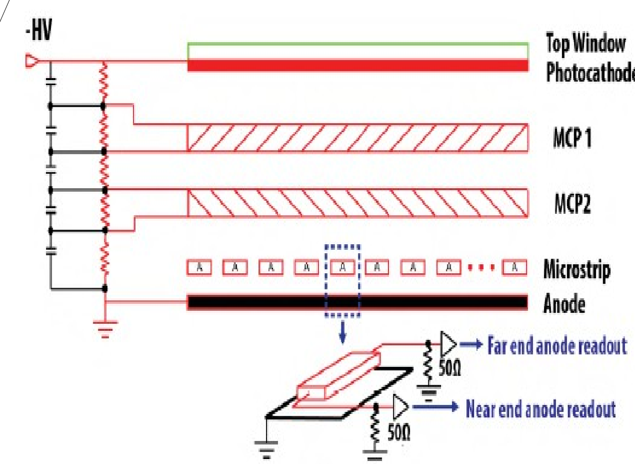

LAPPD

http://psec.uchicago.edu/

The light amplifier approach

Old idea of the smart Philips/Quasar PMT combined with SiPM:
strong focussing of the photoelectrons + a secondary photon readout

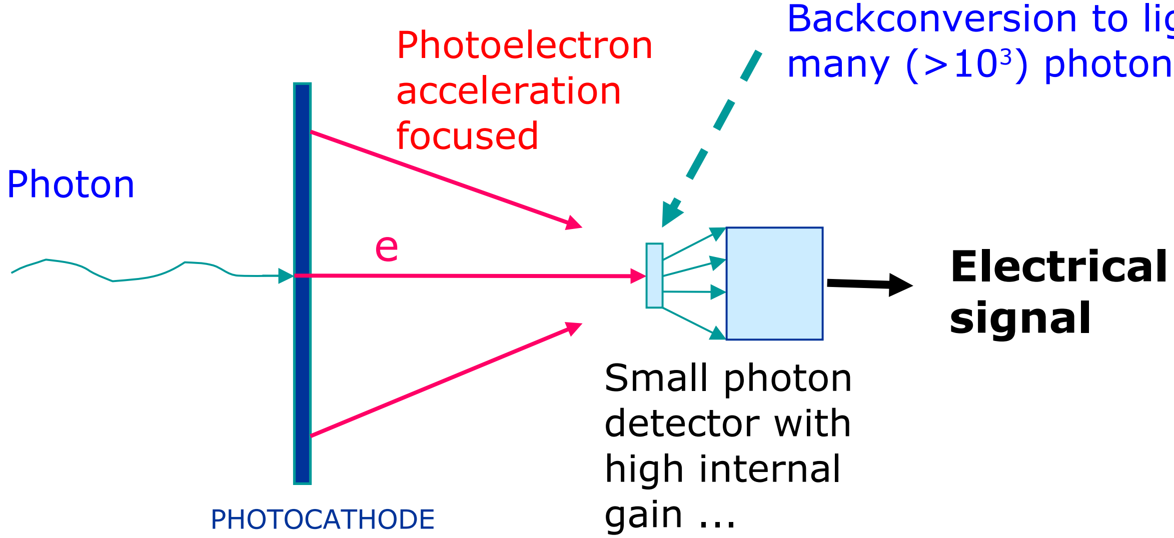

The X-HPD – Conceptual Study of a Large Spherical Hybrid Photodetector

A.Braem[a], C.Joram[a,*], J.Séguinot[a], P. Lavoute[b], C. Moussant[b]

[a] CERN, PH Department, CH-1211 Geneva, Switzerland

[b] Photonis SAS, F-19100 Brive La Gaillarde, France

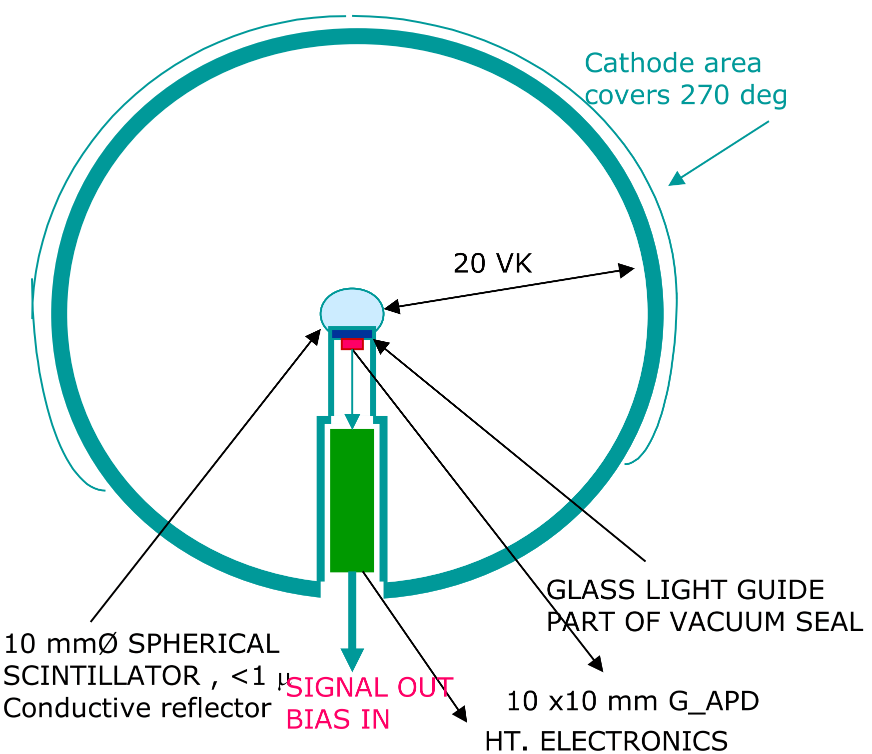

NOTE:
- Simple production (no dynode coating)
  T can be optimized for cathode production
- Today exist very fast and high yield scintillators
- No bleeder current needed: low power HV gen.
- Combined gain very high: easy 10^7
- Insensitive to the earth magnetic field
- Easy to install new very powerful getter pump
- SiPM not be damaged by light (even daylight)

Applications

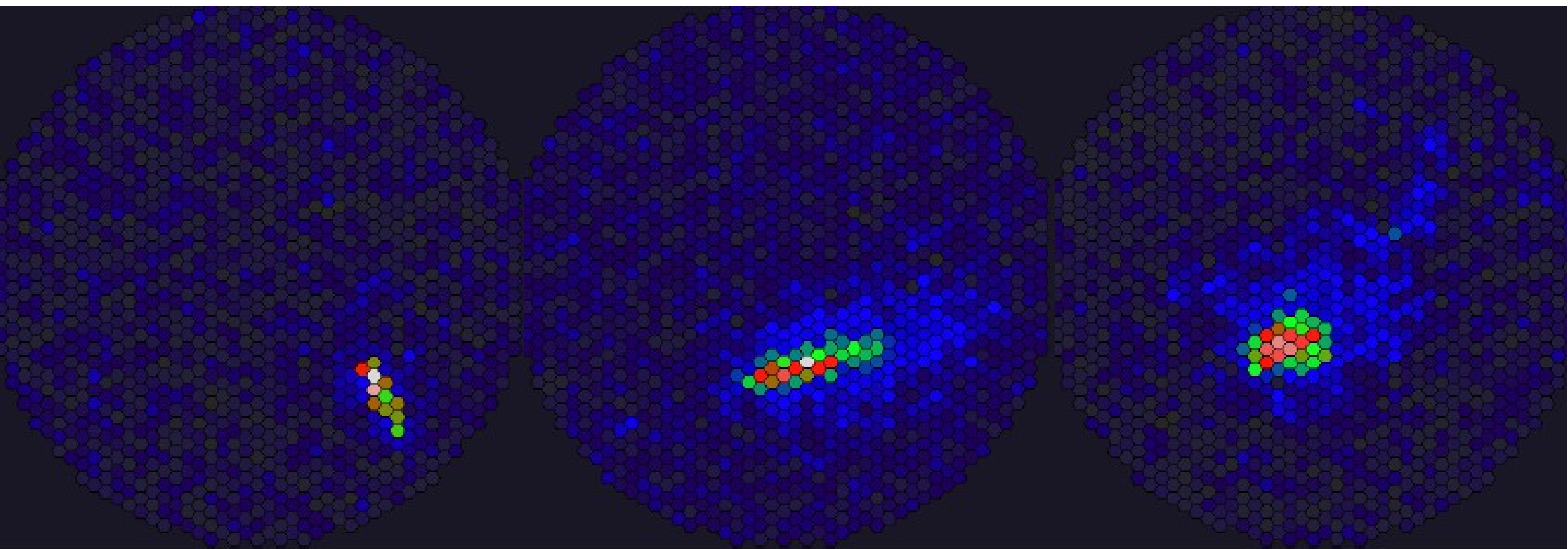

FACT – Selected events of the first nights of data-taking (October 2011)

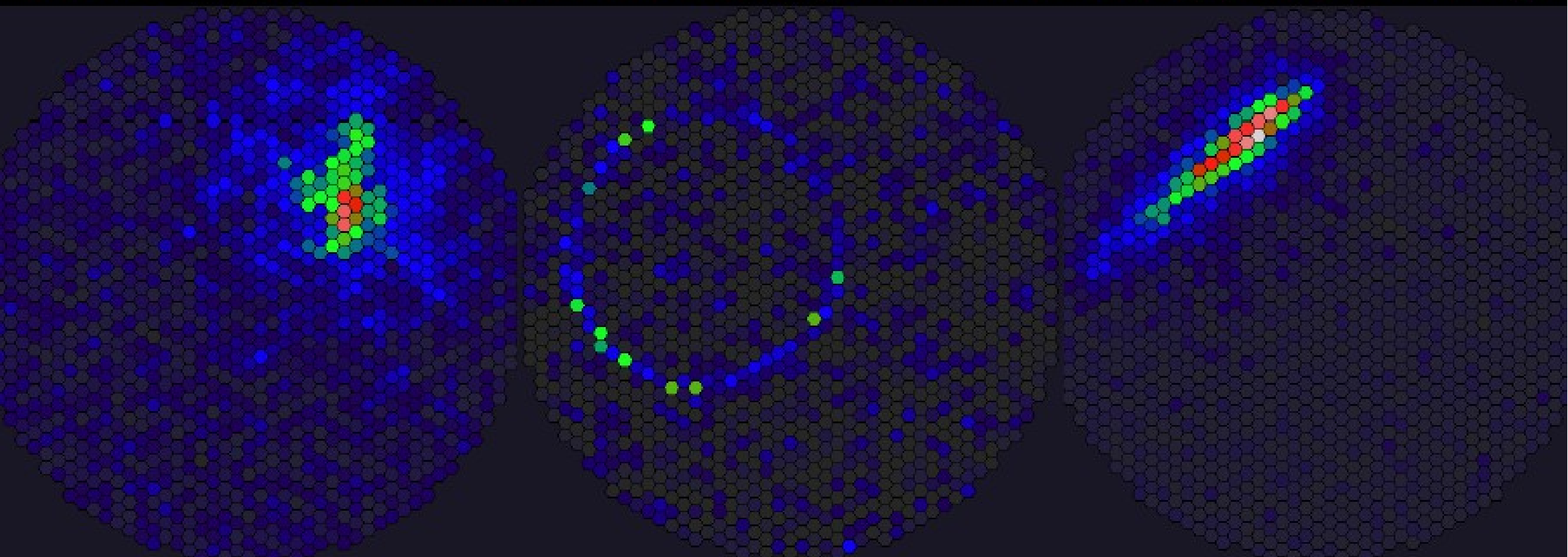

Light guides

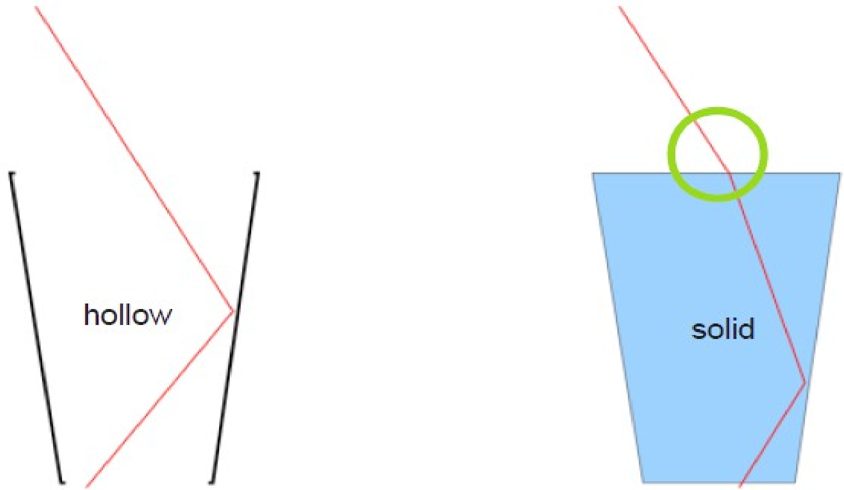

→ **higher concentration than hollow cones due to change of refractive index,** O(12-17)

Solid vs Hollow

Optical coupling

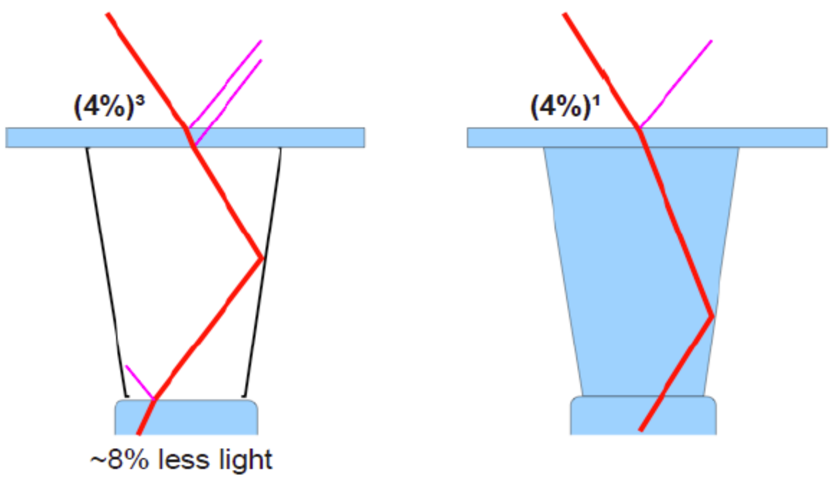

→ **two Fresnel reflections less, ~8% gain**

→ needs *good* optical coupling, i.e. good glueing

Digital SiPM

- Operating frequency: 200MHz
- 2 x TDC (bin width 23ps, 9bit)
- Configurable trigger network
- Validation logic to reduce sensor dead time due to dark counts
- JTAG for configuration and scan test
- Electrical trigger input for test and TDC calibration

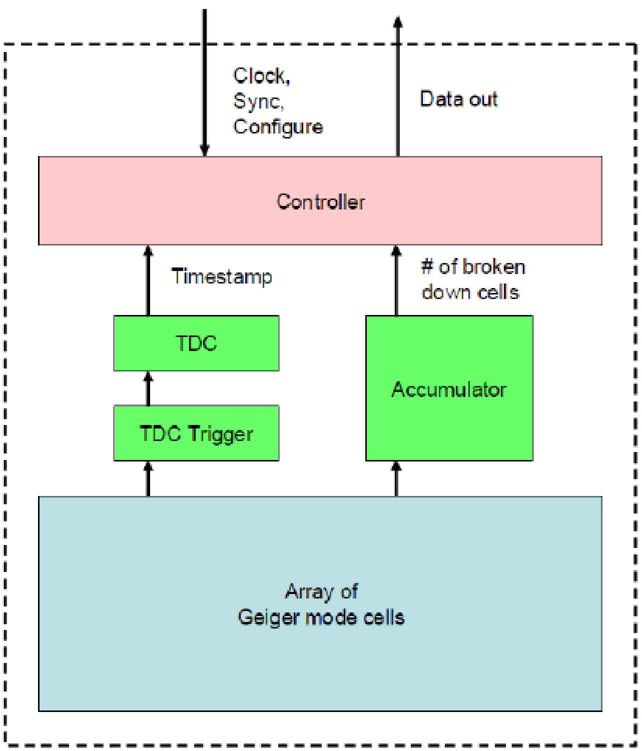

Sensor Architecture

Digital SiPM – State Machine

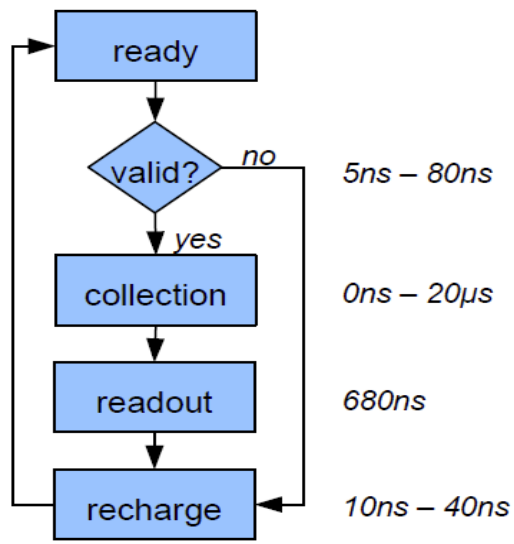

- *200MHz (5ns) system clock*
- *Variable light collection time up to 20µs*
- *20ns min. dark count recovery*
- *dark counts => sensor dead-time*
- *data output parallel to the acquisition of the next event (no dead time)*
- *Trigger at 1, ≥2, ≥3 and ≥4 photons*
- *Validate at ≥4 … ≥64 photons (possible to bypass event validation completely)*

Digital SiPM – Trigger Logic

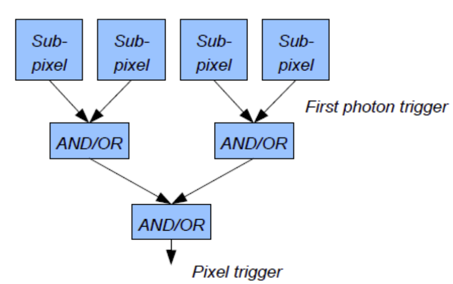

- *Each sub-pixel triggers at first photon*
- *Sub-pixel trigger can be OR-ed or AND-ed to generate probabilistic trigger thresholds*
- *Higher trigger threshold decreases system dead-time at high dark count rates at the cost of time resolution*

T.Frach Heraeus Seminar 2013

FARICH: Stability → radiation and thermal cycles

Note: radiation dose was not monitored during the experiment

Radiation damage: Dark count rate changing

17/06/12: die DCR map

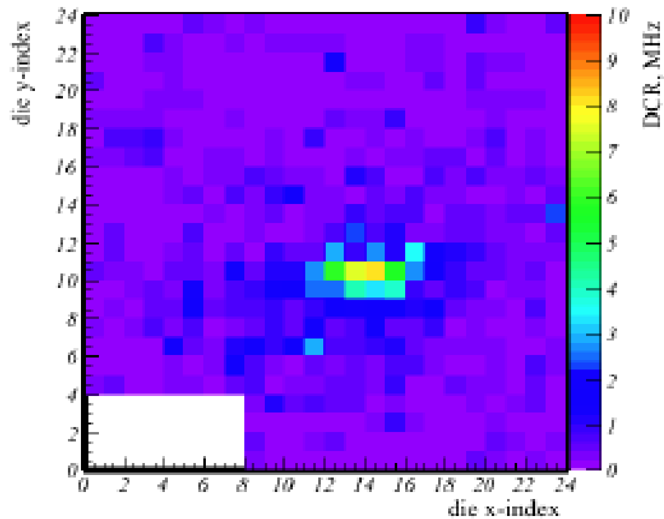

5^{th} day of beam

24/06/12: die DCR map

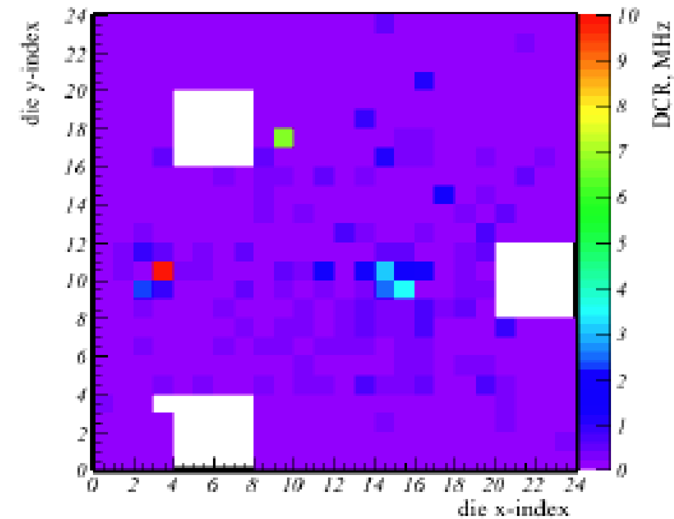

10^{th} day of beam
with 2 days break
at +30°C

Partial recovery is observed after annealing for 2 days at 30°C

Breakage: only 4 of 36 tiles failed after 2 weeks and several thermal cycles.
DPC modules and tiles was not designed to work routinely at low temperature with frequent thermal cycles. It was just a first test.

S.Kononov Vienna Conference on Instrumentation 2013